THE UNIVERSITY *of* EDINBURGH

Identification and characterisation of the E3 ligase, RAP1, in *Arabidopsis*

Manda Yu

Doctor of Philosophy

Institute of Molecular Plant Sciences

The University of Edinburgh

August 2012

Contents

Declaration

I hereby declare that the work presented here is my own* and has not been submitted in any form for any degree to any other university.

Manda Yu

*Remarks: Data shown in Fig 3.2 and Fig 6.2 were generated by Jeum-kyu Hong

Acknowledgements

Firstly, I would like to express my sincere thanks to the Darwin Trust of Edinburgh for financial support during my PhD.

I would also like to express my deepest gratitude to the following people who made my thesis possible;

My supervisor, Professor Gary Loake, who supported me since my PhD application, and who has been providing valuable advice and direction since;

Jeum-kyu, Reza and Hannah who established a good foundation for the project;

Wook, the experienced plant biologist who taught me skills in handling *Arabidopsis*;

Yiqin, who helped me adapt to life in Edinburgh, thus enabling me to find my way around without issue;

Steven, who gave me advice in biotin-switch and experimental design;

All my lab mates who shared happiness and bitterness over the years: Adil, Carols, Corin, Debbie, Edurado, Eunjung, James, John, Kerstin, Kirsti, Krieng, Michael, Minghui, Noor, Priya, Rabia, Rafael, Rumana, Saad, Suzy, Thomas, Usman, Yan and Yuan;

Thierry, for his help in mass spectrometry;

And all my friends in Edinburgh.

I would like to dedicate this work to my wife, for her love and tolerance over the years while we were physically separated, 6,000 miles apart.

My father and grandmother, who bought me up with all their love and strength, without whom, I would be unable to complete my studies.

Abstract

Identification and characterisation of the E3 ligase, RAP1, in *Arabidopsis*

Changes in cellular redox status are implicated in the regulation of developmental and defence-related responses. The absence of S-nitrosoglutathione reductase (GSNOR) function in *Arabidopsis* leads to an accumulation of cellular S-nitrosoglutathione (GSNO), a mobile reservoir of nitric oxide (NO) which impacts the cellular redox tone. Consequently, the *GSNOR* knockout mutant, *atgsnor1-3* displays defects in growth, time to flowering and pathogen resistance. Although it is now well established that GSNO is a key redox signalling molecule, the molecular mechanisms that underpin GSNO function remains largely unknown.

RAP1 (REDOX-ASSOCIATED PROTEIN 1) was identified based on its dynamic changes of expression in *atgsnor1-3* and *sid2* plants upon avirulent *Pseudomonas syringae* pv. tomato (*Pst*) DC3000 (*avrB*) challenge. Pathogen-induced *RAP1* expression was shown to be independent of the plant hormones salicylic acid, jasmonic acid, abscisic acid and ethylene. Recombinant RAP1 protein was shown to exhibit E3 ligase activity in vitro. Application of the NO donors (GSNO and Cysteine-NO (CysNO)) reduced the E3 ligase activity of RAP1 significantly. Biotin-switch analysis showed that RAP1 was S-nitrosylated and site-directed mutagenesis of RAP1 suggested that the S-nitrosylated site is the cysteine residue C325.

The *rap1* line does not show obvious developmental phenotypes, however, overexpressing *RAP1* enhanced lateral root branching in young seedlings. Overexpression of a truncated *RAP1* (*RAP1ΔRING*) led to a loss of apical dominance. In addition, *rap1/rap2* double mutants showed delayed flowering, suggesting *RAP1* might be involved in the regulation of plant growth and development. *RAP1* may also be involved in plant defence, as *rap1*, *rap2* and *rap1/rap2* mutants exhibited increased susceptibility to *Pst*DC3000 and *Arabidopsis* powdery mildew.

Interestingly, *rap1* plants showed enhanced resistance to methyl viologen (MV), which is in line with the phenotype of *atgsnor* mutants. Also, expression of *RAP1* was rapidly inducible by ultraviolet-B (UV-B) light. As *RAP1* expression and RAP1 E3 ligase activity are redox-related, it is speculated that RAP1 may be involved in redox-mediated regulation of a broad range of physiological responses.

Abbreviations

µg	Microgram
µl	Microlitre
35S	Cauliflower mosaic virus 35S promoter
ABA	Abscisic acid
At	*Arabidopsis thaliana*
Avr	Avirulent gene
BAR	The Bio-Array Resource for Plant Biology
Bgt	*Blumeria graminis* f.sp. *tritici*
BLAST	Basic Local Alignment Search Tool
CaM	Cauliflower Mosaic Virus
CaMV	Calmodulin
Col-0	*Arabidopsis* ecotype Columbia
CysNO	S-nitrosocysteine
DNA	Deoxyribonucleic acid
DTT	Dithiothreitol
E.c.	*Erysiphe cichoracearum* or *Golovinomyces cichoracearum*
E. coli	*Escherichia coli*
ETI	Effector Triggered Immunity
GM	Genetically Modified
GSH	Glutathione
GSNO	S-nitrosoglutathione
GSNOR	S-nitrosoglutathione Reductase
GSSG	Glutathione Disulphide
GST	Glutathione-S-Transferase
GUS	β-glucuronidase
H_2O_2	Hydrogen peroxide
HR	Hypersensitive Response
IPTG	Isopropyl- β -thio Galactopyranoside
ICS	Isochorismate Synthase
JA	Jasmonic Acid
kDa	Kilodalton
LB	Luria Bertani medium
MeJA	Methyl Jasmonate
MMTS	S-methylmethanethiosulfonate
MS	Murashige and Skoog medium
MV	Methyl Viologen
NB-LRR	Nucleotide Binding Leucine-rich Repeat
NADH	Nicotinamide Adenine Dinucleotide
NahG	Salicylate hygrogenase gene
NO	Nitric Oxide
NOS	Nitric Oxide Synthase
O_2^-	Superoxide anion radical
$ONOO^-$	Peroxynitrite
PAMP	Pathogen-associated Molecular Pattern
PAGE	Polyarcrylamide Gel Electrophoresis
PBS	Phosphate Buffered Saline
PCD	Programmed Cell Death

PCR	Polymerase Chain Reaction
PDF	Plant defesin
PR	Pathogen Related protein
*Pst*DC3000	*Pseudomonas syringae* pv tomato DC3000
PTI	PAMP-triggered Immunity
R	Resistance gene
RING	Really Interesting New Gene
RNA	Ribonucleic Acid
RNAi	RNA interference
RNI	Reactive Nitrogen Intermediate
ROI	Reactive Oxygen Intermediate
RT	Reverse transcription
SA	Salicylic Acid
SAR	Systemic Acquired Resistance
SNARE	Soluble N-ethylmaleimide-sensitive-factor Attachment Protein Receptor
SNO	S-nitrosothiol
TAIR	The *Arabidopsis* Information Resource
T-DNA	Transfer DNA
TTSS	Type Three Secretion System
Ub	Ubiquitin
UPS	Ubiquitin-proteasome System
UV	Ultraviolet
vir	Virulent gene

List of Tables

Index of Figures

Chapter 1

1 Introduction

1.1 General Introduction

There is an unbreakable link between plants and prosperity in human history: The availability of soil and water for agriculture or animal husbandry has always been the main criteria for selecting the location of residency. Many developing countries predominantly depend on a single crop for calories (e.g. Southeast Asia on rice, Africa on sorghum, maize or cassava) and taking the world as a whole, 80% of human and livestock energy is coming from only four crops (Gressel 2010). However, the world population is expected to reach 9 billion from the current 6.7 billion by 2050, and the arable land and water supply are limited due to urbanization and desertification In addition, crop losses due to diseases and pests are also expected to increase (Roland 2011). A new way to sustain those high food demands for human development will be essential and immediate action is required to prevent social instability.

Development of genetically modified (GM) crops could be a solution, if there are no alternative ways to increase arable land to enhance production. However, the aim of introducing GM crops should not be solely pursuing to increase the yearly production of certain crops, as those GM crops will rapidly consume the minerals in soil. The consequence would be similar to over-farming and the arable land would be further reduced. Therefore the important goal for GM or engineered crops is to make the existing crops more adaptive to abiotic and biotic stresses, for instance, more tolerant to changes in temperature, drought, flooding and more resistant to pathogens and pests. Farmers and consumers have been gradually accepting the benefits of GM crops despite the voices from the international anti-GM movement. The recent report from ISAAA, has shown that in 2010, the accumulated biotech (GM) crop planted land had exceeded 1 billion hectares. It took 10 years from 1995 to 2005 to reach 500 million hectares, but only half that time to gain another 500 million in 2010. More countries have approved the planting of GM crops, such as Pakistan and Myanmar to plant Bt cotton, Sweden - the first Scandinavian country to plant “Amflora” and Germany also resumed adoption of biotech crops (James 2010). Bt cotton secrets an

insecticide originated form a Gram-positive bacterium *Bacillus thuringiensis* and amflora is a genetic engineered potato line that is unable to synthesize amylose (an undesired product for papermaking). These GM-lines are not normally consumed as food but the genetic modifications have significantly improved the cotton yield and the efficiency in papermaking respectively, therefore the use of these crops has been widely accepted by many countries.

However, as more GM crops will be available in the market, more adverse effects might be found in an expanding consumer group, such as the acute allergic effects and more seriously the chronic toxicity or carcinogenic effects upon accumulation of those foreign proteins or metabolites. Therefore new standards have to be introduced for evaluating the potential threats from the GM crops. The European Food Safety Authority (EFSA) has set up a set of risk assessments of GM crops by comparing with the counterpart non-GM crops in order to identify the intended and unexpected impacts on the environment, safety for humans, animals, and nutrition quality. Apart from the classic 90-day rodent feeding test, various *in silico* and *in vitro* methods have been introduced, for instance (i) *in silico* search of the structural similarity of novel proteins or their degradation products to known toxic or allergenic proteins. (ii) *in vitr*o analysis of the stability of the novel proteins under heat or other processing conditions or digestive/intestine fluid. (iii) *in vitro* genotoxicity test methods for screening of point mutations, chromosomal aberrations and DNA damage (van Haver et al. 2008).

Understanding the molecular mechanisms of how plants cope with the abiotic and biotic stresses will help to engineer crops that are more adaptative to the less favourable environment. *Arabidopsis thaliana* (mouse-ear cress) has long been the tool for studying various molecular pathways and plant physiology. It has one of the smallest genomes (~157 Megabase pairs) (Johnston et al. 2005) and was the first fully sequenced plant genome. Other features such as short life-cycle, self-pollination, formation of numerous seeds and easy transformation are also important advantages in plant research. The knowledge and experience extracted from *Arabidopsis* is now being applied into other crops for yield improvement and enhancing resistance to abiotic and biotic stresses.

1.2 Disease Resistance in Plants

Plant diseases are caused by external agents, which can be infectious or non-infectious. A fungus, bacterium, mycoplasma, virus, viroid, nematode, protozoon or parasitic plant that is capable of reproducing and spreading on the host is known as an infectious agent, whilst a disease that is caused by physical factors like extreme temperature, extreme pH, excess or insufficient amount of minerals is non-infectious. Plants have developed various mechanisms to cope with diseases, most notable is the defence mechanism against pathogens which is a highly sophisticated system involving pathogen recognition, signalling and defence gene expression (*Plant Diseases, Encyclopaedia Britannica*).

1.2.1 Basal Disease Resistance

Plants do not have specified cell types to provide protection against pathogen invasions. To prevent entering and spreading of pathogens, plants have established a variety of barriers and inhibitions. The pre-entry protection is given by the physical and chemical barriers, and the observable first barrier is presented by the outer waxy cuticle and preformed antimicrobial compounds (Osbourn 1996; Schulze-Lefert et al. 2008). Antimicrobial compounds can be produced as part of normal plant growth and development (i.e. phytoanticipins) or by transcriptional activation of some biosynthetic pathways in response to microbial attack (i.e. phytoalexins). For example, avenacin, a triterpene glycoside in oat roots and the tomato steroidal glycoalkaloid α-tomatine are constitutively produced. These products confer broad-spectrum disease resistance and pathogens that are capable of degrading these compounds are enhanced in pathogenicity (Bednarek and Osbourn 2009). Some compounds are inactive and stored in healthy tissues; upon tissue disruption, these compounds are converted to biologically active compounds and mobilized to the infection sites. For instance, the indole glucosinolates are stored inside the vacuoles of cells in *A. thaliana* (Ausubel et al. 2009), upon fungus penetration, its activating enzyme myrosinases accumulate at peripheral cells of fungal penetration sites to boost the local concentration of end products (i.e. bioactive isothiocyanate and simple nitrile)(Kim et al. 2008). The accumulation of these end products inhibits the pathogens as well as triggers the deposition of callose and consequently leads to a phytotoxicity and isolation of infected cells from healthy tissues (Bednarek and

Osbourn 2009). Also, phytoalexins are synthesized upon microbial attack, which provide a broad range of disease resistance, possibly by helping the isolation of infected cells from healthy cells. Various phytoalexins have been identified, for example, the stillbenes in grapevine, rishitin and lubimin in potato, camalexin and bassinin in crucifers (e.g. camalexin in *Arabidopsis*), kievitone and phaseollidin in legumes (Morrissey and Osbourn 1999).

1.2.2 Pathogenesis-Related (PR) Genes

PR proteins are not produced, or only at basal concentration in healthy tissue, but are accumulated upon pathogen challenge. Early definitions of PR proteins had also included multifunction enzymes like phenylalanine ammonia lyase which are constitutively present but also increase during most infections. However, recently, the term "PR protein" refers to "inducible defence-related proteins'', with the funtions that are specifically related to host defence. The molecular size of PR proteins is relatively small, ranging from 5kDa to 75kDa. Proteins of a size under 10kDa are often named "PR peptides" (Sels et al. 2008). The first PR protein (PR-1) was identified in the early 1980s from the virus infected tissue of tobacco and is associated with resistance of tobacco mosaic virus (TMV)(Carr et al. 1987). Later on, PR proteins with enzyme activities specifically targeted to pathogens were isolated, for instance PR-2 (β-1,3-Glucanase), PR-2, PR-3, PR-8, PR-11 (chitinases) and PR-5, PR-12, PR-13, PR-14 (membrane targeted). Smaller PR peptides, however, inhibit enzymes of pathogens such as PR-6 as a subclass of serine proteinase inhibitors (PIs), which may act by reducing the ability of the attacker to use its lytic enzymes for pathogenicity (Sels et al. 2008).

1.2.3 Induction of Plant Immunity

A key feature of plant innate immunity is the recognition of microbial- or pathogen-associated molecular patterns (MAMPS or PAMPs) such as flagellin, and lipopolysaccharides (Zipfel and Felix 2005). PAMPs are slowly evolved molecules on the surface of pathogens which are perceived by transmembrane pattern recognition receptors (PRRs) (Zipfel 2008). This is the first layer of plant innate immunity and is also referred to PAMPs-triggered immunity (PTI) (Figure 1.1). Upon recognition, rapid ion influx across plasma membrane leads to MAP kinase activation, ROS production, changes in gene expression and cell wall reinforcement in the plants. However, some successful pathogens are able to interfere with PTI to suppress the induction of defence mechanisms. In many cases, these pathogens secrete some virulence factors (effectors) to evade the recognition or inhibit the subsequent signalling steps (Zipfel 2008). In order to overcome the advancement of pathogens, some plants have evolved resistance proteins (R proteins) to recognize the effectors indirectly or directly by nucleotide binding and leucine rich repeat (NB-LRR) proteins, resulting in effector-triggered immunity (ETI). ETI is a rapid and stronger disease resistance response and is usually accompanied by local cell death known as hypersensitive response (HR) (Jones and Dangl 2006).

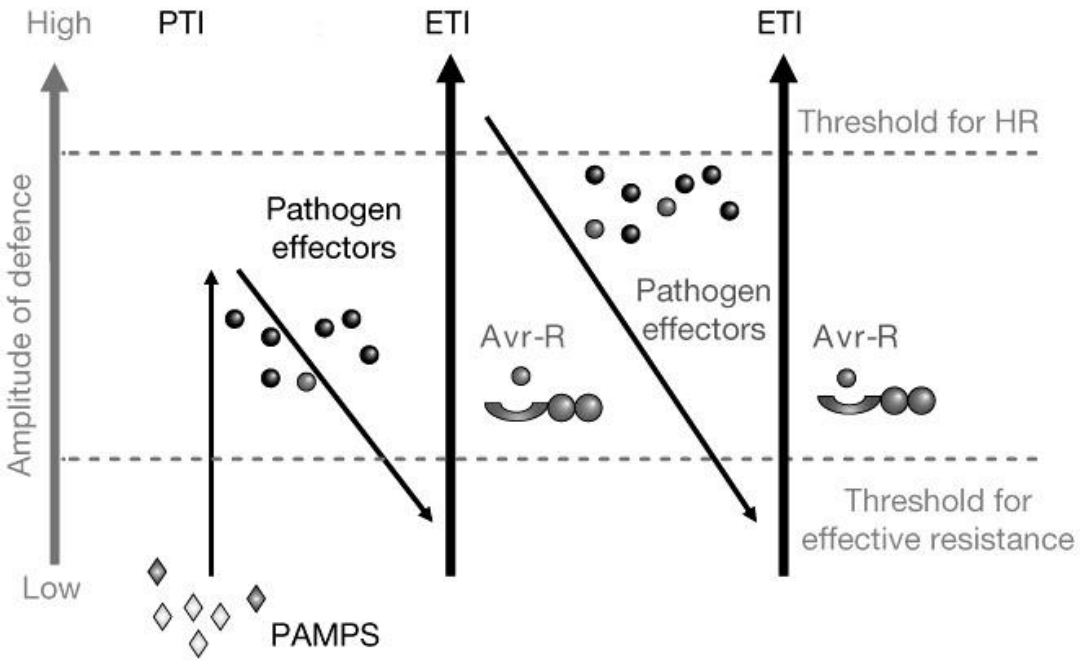

Figure 1.1 A zigzag model illustrates the different phases in plant defence.
Detection of pathogen-associated molecular patterns (PAMPs) triggers the PAMPs-triggered immunity (PTI) to provide effective resistance against pathogens. PTI can be overcome by pathogen effectors, leading to enhanced disease susceptibility. *R*-gene products are then expressed in some adapted plants to neutralize the effects from the effectors and hypersensitive response (HR) is induced to limit pathogen growth in the site of infection by cell-death. However, advanced effectors may be produced to suppress ETI and leading to the competition between invasion and resistance. *Adapted from Jones and Dangl, 2006.*

1.2.4 PTI Induction and Suppression

PAMPs on bacteria such as flagellin (flg22) and Ef-Tu (elf18) are detected by PRRs FLS2 and EFR respectively, while fungal signature proteins xylanase and chitin are recognized by PRRs LeEIX 1/ 2 (tomato) and CEBiP respectively (Bittel and Robatzek 2007). However, PRRs do not signal alone, they require positive regulators such as BRI1-ASSOCIATED KINASE 1 (BAK1). Silencing *BAK1* expression affects responses in tobacco to PAMPs Flg22, CSP22 and oomycete INF1 (Heese et al. 2007) and makes the plants extremely susceptible to necrotrophic fungi in *Arabidopsis* (Kemmerling et al. 2007).

Pathogenic bacteria are able to produce and inject effectors (15-30 effectors per strain) into host cells using a type III secretion system (TTSS) to interfere with PTI (Jones and Dangl 2006). Numerous effectors have been identified and studied; they alter the basal defence functions by suppressing papilla formation (AvrPto1, AvrE1, HopM1, AvrRpm1, and AvrRpt2); altering hormonal responses (AvrB1, AvrRpt2, and Hop(A1,D1, K1,X1 AO1) and suppression of cell death (AvrRpm1, AvrRpt2, AvrB2 and Hop(E1,F2,N1,G1, X1,AB2, AO1 XM1) (Grant et al. 2006). Some effectors have a rather simply mechanism to interfere with host defence, for example, HopM, targets ARF-GEF protein to manipulate host vesicle transport that could be important for bacterial colonization. However, some effectors work sophisticatedly, like the bipartite protein AvrProB of *Pseudomonas syringae*. The N-terminus of AvrPtoB contributes to virulence while the C-terminus is able to block cell death (Jones and Dangl 2006). Further studies have shown that the C-terminus folds into a functional E3 ligase domain, which was a surprise because there is no ubiquitination degradation pathway in prokaryotes. The AvrPtoB E3 ligase was found to interact with a protein kinase Fen in plant cells and targets Fen for degradation. While molecular mimicry of host proteins by bacterial pathogens is common, there is only a handful of bacterial proteins that are known to manipulate the host ubiquitination system (Rosebrock et al. 2007). The disease resistance (*R*) genes will be further discussed in the following section.

1.2.5 Disease Resistance (*R*) Genes

Although PTI can be overcome by effector interference, host resistance (*R*) genes have evolved to recognize effectors and trigger ETI to enhance resistance against pathogen invasion (Figure 1.1). The products of *R* genes are usually NB-LRR proteins and the recognized effectors are termed avirulence (Avr) proteins as ETI leads to immunity to the Avr protein secreting bacteria. However most NB-LRR proteins are known to detect the effectors indirectly and this indirect recognition is known as the "guard hypothesis". NB-LRR proteins manipulate or alter the targets of effectors to reduce the success of interference by effectors. In addition, effectors create a 'pathogen-induced modified self' molecular pattern in host cells, which activates NB-LRR proteins, leading to ETI (Jones and Dangl 2006). For instance, AvrRpm1 and AvrRpt2 are TTSS effectors that target the host plasma membrane associated protein

RIN4 to suppress PTI by either phosphorylation or elimination of RIN4. Action of these effectors activates NB-LRR proteins RPM1 and RPS2 to trigger ETI and leads to hypersensitive response (HR). HR is a form of programmed cell death which confines pathogen in a restricted area (Day et al. 2006). Recent findings have demonstrated a sophisticate mechanism in plants to resist the effects of effector AvrPtoB. The E3 ligase domain of AvrPtoB degrades a protein kinase Fen to reduce PTI. While R protein PtoB shares 80% similarity with Fen but with stronger kinase activity. PtoB phosphorylates AvrPtoB to inactivate its E3 ligase activity. Furthermore, PtoB stabilizes the host protein Prf, which degradation of Prf leads to increased disease susceptibility (Ntoukakis et al. 2009).

1.3 The Roles of Plant Hormones in Defence

Following pathogen recognition, gene transcriptions are initiated, which leads to the shift of concentration of various plant hormones and chemicals. Plant hormones such as salicylic acid (SA), jasmonic acid (JA) and ethylene are produced to trigger different physiological responses locally and systemically. Reactive oxygen intermediates (ROIs) are rapidly produced after pathogen recognition and the process is also termed “oxidative burst”. It is a bi-phasic process, the initial peak of ROI production is seen about 1-2 hours post attempted infection and is followed by a second greater peak at 3-6 hours, but the second peak is only observed with an avirulent pathogen challenge (Grant and Loake 2000). ROIs have a broad role as signals that mediate responses to infection, the abiotic environment, developmental cues, and programmed cell death in different cell types. The subunit (RboH) of NADPH oxidase in plants is regarded as the source of ROI production following pathogen recognition and a variety of other processes (Torres and Dangl 2005). Evidence has also shown that there is a rapid burst of nitric oxide (NO) production in plants upon wounding and pathogen attack (Huang et al. 2004). NO is simple in structure, but its chemistry in biological systems leads to multiple secondary and tertiary reaction products (Ridnour et al. 2004). For instance, NO reacts with other ROIs to from reactive nitrogen intermediates (RNIs)(Hong et al. 2008), contributing the downstream signalling pathway in defence responses. Chapter 1.5 will further discuss the details regarding nitric oxide.

1.3.1 Salicylic Acid (SA) and Defence

Salicylic acid (SA) is an important phytohormone in plant defence against biotrophic pathogens. Pathogen-derived SA is synthesised from chorismate by isochorismate synthase (ICS1). Chorismate is synthesized through the shikimate pathway and components on the pathway are strongly upregulated following pathogen challenge. Pathogen-induced SA is often glycosylated by UDP-glucosyltransferase (UGT) to form non-toxic SA 2-*O*-*β*-D-glucoside (SAG), and other modifications such as methylation (MeSA, a volatile ester) and amino acid conjugation (SA-aa) are also thought to be important in plant defence (Loake and Grant 2007)(Fig 1.2). Over-accumulation of MeSA by expressing rice *OsBSMT1* in *Arabidopsis* reduced SA, SAG and *PR-1* contents, but surprisingly *OsBSMT1* over-expressor triggered *PR-1* induction in neighbouring wild-type plants (Koo et al. 2007). SA-binding protein 2 (SABP2) in tobacco appears to catalyse MeSA to SA, SABP2-silenced plants had attenuated local resistance to tobacco mosaic virus (TMV) and were compromised in systemic acquired resistance (SAR). In addition, jasmonic acid (JA)-induced *AtBSMT1* in *Arabidopsis* explains how the JA pathways may antagonise SA pathways by depleting the SA pool in plants (Loake and Grant 2007). These data suggest MeSA may act as a mobile or volatile signal/inducer in SAR.

Perhaps the strongest evidence that SA plays a critical role in plant defence is the direct impact on defence if the endogenous SA levels are altered. A bacterial gene salicylate hydroxylase (*nahG*) was found to be able to degrade salicylic acid to catechol (You et al. 1991) and the gene was later expressed in tobacco and *Arabidopsis* to reduce endogenous SA levels. Following pathogen infection, these plants were unable to accumulate high SA levels, and they failed to develop SAR or express *PR* genes in the systemic leaves. In addition, these plants were more susceptible to virulent and avirulent pathogens, and the effects were reversible after treatment with synthetic SA. Supressing or mutating genes on the SA-synthesis pathway led to similar observations, for instance, phenylalanine ammonia lyase (PAL), ICS1 (*sid2/eds16* mutant) and a MATE transporter for SA accumulation (*sid1/eds2* mutant)(Vlot et al. 2009).

Another tobacco SA binding protein SABP3 was also identified from the stroma of chloroplasts, exhibiting carbonic anhydrase (CA) activity and antioxidant activity

when expressed in yeast. Silencing the CA activity of SABP3 suppressed the development of hypersensitive cell death (HR) by AvrPto. These findings demonstrate that SA may act through multiple effector proteins in plants (Slaymaker et al. 2002). A homologous *Arabidopsis* protein AtSABP3 was later identified and also possesses CA activity. The nitric oxide (NO) burst during attempted infection promotes increasing S-nitrosylation of AtSABP3 at cysteine 280. S-nitrosylation of AtSABP3 suppressed both binding of SA and CA activity, while the CA activity of AtSABP3 has shown to be required for resistance of *Pst*DC3000(*avrB*). S-nitrosylation appears to be important at the later stage of plant defence response, which contributes to a negative feedback loop to the induced defence genes (Wang et al. 2009c).

The role of SA in monocotyledonous plants is less well understood and may be different to that in dicotyledonous plants. SA induces *PR* genes expression in maize, rice, barley and wheat. The endogenous SA level was elevated to resist the infection of *P. syringae* pv. *syringae* in barley. In contrast, in barley carrying the powdery mildew resistance genes *mlo5*, *Mlg*,or *Mla12*, defence responses (including HR development and H_2O_2 accumulation) were activated without a corresponding rise in SA levels. SA levels also failed to increase in rice inoculated with *P. syringae* or fungus *Magnaporthe grisea* or *Rhizoctonia solani* (Vlot et al. 2009).

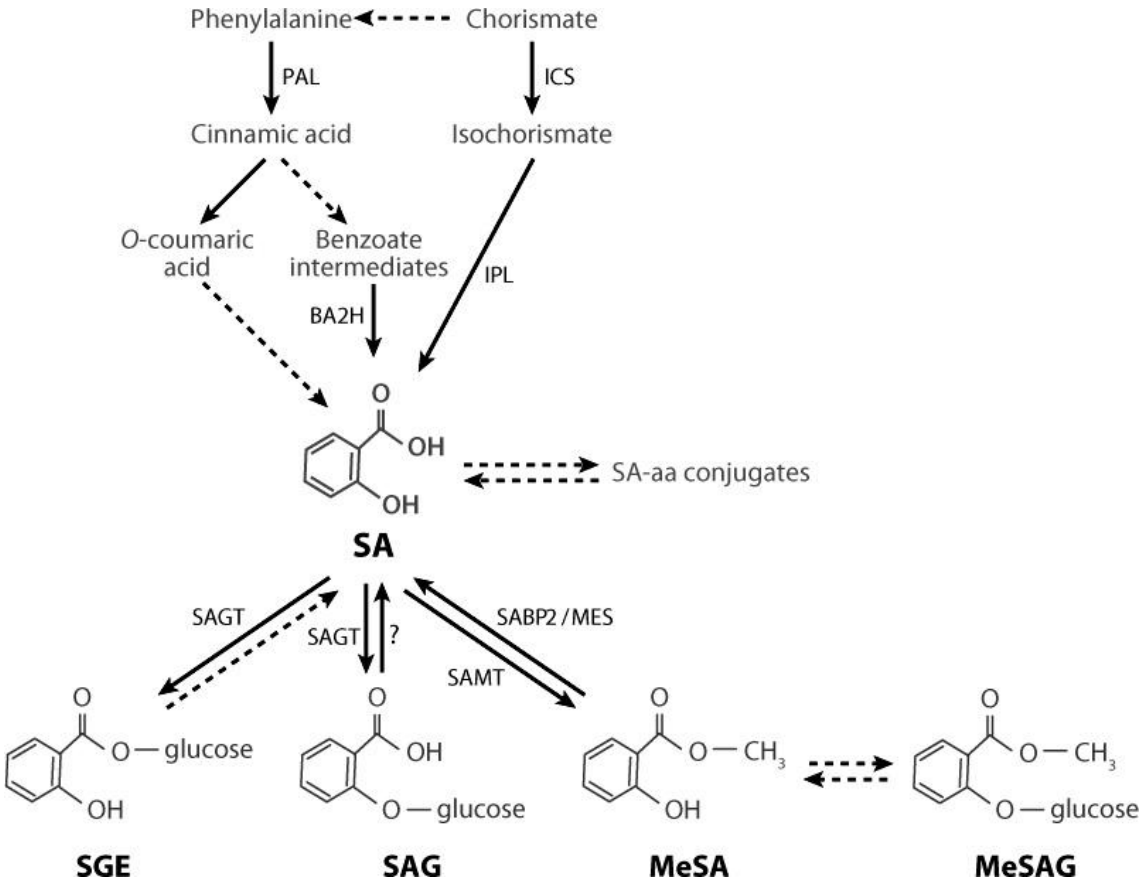

Figure 1.2 SA biosynthesis and SA-derivatives.
SA is synthesized from either chorismate by isochorismate synthase (ICS) or phenylalanine by phenylalanine ammonia lyase (PAL). SA can be further converted to various SA-derivatives such as salicyloyl glucose ester (SGE), SA-*O*-*β*-glucoside (SAG), methyl salicylate (MeSA) and methyl salicylate *O*-*β*-glucoside (MeSAG). Adapted from Vlot et al., 2009.

1.3.2 SA and Systemic Acquired Resistance (SAR)

SA was initially proposed to serve as a signal generated in the infected leaf and transmitted via the phloem to the uninfected portions and leading to resistance in distal tissues (termed "systemic acquired resistance" or SAR), because SA level rise coincidently with or just prior to SAR development and a significant amount of SA is found in the systemic leaves and phloem in pathogen-infected plants (Vlot et al. 2009). However, a classic experiment has reversed this hypothesis, *nahG* expressing plants were grafted onto wild-type tobacco and SAR was still able to be induced in the grafted plants by TMV in the SA-deficient leaves (Vernooij et al. 1994). Another possible mobile signal for SAR is MeSA (Park et al. 2007), which is biological inactive : SA-binding protein 2 (SABP2) converts SA to MeSA and grafting

experiments demonstrated that SABP2's activity is required only in systemic tissues for SAR development. In addition, silencing of *SA methyltransferase 1* (*SAMT1*) or overexpressing a mutant of SABP2 whose MeSA esterase activity is not inhibited by SA, depleted MeSA levels as well as SAR (Vlot et al. 2009).

It is worth noting that MeSA/SA-derivatives are only part of several likely long-distance signals for SAR. Evidence has suggested that SAR signals could be transmitted by JA, a yet undefined lipid-derived molecule, or a group of peptides. Plants possessing a mutation in the lipid-transfer protein DIR1 (DEFECTIVE IN INDUCED RESISTANCE 1) in *Arabidopsis* are incapable to transmit a functional SAR signal, but are not affected in resistance of the inoculated leaf. The lipid-derived molecule associated with DIR1 is unknown, while following the clues with other mutated genes (*FAD7*, *SFD1*, *SFD2*, *MGD1*) have shown that the candidate might be related to chloroplast galactolipid metabolism (Vlot et al. 2008). It was also hypothesized that JA or DIR1-JA could be the mobile signal of SAR, as numbers of JA-dependent gene expression in the systemic leaves of infected plants correlates with SAR and tobacco lipid-transfer protein 1 (LTP1) induces disease resistance only when it is conjugated to JA (Buhot et al. 2004). In addition, small peptides generated by apoplastic aspartic protease CDR1 (CONSTITUTIVE DISEASE RESISTANCE 1) could also be involved in SAR, as at least one receptor has been identified on cell surface. The level of S-nitrosylation (see Chapter 1.5b) could be related to SAR, since GSNOR is localized to phloem companion cells and xylem parenchyma and it was hypothesized that GSNOR plays a role in SAR signal transport through the vasculature (Vlot et al. 2008).

1.3.3 Jasmonic Acid (JA), Ethylene and Defence

SA-dependent defences are largely related to resistance against biotrophic pathogens, whereas jasmonic acid (JA) and ethylene based responses are required for protection against necrotrophic pathogens (Thaler et al. 2012). Jasmonates are small lipid derivatives, and about 20 naturally occurring jasmonates have been described. In *A. thaliana*, JA is necessary for the expression of a number of genes and it can be conjugated to hydrophobic amino acids, usually isoleucine to form JA-Ile by an ATP-dependent JA-amino synthetase JASMONIC ACID RESISTANT 1 (JAR1). The *jar1* mutation led to decreased sensitivity to exogenous JA and increased susceptibility to

certain opportunistic root pathogens without affecting male fertility (a process that requires JA synthesis), suggesting JA-Ile may be a regulator more specific in plant defence (Gfeller and Farmer 2004). Methyl jasmonate (MeJA) is a fragrant volatile compound and is formed by JA carboxyl methyltransferase (JMT) from JA. MeJA formation could be one of several important control points for jasmonate-regulated plant responses, overexpressing *JMT* in *Arabidopsis*, various jasmonate-responsive genes were constitutively expressed in the absence of wounding or jasmonate treatment (Cheong and Choi 2003).

Ethylene is a multifunctional, gaseous plant hormone, which is synthesized as one of the earliest detectable events during plant-pathogen interaction. Some early reports already showed that ethylene was able to induce genes related to phytoalexin and lignin synthesis (Ecker and Davis 1987). Also in certain cases, ethylene modulates programmed cell death (PCD) pathways (such as ethylene-induced leaf senescence) and hypersensitive response (HR). A large burst of ethylene is produced upon HR initiation and treatment of ethylene increased either susceptibility or resistance, depending on the conditions of plant-pathogen interaction (Wi et al. 2012) . Also, in some cases, ethylene can act as a virulence factor of bacterial and fungal pathogens, and in contrast ethylene is involved in disease resistance. The role of ethylene in different stages of infection could be quite different, which might be due to the antagonistic interactions between SA and JA/ethylene or the synergistic action of SA and ethylene (Bouchez et al. 2007).

1.4 Defence Signalling Pathways

After recognition of pathogens, a complex genetic signalling network is switched on. Emerging evidence has given a better picture to show how these signals are being perceived, relayed and regulated. Salicylic acid (SA), jasmonic acid (JA) and ethylene are the major plant hormones involved in defence responses. SA signalling is generally important for immunity against biotrophs or hemibiotrophs, while JA and ethylene signalling are generally important for immunity against necrotrophs and herbivores (Tsuda and Katagiri 2010).

NPR1 (NONEXPRESSOR OF PATHOGENESIS-RELATED GENES 1)(also known as NIM1 and SAI1) is a key regulator in the SA signalling pathway. NPR1 oligomers

are held together by disulphide bonds in the cytosol in the absence of pathogen challenge. Upon SA induction, NPR1 oligomers are dissociated to become monomers. NPR1 monomers are formed due to changes in the cellular redox state leading to reduction of two cysteine residues Cys82 and Cys216 by THIOREDOXIN (TRX)-H5 and/or TRX-H3 (Tada et al. 2008). The NPR1 monomers translocate to the nucleus where the monomers activate the expression of a variety of pathogenesis-related (*PR*) genes. In the nucleus, NPR1 interacts with several members of the TGA family of bZIP transcription factors, as well as with three other proteins, NIMIN1, 2, and 3 (Weigel et al. 2005). Interaction between NPR1 with TGA1 and TGA4 only occurs in SA-induced leaves, due to the reduction of two conserved cysteines of TGA1 and TGA4, while interaction between TGA2 and NPR1 can be detected in the absence of SA, but is enhanced by SA treatment of leaves (Durrant and Dong 2004). Reversely, S-nitrosylation (at Cys156) takes part in facilitating NPR1 to form back to oligomer, which could act as a negative feedback loop for SA mediated resistance (Tada et al. 2008). (Fig 1.3)

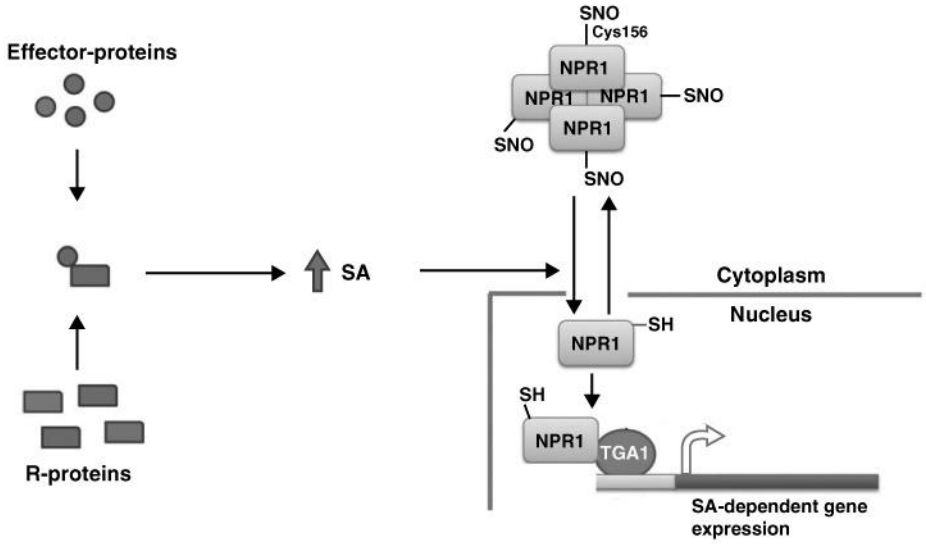

Figure 1.3 Salicylic acid (SA) signalling is regulated through the dynamic equilibrium between monomeric and oligomeric forms of NPR1.
Pathogen recognition results in increased SA accumulation which favours the NPR1 monomer formation. The NPR1 monomers translocate to the nucleus where it binds TGA1 and functions as a transcriptional co-activator of SA-dependent gene expression. Conversely, S-nitrosylation of NPR1 at Cys 156 favours oligomer formation. *Adapted from (Yu et al. 2012).*

Jasmonates (JAs) are important in plant defence against pathogens and also have a significantly role in wounding and herbivore defence. The first key JA signalling component was isolated from a *coi1* (*coronatine insensitive 1*) mutant using a map-based strategy, and the *COI1* locus was found to encode an F-box protein. The *coi1-1* mutant displays defects in many JA-dependent functions, such as fertility, secondary metabolite biosynthesis, pest and pathogen resistance, and wound responses (Xie et al. 1998). COI1 is one of the components of an integral part multi-protein complex called the SCF E3 ubiquitin ligase complex (SCF^{COI1}). The SCF complexes are found in all eukaryotes and consists of a Skp1 (S-phase kinase-associated protein)-related protein, a cullin, a RING-box protein, and an F-box protein. F-box proteins (i.e. COI1) are known to be responsible for the specificity of SCF complexes to target protein(s) for degradation through the 26S proteasome. In yeast cells, *Arabidopsis* COL1 and JAZ1 interact but only when JA-Ile is added to the growth medium and interestingly but not other jasmonate-derivatives such as jasmonate, 12-oxo-phytodienoic acid, or MeJA. (Thines et al. 2007). In *Arabidopsis*, two conserved signatures are found in JAZ proteins, ZIM (Zinc-finger inflorescence meristem) domain and Jas motif. Elimination of the Jas motif in JAZ3 protein in a *jaz3* mutant, results in a dominant jasmonate-insensitive phenotype, and deletion of the JAZ1 Jas motif also disrupted jasmonate signalling in a dominant manner. JAZ proteins work as transcriptional repressors, therefore overexpression of JAZ proteins does not impact the normally repressed transcriptional state. Upon activation of JA-mediated signalling pathway, elevated JA-Ile level induces the interaction of JAZ protein (JAZ1) and COI1 and leads to the ubiquitin-mediated degradation of JAZ1. JAZ proteins are unlikely to bind DNA directly but through the interaction with transcription factor like MYC2, for instance JAZ3 physically interacts with MYC2, requiring the Jas motif, so MYC2 is probably regulated (inhibited) by JAZ3. MYC2 positively regulates a variety of genes involved in wound and/or insect responses, oxidative stress response and flavonoid synthesis, and negatively affects genes for pathogen defence and tryptophan metabolism; degradation of JAZ3, therefore releases MYC2 from inhibition, leading to transcription of JA response genes (Chico et al. 2008; Staswick 2008).

Ethylene is a volatile and gaseous molecule which is detected by a set of well-characterized ethylene receptors. In *Arabidopsis*, from structure analysis, ethylene receptors are categorized into two main subfamilies: Subfamily I, composed of ETR1

and ERS1, is characterized by the presence of three transmembrane domains and a C-terminus histidine kinase domain, whereas Subfamily II, which includes ETR2, EIN4, and ERS2 have four transmembrane regions and a C-terminus serine–threonine kinase domain (Kendrick and Chang 2008). Downstream of ethylene receptors is Raf-like protein kinase CTR1, which physically interacts with the kinase domain of ETR1 and ERS1 and co-localizes in the ER. Signals are further transduced by MKK9–, MPK3/6 MAP kinase cascade to reach EIN3 and EIL1 transcription factors (Stepanova and Alonso 2009). EIN3 binds to the 5'- upstream of the *Arabidopsis ERF1* gene and is considered as an immediate target of EIN3. EIN3 drives the expression of ERF1 and results in activation of several ethylene-inducible genes that contain the GCC box in the promoter (Ohme-Takagi et al. 2000). A variety of defence-related genes are ethylene responsive through the GCC-box element such as vacuolar β-1,3-glucanases (PR-2), vacuolar basic-chitinases (PR-3), acidic hevein-like proteins (PR-4), and plant defensins (PDFs; PR-12). In addition, the *Arabidopsis* defensin *AtPDF1.2* gene contains a GCC box promoter elements and is inducible by both ethylene and JA through activation of AtERF1 but is repressed by SA. Therefore, *AtPDF1.2* has been regarded as a marker for ethylene/JA mediated defence responses (Broekaert et al. 2006).

1.4.1 Cross Talk between Hormones in Defence

SA and JA are responsible to combat different targets. SA is predominantly related to biotrophic pathogens and viruses, whereas JA protects against necrotrophic pathogens and insects (Tsuda and Katagiri 2010). The signalling between SA and JA is generally antagonistic to each other through the regulation on NPR1, SSI2, WRKY transcription factors, and MPK4, although synergism between both signalling pathways has been observed. Competition experiments using biotrophic and necrotrophic pathogens or insects revealed that SA has a higher priority over JA pathway in *Arabidopsis* (Vlot et al. 2009). Transcription of JA-responsive marker genes, such as *PDF1.2* and *VSP2*, is highly sensitive to suppression by SA. The SA-mediated suppression of JA signalling might be due to an increase in cellular glutathione levels, as inhibition of glutathione biosynthesis suppresses the antagonistic effect of SA on JA signalling (Koornneef et al. 2008). Furthermore, SA-inducible glutaredoxin 480 (*GRX480*) represses *PDF1.2* expression in *Arabidopsis*.

Overexpression of *GRX480* also abolished induction of *PDF1.2* by MeJA in an *NPR1*-independent, *TGA2/5/6*-dependent manner (Vlot et al. 2009).

On the other hand, the ethylene- and JA- mediated signalling pathways act synergistically in defence responses. Microarray analysis has indicated that clusters of genes are induced by ethylene and JA. Furthermore, the AtERF1 binding GCC-box is also present in the promoter of the JA-induced *AtPDF1.2* gene and has also been identified as a JA-responsive element. JA-induced transcription factor also interacts cooperatively with EIN3 in the promoter of *AtERF1* (Broekaert et al. 2006). Similar to JA, ethylene pathway acts independently or antagonistically with respect to the SA-dependent pathway. Transgenic *Arabidopsis* plants that are impaired in accumulation and synthesis of SA (e.g. *nahG*-expressing, *sid2* and *eds5*) or SA signalling (e.g.,*npr1/nim1*) show an equal or even stronger induction of ethylene/JA-dependent *PR*-genes. In addition, enhanced resistance to *B. cinerea* by overexpression of *AtERF1* reduced the SA-mediated resistance to *P. syringae* pv. *tomato*.

1.5 Nitric Oxide (NO)

1.5.1 Origin of NO

NO, a free radical, is a by-product of oxidative metabolism. Animal cells synthesise NO by the activity of NO synthase (NOS), which is a NADPH-dependent reaction (oxidation) of $_{L}$-Arg to NO and $_{L}$-citrulline. However, there have been only false clues after a long search for a plant NOS. Endogenous NO synthesis in plants was initially demonstrated by the application of the inhibitors of NO synthesis which resulted in compromised disease resistance (Delledonne et al. 1998). It has been shown that NO can be synthesised by the reduction of nitrite to NO by nitrite reductase (NR)(Yamasaki et al. 1999). However, the efficiency is low and NR is required during flowering, auxin-induced lateral root development and abscisic acid (ABA)-induced stomatal closure but not in many other responses (Gas et al. 2009). While other reports suggested various sources of nitrite-dependent NO synthesis and non-enzymatic synthesis, the origin of $_{L}$-Arg dependent NOS activity in plant cells has not been uncovered.

Analysis of the full sequenced genome of *Arabidopsis* and rice have not retrieved any gene that is homologous to animal NOS, suggesting the NOS activity in plant cells comes from an enzyme distinct to the mammalian proteins. A protein, initially named At-NOS1 in *Arabidopsis* was identified based on its homology to a snail protein wihich coeluted with NOS activity and cross-reacted with antibodies against mammalian NOS enzymes (Huang et al. 1997). Mutant *nos1* displayed decreased NO accumulation/burst in response to ABA, salicylic acid, salt, elicitor treatments. However, NOS1 protein fails to display NOS activity in vitro and does not reduce NO accumulation in some responses such as H_2O_2-induced NO accumulation in guard cells, suggesting NOS1 is not a NOS enzyme and consequently has been renamed nitric oxide associated protein1 (NOA1) or RIF1 (Resistant to Inhibition by fosmidomycin). Fosmidomycin inhibits 1-Deoxyxylulose 5-phosphate reductoisomerase (DXR) which results in a specific block in the biosynthesis of chlorophylls and carotenoids (Flores-Perez et al. 2008b). Further evidence has suggested that the GTPase activity of NOA1/RIF1 is unrelated to plant NO production (Moreau et al. 2008) but linked to plastid RNA binding/processing (Flores-Perez et al. 2008a).

1.5.2 S-Nitrosylation

There is considerable evidences that NO and its metabolites play an essential role in signal transduction in plants and animals. For instance, the NO-related S-nitrosothiols (SNOs) have been shown to be involved in many physiological regulation pathways. In mammals, SNOs circulate in the blood as S-nitrosohaemoglobin (SNO-Hb), which is linked to hypoxic vasodilation (Reynolds et al. 2007). The free radical NO, however, is an unstable product, which requires to be stabilized in the cell to provide sustainable effects after synthesis. NO reacts rapidly with glutathione (GSH) to form S-nitrosoglutathione (GSNO), the reaction is reversible and GSNO is considered to represent a functionally relevant signalling molecule that acts as an NO reservoir and donor. NO is also reactive with thiol group of cysteine residues in proteins through the donation of NO, a reaction known as S-nitrosylation, which often alters protein stability and activity. Protein S-nitrosylation in humans has been extensively studied and constitutes a large part of the ubiquitous influence of nitric oxide on cellular signal transduction both in normal physiology and in a broad spectrum of diseases (Foster et al. 2009). Although some proteins can transfer an NO group onto another protein (i.e. trans-nitrosylation), a specific enzyme to catalyse the S-nitrosylation of proteins is not yet described. S-nitrosylation of proteins is mainly regulated by the availability of NO or NO donors. The activity of NOS can be modulated through altered expression or activity of enzymes that control the availability of endogenous NOS substrates (e.g. $_{L}$-Arg) or by endogenous NOS inhibitors. (Hess et al. 2005). Enzymes on the NO synthesis pathway are also regulated by S-nitrosylation. For instance arginase 1 (Arg1) is activated through enhanced multimerization resulting from S-nitrosylation at cysteine 303 (Santhanam et al. 2007). Arg1 competes with NOS for $_{L}$-Arg and hence reduces the production of NO (Bronte and Zanovello 2005). Some enzymes promote S-nitrosylation, such as Cu/Zn superoxide dismutase (SOD) which catalyses the S-nitrosylation of haemoglobin by NO or (NO from GSNO) and Cu^{2+}-containing protein ceruloplasmin which catalyses S-nitrosylation of the heparan-sulphate proteoglycan glypican, *in situ* (Hess et al. 2005). Protein-bound transition metals, in particular Cu^{2+} or Fe^{2+} bound near the thiol sites can also catalyse the transfer of NO-group from GSNO/nitrite to cysteine residues within serum albumin, haemoglobin and calbindin (Hess et al. 2005).

Protein conformation, electrostatic environment, hydrophobicity, contiguity and orientation of aromatic side chains, proximity of target thiols to transition metals, redox centres or other thiols (formation of disulphide bond) and protein-protein interaction determine the site of S-nitrosylation. Some common features of SNO sites are: electrostatic interactions that control thiol pKa (NUCLEOPHILICITY); hydrophobic compartmentalization; allosteric regulators (e.g. Ca^{2+}, Mg^{2+} and O_2/redox) that can modulate thiol (solvent) accessibility or reactivity and interaction between NO and target proteins. Motifs that are likely to be S-nitrosylated, are termed SNO motifs. An example is the "acid-base" motif found on the β-Cys93 of haemoglobin (Hess et al. 2005). The acid–base motif comprises flanking acidic (Asp, Glu) and basic (Arg, His, Lys) residues, and it has been illustrated to catalyse GSNO-induced S-nitrosylation of hepatic methionine adenosyltransferase (Perez-Mato et al. 1999). High local hydrophobicity of a protein region (due to tertiary protein structure and protein–protein interactions) also promotes S-nitrosylation. The only one of ~50 free thiols (Cys3635) of the ryanodine receptor of skeletal muscle (RyR1) that is S-nitrosylated is intercalated within a hydrophobic region of calmodulin (CaM)-binding domain (Jourd'heuil et al. 2003).

1.5.3 Denitrosylation

The level of S-nitrosylation of cellular protein depends on the balance between nitrosylation and denitrosylation. Research has mainly focused on the mechanisms that promote S-nitrosylation, and work on denitrosylation has lagged behind. Recent reports suggest that in particular, two enzymatic systems are directly involved in the process of denitrosylation. They are important in protecting cells from nitrosative stress and regulate manifold NO-related cellular and systemic responses (Benhar et al. 2010). One enzyme system is the thioredoxin/thioredoxin reductase (Trx/TrxR). Thioredoxins (Trxs) are ubiquitous and have a conserved Cys-Gly-Pro-Cys redox active site that is essential for their function as oxidoreductases. The denitrosylase activities of Trxs are coupled to cognate Trx reductases (TrxR), flavin containing selenoenzymes that have been shown to safeguard microbial and mammalian organisms against nitrosative stress. Trx was shown to have caspase-3 denitrosylase activity in the presence of NADPH *in vivo* (Benhar et al. 2008). The denitrosylase activity of Trx requires the activity of TrxR which catalyses NADPH to $NADP^+$ to

recycle the oxidized thioredoxin (Trx-S_2) to reduced thioredoxin (Trx-$(SH)_2$)(Benhar et al. 2009; Holmgren 2008). A number of enzymes such as glutathione peroxidase, γ-glutamyl transpeptidase, and xanthine oxidase are able to decompose SNO in vitro, but none has been shown to regulate levels of endogenous SNO or to be involved in any NO or SNO-mediated response (Liu et al. 2001)(Fig 1.4).

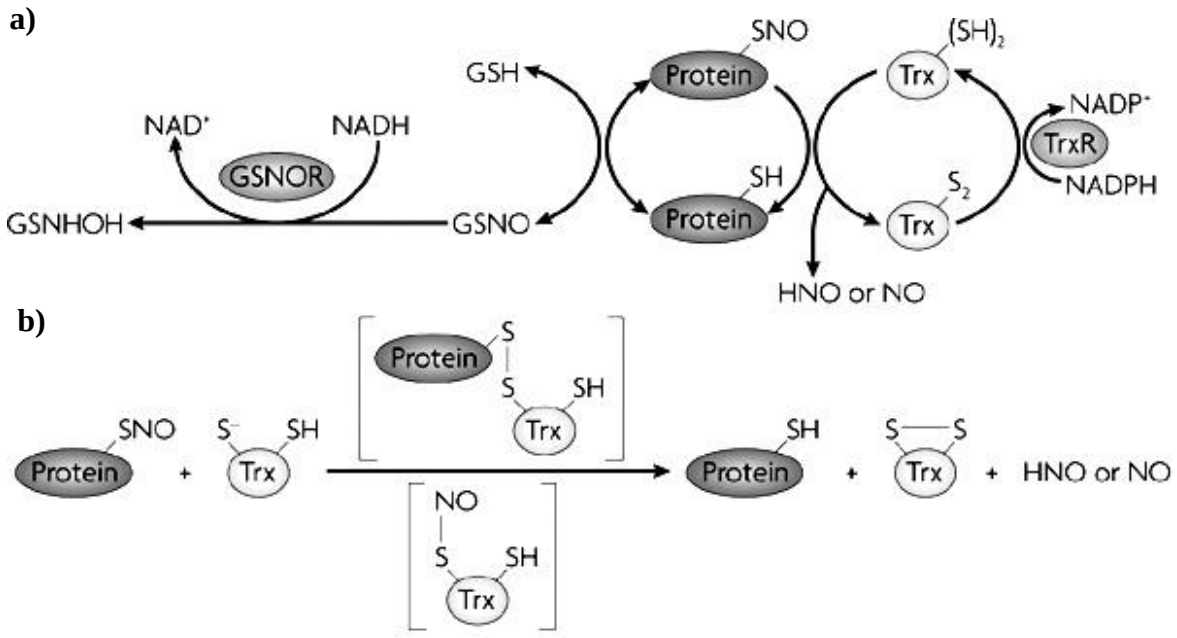

Figure 1.4 Denitrosylation by Trx and GSNOR.
(a) S-nitrosylated protein can be denitrosylated non-enzymatically with GSH, subsequently GSNOR rapidly and irreversibly metabolizes GSNO to GSNHOH to drive the equilibrium from S-nitrosyalted proteins towards GSNO. Trx denitrosylates S-nitrosylated proteins through its dithiol moiety, thereby forming a reduced protein thiol (-SH) and oxidized Trx. Oxidized Trx is "recycled" by ThxR in the presence of NADPH. **(b)** Alternative proposed mechanisms of Trx-mediated denitrosylation, suggesting that the formation of an intermolecular disulphide intermediate between S-nitrosylated protein and Trx or direct transnitrosylation from S-nitrosylated protein. *Adapted from Benhar et al., 2009.*

1.5.4 S-Nitrosoglutathione Reductase (GSNOR)

S-nitrosoglutathione (GSNO) serves as the NO reservoir and NO donor for S-nitrosylation, therefore the level of cellular GSNO directly impacts on NO bioactivity and consequently on transduction pathways in host defence. An *Escherichia coli* enzyme, glutathione-dependent formaldehyde dehydrogenase (GS-FDH) was firstly identified to have a robust activity of reducing GSNO to glutathione disulphide (GSSG) and ammonia (NH_3), and was NADH dependent. The activity of GS-FDH was also highly GSNO specific: no activity was seen towards S-nitrosocysteine (CysNO) and S-nitrosohomocysteine and only ~1 % with cysteinyl-glycine and g-glutamylcysteine. A mouse GS-FDH or alcohol dehydrogenase class III (ADH III) was also identified based on the GSNO-metabolizing activity of RAW 264.7 cell lysates. Mouse GS-FDH shares over 60% sequence identity with the yeast protein GS-FDH (*SFA1*) and deletion of this gene in yeast lead to 11-fold higher SNO. Moreover growth of yeast *sfa1* mutant cells was inhibited by a GSNO concentration that had little effect on wild-type Y190 cells, suggesting the GS-FDH is essential to protect against nitrosative stress from GSNO (Liu et al. 2001). GS-FDH was renamed as S-nitrosoglutathione reductase (GSNOR). Arabidopsis GSNOR was identified which was able to fully complement the GSNO hypersensitive in yeast *sfa1* mutant (Sakamoto et al. 2002). In addition, *Arabidopsis* GSNOR also contains glutathione-dependent formaldehyde dehydrogenase (FADLH) activity, which confers high resistance to formaldehyde when overexpressed in yeast *sfa1* mutant (Achkor et al. 2003). GSNOR is related to many physiological responses, and knocking out of *GSNOR* in *Arabidopsis* leads to a variety of developmental phenotypes such as delayed seed germination, reduced plant growth, loss of apical dominance, and increased numbers of highly branched shoots (Feechan et al. 2005; Holzmeister et al. 2011).

1.5.5 GSNOR and Defence

NO is ubiquitously produced in almost all mammalian immune cells and is recognized as an immunoregulatory molecule. NO and GSNO are able to induce apoptosis in macrophages, thymocytes, lymphocytes, and endothelial cells through S-nitrosylation/denitrosylation of proteins in the signalling pathway. There is evidence that NOS and GSNOR act as a double gate control of S-nitrosylation in the immune

response (Duan and Chen 2007). In *Arabidopsis*, loss of GSNOR function increases cellular SNO levels, disabling plant defence responses conferred by distinct resistance (*R*) gene subclasses and compromising basal and non-host disease resistance (Feechan et al. 2005). The knockout mutant *atgsnor1-3* exhibits 21% of GSNOR activity than in wild type plant, while gain-of-function mutants *atgsnor1-1* and *atgsnor1-2* have increased activity of 189% and 165% respectively. Challenging *atgsnor1-3* plant with avirulent pathogen *Pseudomonas syringae* pv. tomato (*Pst*) strain DC3000 (*avrB*) increased cellular SNO to 220% of wild type level, and the resistance was abolished. The *atgsnor1-3* plants were also more susceptible to avirulent *Pst*DC3000 (*avrRps4*), virulent *Pst*DC3000, *Hyaloperonospora parasitica* Noco2, *Blumeria graminis* f.sp. *tritici* (*Bgt*); and *Pseudomonas syringae* pv. *phaseolicola* (*Psp*) (NPS3121) (Feechan et al. 2005).

A study in tobacco (*Nicotiana attenuata*) has showed that GSNOR is also involved in plant-herbivore defence. Silencing GSNOR decreased the herbivore-induced accumulation of jasmonic acid (JA) and ethylene (Wunsche et al. 2011).

1.6 Cellular Redox Status and Defence

Redox (reduction-oxidation) reactions refer to all chemical reactions which lead to the change in oxidation state of atoms. Reactive oxygen species (ROS) are produced during normal metabolism, certain development process and stress conditions. Formation of ROS changes the redox status of the cellular environment and ROS need to be detoxified as it can potentially damage DNA, RNA and proteins. In plants, ROS such as superoxide (O_2^-) can be produced at any location where an electron transport chain is present, including mitochondria, chloroplasts, microsomes, glyoxysomes, peroxisomes, apoplasts, and the cytosol. ROS can be removed enzymatically by superoxide dismutases (SODs) which catalyse the dismutation of superoxide into oxygen and hydrogen peroxide. In plants, SODs are classified into three groups: iron SOD, maganese SOD and copper-zinc SOD which locate in difference compartment of the cells as the first line of defence against ROS (Alscher et al. 2002).

On the other hand, change in ROS levels can be exploited to redox signals that are important for the organisms to respond to different biotic and abiotic stresses. Glutathione (γ-glutamyl-$_L$-cyteinly-glycine) is the most abundant low-molecular

weight thiol in the cellular redox system and is used for detoxification of ROS. Detoxification of ROS through the glutathione-ascrobate cycle (Noctor 2006) leads to a transient change in the cellular glutathione redox potential. The shift of glutathione redox potential can be sensed by glutaredoxins (GRXs), which transfer electrons between glutathione redox buffer and thiol groups of proteins. These target proteins might be transcription factors altering the expression of stress-related genes or metabolic enzymes. As a result, even minor deviation in glutathione redox potential due increase in oxidation can be exploited for fine tuning of the activity of target proteins (Meyer 2008). Apart from glutathione (GSH/GSSG), there are other redox-couples such as NAD(P)H/NAD(P)$^+$ and reduced/oxidized ascorbate (ASC/DHASC) to detect the changes in cellular reduction potential. The gradually increasing redox potential in the cells leads to an electron flow from NAD(P)H to glutathione to ascorbate. Changes in the ratio between oxidised versus reduced of these redox-couples are detected by the reactive cysteines of redox sensor (target) proteins (Spoel and Loake 2011)(Fig 1.5).

ROS is produced upon infection and lead to a change in cellular redox potential. Also, application of defence-related hormones SA or JA changes the total amount of cellular glutathione as well as the ratio between oxidized and reduced forms of glutathione. NPR1, the SA-response coactivator contains at least 10 cysteine residues and serves as a redox sensor protein. Upon infection, oligomer NPR1 is monomerized through the reduction of two cysteine residues Cys82 and Cys216 by TrxH3 and TrXH5 and conversely, S-nitrosylation of Cys156 facilitates the oligomerization of NPR1(Mou et al. 2003). In addition, a subset of the NPR1-interacting TGA transcription factors is allowed to interact with NPR1 because of the reduction of disulphide bridge in the TGA proteins. Furthermore, S-nitrosylation of SABP3 inhibits its SA-binding and carbonic anhydrase activities, and S-nitrosylation of PrxIIE and Metacaspase 9 (MC9) suppresses $ONOO^-$ detoxification and cysteine protease activities, respectively, both of which may be involved in programmed cell death regulation (Spoel and Loake 2011).

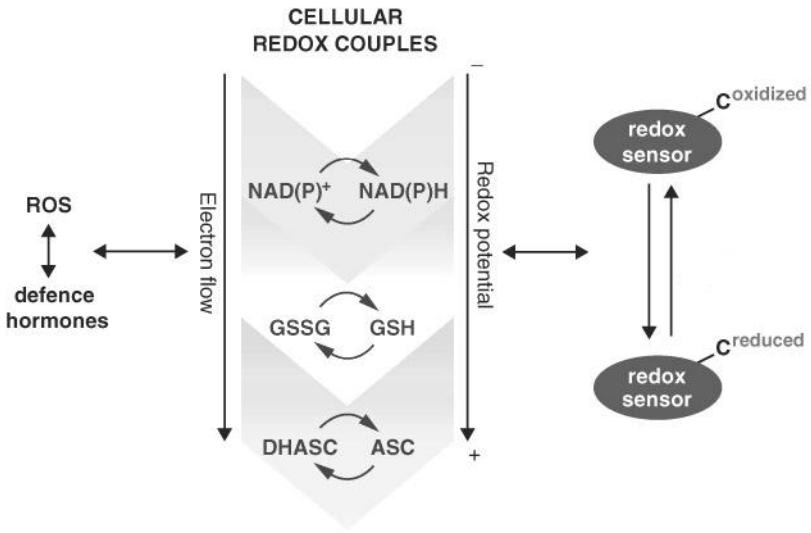

Figure 1.5 Redox coupes detect changes in cellular redox potential.
Upon infection the production of ROS and defence hormones leads to the change in cellular redox potential. The increasing redox potential establishes the flow of electron from NAD(P)H to glutathione to ascorbate. The reactive cysteines of redox sensor proteins detect the changes in the ratio between oxidised and reduced redox couples. *Adapted from Spoel and Loake, 2011.*

1.7 Ubiquitination and Defence

1.7.1 Ubiquitination and 26S Proteasome Degradation

Cellular proteins turn over rapidly and the lysosomal compartment once was considered the principal site of protein degradation by acid-dependent protease. However, the observation that the half-lives of most cellular proteins are insensitive to alkalinisation of the lysosomes, led to the discovery of ubiquitin-proteasome degradation system as the major route to protein degradation. Proteins to be degraded (substrates) are modified with a polypeptide ubiquitin tag (i.e. ubiquitination) and directed to the large (26S) proteolytic complex known as the proteasome. Recent discoveries also revealed that ubiquitin tagging provides a signal to route endocytosed receptors to the lysosomal degradation pathway and by the third major cellular degradative pathway of autophagocytosis in organelles (Clague and Urbe 2010). Three enzymes are required for the ubiquitination of a substrate: ubiquitin-activating enzyme (E1), ubiquitin-conjugating enzyme (E2) and ubiquitin–protein ligase (E3). Ubiquitin's C-terminal Gly is initially activated by linkage to a Cys residue of an E1 in the presence of ATP and then the activated ubiquitin is linked to an E2 through trans(thio)esterification and finally an E3 ligase catalyses the formation of an isopeptide bond between a Lys residue of a substrate and the C-terminal Gly residue of ubiquitin.

In *Arabidopsis*, there are 16 known ubiquitin, whereas 8 in *Saccharomyces cerevisiae* and 38 in humans. All these genes encode precursor proteins and ubiquitin specific proteases are required to release mature ubiquitin. Ubiquitin-activation by E1 is generally not considered to be involved in regulatory step during ubiquitination and there are only two E1 isoforms (UBA1 and UBA2) in *Arabidopsis* (Bachmair et al. 2001). On the other hand, there are 41 predicted E2s. Expression analysis in specific organs or under specific environmental conditions revealed that some E2s and E3s showing unique patterns of expression and may interact specifically (Kraft et al. 2005). In contrast to the numbers of E1 and E2 isoforms, more than 1,300 genes are predicted to encode for E3 components in *Arabidopsis*, accounting for the majority of the proteins involved in the 26S proteasome degradation. E3 ligases can be grouped into three classes based on the presence of the HECT, U-box, or RING domain, in addition RING-type protein can be subdivided into simple and complex E3s. The

simple RING E3s contain both the substrate-binding domain and the E2-binding RING domain in a single protein others act as a homodimer or heterocomplex with another RING protein. The multi-subunit Skp1-Cullin-F-box (SCF)-type ligase is an example of a complex RING E3s, in which the F-box protein is responsible for substrate recognition and the RING-containing protein, Rbx/Roc/Hrt, recruits the E2-ubiquitin intermediate to the SCF complex. The huge number of E3 ligases as well as about 700 predicted *F-box* genes in the *Arabidposis* genome, reveals that E3 ligases play a significant/regulatory role in recognition of proteins for 26S proteasome degradation (Stone et al. 2005).

The ATP-dependent 26S proteasome is comprised of 31 subunits divided into two subcomplexes, the 20S core protease (CP) and 19S regulatory particle (RP), leading to a huge complex of 2MDa. The CP serves as a non-specific protease which is independent of ATP and ubiquitin. It has peptidylglutamyl, trypsin-like, and chymotrypsin-like activities to cleave most peptide bonds. The RP is composed of 17 subunits and associates with either end of the CP. It confers ATP dependence and poly-ubiquitin recognition to the proteasome. Two subcomplexes in RP termed Lid and Base work cooperatively to recognize the substrate-poly-ubiquitin chains, to remove covalently bound ubiquitin moieties, to unfold targeted substrates, to gate pore, and to import substrates into the proteasome (Craig et al. 2009).

1.7.2 E3 Ligases and Defence

Evidence for the role of E1 and E2 enzymes in plant defence is limited. A report has showed that the deletion of 15-bp of *AtUBA1* (*mos5*) suppressed the constitutively activated defence responses of a mutant *npr1-1 constitutive 1* (*snc1*) (Goritschnig et al. 2007). Conversely, there is emerging evidence that E3 ligases have regulatory roles in plant defence signalling. A well-characterized mechanism is the involvement SCF E3 ligase complexes are involved in the regulation of transcription factors of defence responsive genes. For instance, the stability of EIN3-type transcription factors is regulated by F-box proteins EBF1 or EBF2 (EIN3 binding F-box)(Delaure et al. 2008). Furthermore, the JA-mediated defence responses are regulated by JAZ proteins (i.e. JAZ1 and JAZ3). JAZ proteins are recognized by F-box protein COI1, and through the degradation of JAZ, MYC2 transcription factor is released to activate transcription of defence related genes. The F-box protein SON1 is involved in the SA

independent resistance to *Peronospora parasitica*. NPR1 mutant (*nim1-1*) is highly susceptible to *P. parasitica*, and *son1* mutation in *nim1-1* background fully restores *P. parasitica* resistance without the induction of SAR-associated genes (Kim and Delaney 2002). In tomato, F-box ACIF1 is important to trigger HR through effectors Avr9, Avr4, AvrPto, Inf1, and the P50 helicase of tomato mosaic virus (TMV). Silencing of *ACIF1* leads to compromised resistance in many aspects, such as N gene-mediated responses to TMV infection, reduced confluent cell death induced by *Pseudomonas syringae* pv *tabaci* and *R-gene Cf-9*-dependent HR (but not *Cf-9* resistance to *Cladosporium fulvum*). Expression profiling showed that ACIF1 homologs regulate defence responses via MeJA- and ABA-responsive genes. Apart from the SCF complexes, simple RING E3 ligases are involved in defence responses. For instance, *Arabidopsis* RIN2 and RIN3 are RING E3 ligases with 6 transmembrane domains and an ubiquitin-binding CUE domain. RIN2 is predominantly localized to the plasma membrane, as are *R*-gene proteins RPM1 and RPS2. The C-terminal regions of RIN2 and RIN3 interact strongly with an RPM1 N-terminal fragment and weakly with a similar domain from the RPS2 protein. A *rin2/rin3* double mutant showed reduction in RPM1-/RPS2-dependent HR but no alteration of pathogen growth, suggesting RIN2/RIN3 may act on the substrate that regulates RPM1- /RPS2-dependent HR (Kawasaki et al. 2005).

U-box E3 ligases also play an important role in during plant defence. *Arabidopsis* U-box proteins PUB22, PUB23, and PUB24 are negative regulators of PTI in response to several distinct PAMPs. Single, double, and triple *pub22/pub23*/*pub24* mutants exhibited progressive loss of suppression in the flg22-induced ROI burst, and the triple mutant displayed derepression and impaired downregulation of responses triggered by PAMPs (Trujillo et al. 2008). Another U-box protein, tomato ACRE276, is involved in the *R* genes Cf-9 and N for efficient development of HR. Mutation of its orthologue PUC17 in *Arabidopsis* (*puc17*) was shown to have increased susceptibility against avirulent strains of *P. syringae* (Craig et al. 2009). The tobacco U-box protein CMPG1 mediates Cf-9-triggered HR. Recent research has shown that potato resistance protein R3a, strongly suppresses infestin 1 (INF1)-triggered cell death (ICD) through the recognition of effector AVR3a from potato blight pathogen *Phytophthora infestans*. AVR3a is required for virulence and it stabilized CMPG1 during infection to suppress PTI but CMPG1 activity is required for *P. infestans*

during the late, necrotrophic phase of infection. The stability of CMPG1through the interaction with AVR3a is a key event to determine cell death (Bos et al. 2010).

The RAR1-SGT1-SCF complex has merged the relationship between ubiquitination and resistance mediated by multiple *R* genes in monocot and dicot plant species. RAR1 is conserved in all eukaryotes except yeast and was initially implicated in disease resistance against powdery mildew in barley. RAR1 interacts with SGT1 (SUPRESSOR OF THE G2 ALLELE OF SKP1) through the C-terminal CS motif. SGT1 regulates SCF E3 ligase complexes with which it associates through the SKP1 subunit in yeast, *Arabidopsis*, barley, and *Nicotiana benthamiana* (Azevedo et al. 2002). F-box-mediated auxin- and JA-dependent signalling is disrupted in *Arabidopsis sgt1b* mutants and SGT1 is also required for *R*-gene mediated resistance against a variety of pathogens, suggesting that SGT1 is a key component of multiple SCF-regulated pathways (Craig et al. 2009). Furthermore, silencing *SKP1* and subunits of the COP9 signalosome (*CSN*) in *N. benthamiana*, resulted in the loss of N-mediated TMV resistance. It is also proposed that RAR1 and SGT1 function as co-chaperones with HSP90 in close proximity to R proteins, possibly to assist in the maintenance of conformation-sensitive signalling states during R protein activation (Shirasu and Schulze-Lefert 2003).

1.7.3 S-Nitrosylation of E3 Ligases

Studies of redox regulation in ubiquitination in plants are rare, and to date, no reports of E3 ligase S-nitrosylation are published. Conversely, in mammals, there is emerging evidence that S-nitrosylation is a key regulatory mechanism in ubiquitination especially during nitrosative stress. Most neurodegenerative disorders are related to excess of reactive nitrogen and oxygen species (RNS/ROS) in neuronal cells, which can lead to cell injury and death. In general, accumulation of aberrant proteins such as misfolded and aggregated proteins in neuronal cell affect neuronal connectivity and plasticity and trigger cell death signalling pathways. For example, α-synuclein and synphilin-1 are involved in Parkinson's disease (PD), and β-amyloid (Aβ) and tau are involved in Alzheimer's disease (AD). In unstressed and healthy neurons, these aberrant proteins do not accumulate due to removal through ubiquitin-mediated degradation. Extreme nitrosative/oxidative stress can facilitate protein misfolding and aggregation. Recent studies have implied that NO-related species may significantly

contribute of protein misfolding through protein S-nitrosylation under degenerative conditions (Gu et al. 2010). In the case of PD, mutation in an E3 ligase, parkin, can simulate the sporadic phenotype, which is believed to be induced by oxidative/nitrosative stress to the ER and ubiquitin–proteasome systems (UPS). Nitrosative stress leads to S-nitrosylation of parkin and both *in vitro* and *in vivo*, and interestingly a dramatic increase was followed by a decrease in the parkin E3 ligase activity (Yao et al. 2004). The initial increase in activity leads to enhanced ubiquitination of parkin substrates. The subsequent decrease in parkin activity may allow misfolded proteins to accumulate, leading to neuronal cell death and PD (Nakamura and Lipton 2007). Another neuronal neurodegenerative disorders associated RING E3 ligase, XIAP (X-linked inhibitor of apoptosis), is regarded as an important regulator of apoptosis through the association with active caspases and repression of their catalytic activity. XIAP interacts with active caspases-3/-7/-9 in the cytosol and is thought to be the most potent endogenous caspase inhibitor. It has been reported that S-nitrosylation of the RING domain of XIAP decreases its E3 ubiquitin ligase activity both *in vitro* and in intact cells. In addition, SNO-XIAP formation is found in brains of patients with Alzheimer's, Parkinson's, and Huntington's diseases, implicating S-nitrosylation in the etiology of neuronal damage. An unexpected finding associated to XIAP is the transfer of NO groups (transnitrosylation) from SNO-caspase to XIAP to form SNO-XIAP (Nakamura et al. 2010). These findings provide insights that S-nitrosylation of E3 ligases is an important regulatory mechanism to protect against nitrosative stress in neuronal cells (Fig 1.6).

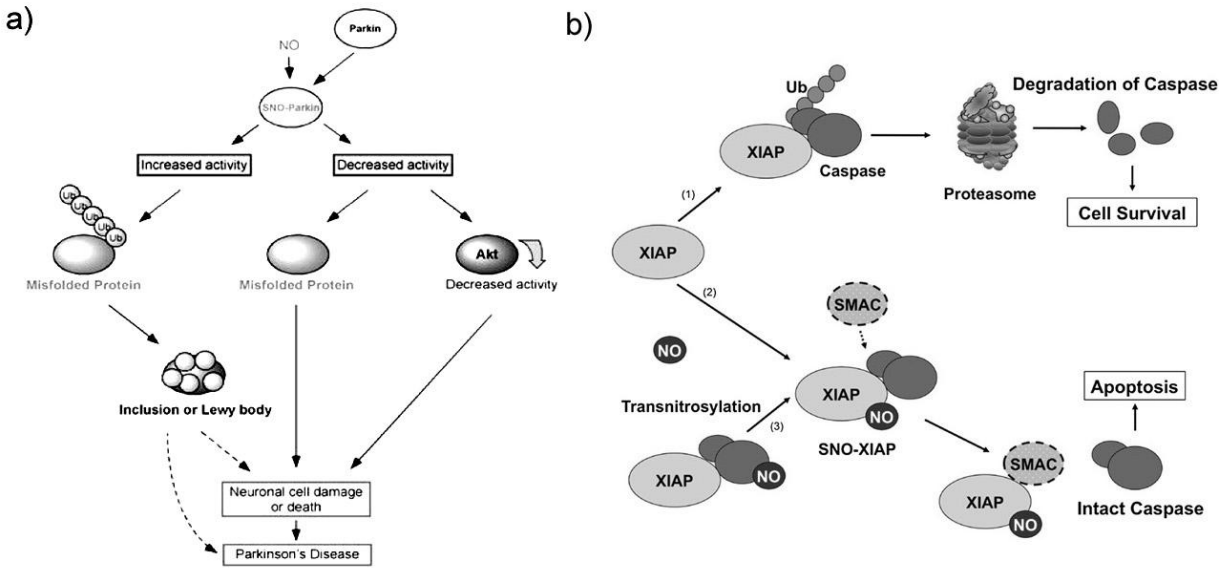

Figure 1.6 Two examples illustrate the regulation of E3 ligase activity through S-nitrosylation in neuronal cells.
a) S-nitrosylation increases parkin activity at the early stage of nitrosative stress, while later on, decreased activity leads to the accumulation of aberrant proteins and neuronal cell damage. **b)** Under normal conditions, caspases are efficiently blocked and guided to proteasomal degradation by XIAP. However under nitrosative stress, NO inactivates the XIAP E3 ligase activity via S-nitrosylation, thus stabilizing caspases and sensitizing neurons to apoptotic stimuli. *Adapted from Nakamura et al., 2007 and Nakamura et al., 2010.*

1.8 Aim of the study

It is now well studied that GSNOR is important in regulation of cellular SNO levels. Loss of function *atgsnor1-3* mutant has shown compromised growth and disease resistant (Feechan et al. 2005). However, the signalling pathways between S-nitrosylation and the consequential phenotype of *atgsnor1-3* remain largely unknown.

Arabidopsis *RAP1* (*Redox Associated Protein 1*) was identified from microarray analysis which shows related expression profile with the *atgsnor1-3* mutant (Chapter 3.2). Two conserved domains: RING and Ankyrin are found in the amino acid sequence of RAP1. RING domain is known to possess E3 protein ligase activity in the ubiquitin-dependent degradation pathway, while ankyrin domain mediates the attachment of integral membrane protein to the membrane. A previous report shows that RAP1 lacks of E3 ligase activity(Stone et al. 2005) . Therefore, one of the main targets of this project is to demonstrate the molecular function of RAP1 (Chapter 4.3). If RAP1 contains the E3 ligase activity whether the activity can be regulated by S-nitrosylation (Chapter 4.4) and where is the S-nitrosylation site in RAP1(Chapter 4.5).

The other target of this project is to identify the roles of *RAP1* in Arabidopsis, which is achieved by the study of *RAP1* knockout mutants and *RAP1* overexpressing line. The *atgsnor1-3* mutant has a phenotype of retardation in growth and development, compromised disease resistant and enhanced resistant to methyl viologen. It is speculated that the *RAP1* mutants also show the similar phenotype. Therefore, the *RAP1* mutants will be analysed in three main aspects: the developmental phenotype (Chapter 6.1), disease-related phenotype (Chapter 6.2) and resistance to methyl viologen (Chapter 6.3).

Through this study, it is hopefully to show that *RAP1* is involved in redox-mediated signalling pathway in Arabidopsis, which could also be a clue to identify novel redox-related regulators in other plant species.

Chapter 2

2 Methods and materials

2.1 *Arabidopsis* Seeds and Growth Conditions

Arabidopsis thaliana (*Arabidopsis*) ecotype Columbia (Col-0) was used. Seeds were soaked in water for 2 days at 4^{o}C and were placed on potting medium consisting of peat moss, vermiculite and sand (4:1:1). And then were placed in a growth room and grown in long days (16 hours light, 8 hours night) with light intensity 110µmolm^{-2}s^{-1} at 20^{o}C. Table 2.1 lists the *Arabidopsis* transgenic lines and mutant strains and their phenotypes.

Table 2.1 *Arabidopsis* transgenic lines and mutant strains.

Strains	Phenotype	Reference	Source
Col-0	wild-type		NASC
atgsnor1-3	Loss of apical dominance, Resistance to methyl viologen		Gabi-Kat
rap1	Semi-resistance to methyl viologen	This study	NASC
rap2	Semi-resistance to methyl viologen	This study	NASC
rap1/rap2	Reduced resistance to *Pst*DC3000	This study	Yu & Loake
35S::*RAP1*	Enhanced root branching	This study	Hong & Loake
35S::RAP1 -ΔRING	Dwarf and loss of apical dominance	This study	Hong & Loake
pAgrikola-*RAP1*-RNAi	Enhanced resistance to methyl viologen	This study	Hong & Loake

2.2 Cotyledons Development Assay with Methyl Viologen

Arabidopsis seeds were surfaced steriled in 10% (v/v) bleach with a drop of Triton X-100 for 20 minutes. The seeds were washed at least 5 times with sterile water and placed on ½ MS agar plates with or without methyl viologen (1 µM final concentration) and incubated in long days at 20^{o}C for 5 days.

2.3 Inoculation of *Pseudomonas syringae* Pv Tomato DC3000 (*Avrb*) and Trypan Blue Staining

Pseudomonas syringae pv tomato (*Pst*) DC3000 (*avrB*) was grown in LB medium supplemented with $MgCl_2$ (6 mM final concentration), 50 mgL^{-1} rifampicin and 50 mgL^{-1} kanamycin at 30^{o}C at 250 rpm. Cells were harvested at cell density around

OD_{600}=0.2 by centrifugation at 3000 g for 10 minutes. Cell pellet was washed twice and re-suspended in 10mM $MgCl_2$ and the cell density were further adjusted to OD_{600}= 0.002. Four week *Arabidopsis* plants were infiltrated with *Pst* DC3000 (*avrB*) on the abaxial side of the leave (half leaf) using a 1mL syringe.

Leaves after 1 day of inoculation with *Pst* DC3000 (*avrB*) were cut out from the plant and soaked in trypan blue solution (2.5 gL^{-1} trypan blue, 25% (w/v) lactic acid, 23% (w/v) water saturated phenol, 25% (w/v) glycerol and water) and boiled at 100^{o}C for 2 minutes. After cool down, the trypan blue solution was replaced by saturated choral hydrate solution (1 kgL^{-1}). After 24 hours, the leaves were taken out and mounted onto a microscopic slide.

2.4 *Pseudomonas syringae* pv Tomato DC3000 Resistance Assay

Pst DC3000 was grown in LB medium supplemented with $MgCl_2$ (6mM final concentration) and 50mgL^{-1} rifampicin. Four week old plants were infected with a *Pst* DC3000 suspension (OD_{600}= 0.0002) in 10mM on the abaxial side of the leaf using a 1ml syringe. Three leaves per plant and three plants per line were infected. Leave were harvested at 3 day and 5 day after inoculation. Three leaf discs (0.5cm^2) from each plant were collected and ground in 500µL 6mM $MgCl_2$ solution in a 1.5mL eppendorf tube. Serial dilutions of bacterial suspension were made and 100 µL of each dilution was spread onto LB plates containing $MgCl_2$ (6mM final concentration) and 50mgL^{-1} rifampicin. The plates were incubated for 2 days at 30^{o}C and the number of bacterial colonies for each sample were counted and recorded.

2.5 Inoculation of *Erysiphe cichoracearum*

Arabidopsis powdery mildew, *Erysiphe cichoracearum* (*E. c.*) was maintained on Col-0 plants in the greenhouse. Leaves with infected *E.c.* were cut, and spores were collected from the infected leaves by a cotton bud. Spores were transferred on the healthy leaves via rubbing the cotton bud with spores from two infected leaves. At least six leaves were inoculated per plant line. The inoculated plants were left in the greenhouse (~25^{o}C) and leaves were collected for either trypan blue staining (3 day post-inoculation) or protein extraction (10 day post-incoulation).

2.6 Extraction of Genomic DNA from *Arabidopsis*

A leaf of *Arabidopsis* plant was ground in 300µL of CTAB buffer in a 1.5mL eppendorf tube and incubated at 65^{o}C for 20 minutes. The plant extract was mixed with 300µL of chloroform by vortex vigorously and centrifuged at 15,000 rpm for 5 minutes. The upper aqueous layer was transferred to a new eppendorf with 300µL of isopropanol followed by centrifugation at 15,000 rpm for 5 minutes. The supernatant was removed and the pellet was washed by 1mL 70% ethanol. The ethanol was then removed and the pellet was air-dried and dissolved in 50 µL of water.

2.7 RNA Extraction and Reverse-Transcription (RT)

Total RNA was extracted from 4 weeks old plant using TRI reagent (Sigma) according to the manufacturer's protocol. Ominiscript RT Kit (Qiagen) was used for first-strand cDNA synthesis, which extracted total RNA (1µg) were mixed with 1x Buffer RT, oligo-dT (20 pmole), dNTP mix (100 nmole),RNase inhibitor (10 units), Ominiscript Reverse Transcriptase (4 units) and RNase-free water to 20µL in total. The reaction mix was incubated at 37^{o}C for 60 minutes. The reaction product was stored at -20^{o}C or immediately used in a PCR reaction.

2.8 Polymerase Chain Reaction (PCR) Based Methods

2.8.1 RT-PCR

RT-PCR was carried out in the following condition: 1μL of RT-product (cDNA), dNTP mix (5 nmole), forward and reverse primer (5 pmole each) (

Table 2.2), 1X Buffer, *Taq* polymerase (1 unit) (Promega) at cycle 95^{o}C (30s), 55^{o}C (30s) and 72^{o}C (2 min) for 25 cycles. Reaction product (5 μL) was taken out to analyze in agarose gel electrophoresis.

Table 2.2 Primers used in RT-PCR.

Gene	Forward	Reverse	Product size
GSNOR	GAGGTTCGGATCAAGATCCT	GTTGGAACGGACGAGTTGAT	826bp
RAP1	GTATCAAATCACTTCACCATGAAG GAGCA	CATTGGCTGTGGAACTCCTTT	767bp
RAP2.1	GGATGAAGAAACGAAGGGTCTG	AGGATATAGATAATCCCATGTTG TTGTTG	752bp
RAP2.2	GATAACTCCACAAAAACACGTCTT	AGGATATAGATAATCCCATGTTG TTGTTG	705bp
ACTIN1	CATCAGGAAGGACTTGTACGG	GATGGACCTGACTCGTCATAC	240bp

2.8.2 Genotyping PCR

Genotyping PCR was carried out in the following condition: 1μL genomic DNA, dNTP mix (5 nmole), forward and reverse primer (5 pmole each) (Table 2.3), 1X Buffer, *Taq* polymerase (1 unit) (Promega) at cycle 95^{o}C (30s), 52^{o}C (30s) and 72^{o}C (2 min) for 35 cycles. Reaction product (5 μL) was taken out to analyze in agarose gel electrophoresis.

Table 2.3 Primers used in genotyping.

Gene	Forward	Reverse	Product size
GSNOR	GGATCGATAAGGTTCCCAGTCTAG CTACGTA	CAGCAGCCTCATGACCTAGAATA CAAGGAA	939bp
RAP1	GTATCAAATCACTTCACCATGAAG GAGCA	CATTGGCTGTGGAACTCCTTT	1555bp
RAP2	GGATGAAGAAACGAAGGGTCTG	AGGATATAGATAATCCCATGTTG TTGTTG	1038bp
ACTIN1	CATCAGGAAGGACTTGTACGG	GATGGACCTGACTCGTCATAC	351bp
RAP1-TDNA	GCCTTTTAGAAGGATAAAAGCCTG CTCC	CATGGACTTTGGACTTCTGGAGT CATCAATAAT	~1200bp
RAP2-TDNA	GGATGAAGAAACGAAGGGTCTG	GCGTGGACCGCTTGCTGCAACT	~550bp

2.8.3 PCR Reaction for Protein Expression

PCR reactions were carried out in the following conditions: 1μL of cDNA, dNTP mix (5 nmole), forward and reverse primer (5 pmole each) (Table 2.4), 1X Buffer, *Pfu* polymerase (1 unit) (Promega) at cycle 95^{o}C (30s), 55^{o}C (30s) and 72^{o}C (2 min) for 35 cycles. *Taq* polymerase (0.5 unit) was added after the PCR reaction and incubated at 72^{o}C for 10 minutes to add a 3'A overhang for TA cloning purpose. The desired PCR product was separated in agarose gel electrophoresis and purified in distilled water by a gel extraction kit (Qiagen).

The purified PCR product was cloned into pGEM-T Easy (Promega) for amplification and sequencing. Confirmed DNA fragment was then subcloned into an expression vector pGEX4T-1(GE Healthcare) through the designed restriction sites and transformed into *E. coli* BL21 for expression purpose.

Table 2.4 Primers used in protein expression.

Gene	Forward	Reverse	Product size
CIP8	GGATCCATGTCCGATGCTCCGTC GTCTTCCCCG	CTCGAGTCAGTAACGAGAAGTTG AAGAAGAAGAAGAAG	1005bp
UBC1	GGATCCATGTCGACGCCAGCAAG GAAGAGGTT	CTCGAGCTAGTCAGCAGTCCAGC TTTGCTCAA	459bp
RAP1	GGATCCATGGGGCAACAACAAT CACAGTCCA	GTCGACTCAAACATGATATAGCT TAATGACCTGATC	1131bp
RAP2.1	GGATCCATGGGACAACAGCAAT CAAAAGGG	CTCGAGTCAGACACGGTACAGCT TAATAACCTGATC	1317bp
RAP1-RING	AAAAAGGATCCAAAGGAGTTCC ACAGCCAATG	AAAAACTCGAGTCAAACATGAT ATAGCTTAATGACCTG	315bp

2.8.4 Site-Directed Mutagenesis

Codon replacement in expression vectors was carried out by QuikChange® II XL Site-Directed Mutagenesis Kit (Stratagene). Two complimentary primers containing the desired mutation were synthesized (see Table 2.5) and used in the PCR reaction in the following condition: 10× reaction buffer (5 μL), expression vector (pGEX-RAP1 or pGEX-RAP1-RING)(10 ng), complimentary primers (125 ng each), dNTP mix(1 μL), QuikSolution reagent (3 μL), *Pfu*Ultra HF DNA polymerase (2.5 U) and distilled water to a final volume of 50 μL. The cycling parameter was set as follow: 95^{o}C (50 s), 52^{o}C (50 s) and 68^{o}C (5min) for 18 cycles. The parental plasmid was digested by *Dpn* I (10 U) at 37^{o}C for 1 hour and the *Dpn* I-treated DNA was transformed into supplied XL10-Gold ultracompetent cells. The mutated expression plasmid was purified and the mutated site was confirmed by DNA sequencing.

Table 2.5 Primers used in site-directed mutagenesis.

Gene	Forward	Reverse
C325H	GAAGATGGACTGCATGTGATTTGTGTG	CACACAAATCACATGCAGTCCATCTTC
C328H	CTGTGTGTGATTCATGTGGATGCACCA	TGGTGCATCCACATGAATCACACACAG
C337H	TCTGAAGCAGTGCATGTGCCGTGTGGA	TCCACACGGCACATGCACTGCTTCAGA
C340H	GTGTGTGTGCCGCATGGACATGTCGCC	GGCGACATGTCCATGCGGCACACACAC

2.9 Expression and Purification of Recombinant Proteins in *E. coli* BL21

E. coli BL21 cells harbouring expression plasmid were grown in 5mL LB medium supplemented with ampicillin (50 mgL^{-1}) at 37^{o}C for overnight. The overnight culture was subcultured into 100 mL LB medium with ampicillin (50 mgL^{-1}) at 1:100 ratio in 500 mL conical flask and incubated at 37^{o}C, 250 rpm until cell density OD_{600}=0.5-0.6. The culture was chilled on ice for 10 min and IPTG was added to the cell culture to a final concentration of 0.1 mM and further incubated for 8 hours. The cells were harvested by centrifugation at 3000 g for 20 minutes, washed twice with phosphate-buffer saline (PBS) and resuspended in 1mL PBS or stored at –80^{o}C without PBS.

Lysozyme (final 2 mg mL^{-1}), protease-inhibitor cocktail (Roche) were added to the cells that were resuspended in 1 mL PBS and incubated on ice for 30 minutes. Sonication was applied at 10 times at 10s intervals and immediately centrifuged at 20,000 g at 4^{o}C for 20 minutes. The supernatant was mixed with 100 μL of PBS washed gluthathione-sepharose 4B matrix (GE Healthcare) and incubated at 4^{o}C (with shaking) for 30 minutes. The protein-bound matrix was washed 4 times with ice-cold PBS and the fusion proteins were eluted in elution buffer (100 μL of 50mM TrisCl, 100mM NaCl, 10mM glutathione, pH 8.0). The fusion protein was analyzed in a SDS-PAGE gel and mass spectrometry.

The GST-tag of the fusion protein was removed by application of thrombin protease (1U)(GE Healthcare) into 100 μL of protein solution at room temperature for 16 hours. Gluthathione-sepharose 4B matrix (30 μL) was added and incubated at room temperature at room temperature for 1 hour with shaking. The GST-tag bound matrix was removed by centrifugation at 13,000 g for 5 minutes. The cleaved protein in supernatant was analyzed in a SDS-PAGE gel.

2.10 In-Gel Digestion and Mass Spectrometry Analysis

Protein band with expected size was excised from a SDS-PAGE gel and was shrunk in methanol (200 μL) for 10 minutes and the methanol was replaced by ammonium bicarbonate (ABC) solution (50mM) and incubated for 10 minutes. This procedure (methanol/ABC exchange) was repeated at least 3 times and the gel was finally shrunk in methanol and dried in a laminar flow hood. The dried gel was then soaked in trypsin solution (0.4 μg in 20 μL ABC solution) at 37^{o}C for 16 hours. The solution

with digested peptides was transferred to a new eppendorf and the remaining peptides in the gel were further extracted by 0.5% formic acid and 50% methanol. The peptide solution was dried completely in a speedvac concentrator. Capillary-HPLC-MSMS analysis was performed on an on-line system consisting of a micro-pump (1200 binary HPLC system, Agilent, UK) coupled to a hybrid LTQ-Orbitrap XL instrument (Thermo-Fisher, UK). Samples were reconstituted in 10 µl loading buffer before injection, and analyzed on a 1 hour gradient for data dependent analysis. MSMS data were searched using MASCOT Versions 2.2 and 2.3 (Matrix Science Ltd, UK).

2.11 *In vitro* S-Nitrosylation

The original buffer in the expressed proteins (Chapter 2.8) was exchanged to 100 µL of HEN buffer (250 mM HEPES-NaOH pH7.1, 1m EDTA and 0.1 mM neocuproine) by a Zeba spin desalting column (Thermo Scientific). NO donor (GSNO or CysNO) or GSH (control) was added to the protein solution (final concentration from 0.1 mM to 1 mM) and incubated in dark for 20 minutes at room temperature. The unreacted NO donor was removed by HEN-pretreated Zeba spin desalting column. The NO donor treated protein was then ready for a biotin-switch assay or an E3 ligase activity assay.

2.12 Biotin-Switch Assay

Protein solution (100 µL) was mixed thoroughly with 300 µL of blocking solution (HEN buffer, 2.5% SDS and 20 mM S-methylmethanethiosulfonate (MMTS)) in dark at 50^{o}C for 20 minutes. Ice-cold acetone (800 µL) was then added and incubated at -20^{o}C for 1 hour. The protein was then pelleted by centrifugation (10,000 x g, 10 minutes), air-dried and resuspended in 50 µL HEN-S buffer (1% SDS in HEN buffer). The protein solution was incubated with 13 µL of Biotin-HPDP (N-[6-(Biotinamido) hexyl]-3'-(2'-pyridyldithio)-propionamide) (5 mM in DMSO) and 3 µL of sodium ascorbate (100mM) for 1 hour at room temperature. Biotinlyated protein was detected by anti-biotin antibody or pulled down by streptavidin.

Pulldown of biotinylated proteins by streptavidin was performed as previously described (Forrester et al. 2009). The buffer solution in protein samples were exchanged to neutralization buffer (20mM Hepes pH7.7, 100 mM NaCl, 1 mM EDTA and 0.5% Triton) by a Zeba desalting column. Streptavidin agarose (Fluka) was added

to the protein samples in 1:10 ratio and incubated at 4^{o}C for 12 hours. Avidin beads were collected by centrifugation at 200 g for 10 seconds, followed by washing with wash buffer (neutralization buffer containing 600 mM NaCl) for four times. The washed protein was resuspended in non-reducing protein loading buffer and boiled at 95^{o}C for 5 minutes. The boiled protein solution was analyzed in a SDS-PAGE or a western blot (detection by anti-GST or anti-biotin).

2.13 Protein Extraction from *Arabidopsis*

Tissue of *Arabidopsis* (100mg) was ground in liquid nitrogen into fine powder. Ice-cold extraction buffer (1x PBS, 1mM PMSF and 5mM DTT) was added to the leaf powder and vortex vigorously for 1 minutes. Samples were centrifuged for 20 minutes at 13,000 x g in 4^{o}C and supernatant was collected. The protein concentration was determined by Bradford analysis (Bradford 1976).

2.14 SDS-PAGE and Western Blot Analysis

SDS-PAGE and western blot analysis were carried out as described by Sambrook & Russell (Molecular Cloning, 3rd edition, CSHL Press) with following adjustments. Proteins were separated in a 10% SDS-PAGE (without SDS for in-gel activity assay) at 120V for 1 hour. Blotting was carried out in a tank transfer using the Mini Trans-Blot cell (Bio-Rad) in transfer buffer (25mM Tris, 200mM glycine and 20% Methanol) at 80^{o}V, 4^{o}C for 1 hour. Proteins were then transferred onto a PVDF membrane (GE Healthcare). The membrane was then blocked with 5% (w/v) of skimmed-milk powder in phosphate-buffered saline (PBS) and 0.1% Tween (PBS-T). The blocked membrane was incubated with antibody as described (Table 2.6) and followed by 3 times washing with PBS-T. Protein was detected by an ECL Plus Western Blotting Detection System (GE Healthcare). The blot was incubated with 1 mL of solution A and 25 μL of solution B for 1 minute. The illuminant signal was detected by exposure of the blot to an X-ray film (Thermo Scientific).

Table 2.6 Western blot condition for different targets.

Target	1^{o} antibody	dilution	2^{o} antibody	dilution
GST	Mouse monoclonal anti-GST HRP-conjugated antibody (GE Healthcare)	1:5000	-	-
Biotin	Monoclonal anti-biotin HRP-conjugated antibody (Cell Signaling Technology)	1:5000	-	-
RAP1	Rabbit polyclonal anti-RAP1 antiserum	1:250	Goat monoclonal anti-rabbit IgG HRP-conjugated antibody (Promega)	1:5000
AtGSNOR	Rabbit polyclonal anti-AtGSNOR antiserum (Agrisera)	1:1000	Goat monoclonal anti-rabbit IgG HRP-conjugated antibody (Promega)	1:5000
Ubiqutin	Mouse monoclonal anti-ubiquitin antibody (Sigma-Aldrich)	1:5000	Monoclonal anti-mouse IgG HRP-conjugated antibody (Cell Signaling Technology)	1:5000

2.15 E3 Ligase Activity Assay

E3 ligase activity assay was carried out as described (Kawasaki et al. 2005; Stone et al. 2005) with modifications. Expressed recombinant E3 ligase (100 ng) was co-incubated with 50 ng of recombinant human E1 enzyme (Sigma-Aldrich), 5 μL of E2 enzyme extract (AtUBC1) (This study) and 2 μg of ubiquitin (Sigma-Aldrich) in a reaction mixture containing 50mM TrisCl, 10mM $MgCl_2$ and 0.05mM $ZnSO_4$. The reaction mixture was incubated at 30^{o}C for 2 hours and stopped by adding of 4X SDS loading buffer. The proteins in the reaction were separated by a SDS-PAGE and transferred to a PVDF membrane by tank transfer system. Polymerization of ubiquitin was detected by a western blot using anti-ubiquitin antibody as the primary antibody and HRP-conjugated anti-mouse IgG (Cell Signaling Technology) as the secondary antibody.

2.16 GSNOR In-Gel Enzyme Activity Assay

GSNOR activity was detected as previously reported (Barroso et al. 2006). Extracted proteins from *Arabidopsis* were separated in a native polyacrylamide gel 7.5% (w/v) at 4^{o}C. The gel was incubated in 0.1 M sodium phosphate buffer (pH 7.4) containing 2 mM NADH for 15 minutes at 4^{o}C. The gel was covered with filter paper soaked in 3 mM GSNO (freshly prepared) for 10 minutes. The filter paper was removed and the gel was illuminated under ultraviolet light in an UV illuminator. The GSNOR activity was detected referring to the disappearance of the NADH fluorescence.

Chapter 3

3 Identification of *RAP1* in *Arabidopsis*

3.1 Introduction

S-nitrosoglutathione reductase (GSNOR) catalyses the conversion of S-nitrosoglutathione (GSNO) into oxidized glutathione (GSSG). GSNOR is also the key enzyme in regulation of S-nitrosylation in *Arabidopsis* and previously, a loss-of-function mutant *atgsnor1-3* was isolated which shows distinct phenotypes such as slow growth, loss of apical dominance, reduced fertility and increased susceptibility to pathogen (Feechan et al. 2005). Compared to WT plants, *atgsnor1-3* plants display higher SNO levels upon pathogen infection, suggesting SNOs produced during infection are not effectively removed due to the loss of GSNOR. Excess NO or GSNO shifts the equilibrium towards S-nitrosylation of a variety of proteins, thereby leading to changes of protein function and structure. Activities of certain proteins may be altered due to S-nitrosylation, these proteins could be important regulators of plant development, resistance to abiotic stress as well as defence against pathogens. The cross-talk between SA and GSNO has been described in some reports, for instance, both WT and *atgsnor1-3* plants were able to respond to SA treatment to trigger *PR-1* expression in 6 hours, however *PR-1* mRNA transcript accumulation was substantially reduced in *atgsnor1-3* plants. Thus, the SA-signalling pathway is affected due to accumulation of GSNO (Feechan et al. 2005). Further, the SA binding protein 3 (SABP3) in *Arabidopsis* has been shown to be S-nitrosylated, and *atsabp3* mutants were found to be more susceptible to bacterial infection (Wang et al. 2009c), revealing that S-NO/redox-regulation is actively involved in the control of defence responses. However, the precise regulatory mechanism (such as NO perception, signal relaying and transcription activation) against nitrosative stress remains unclear, and some uncharacterized genes may be specifically involved in pathogen responses under nitrosative stress.

The availability of *atgsnor1-3* mutants has provided a convenient tool to study the role of NO/GSNO in plant defence. Previously, a microarray analysis was carried out to explore differential gene expression upon *Pst*DC3000(*avrB*) treatment of plant lines with different genetic backgrounds (i.e. Col-0, *atgsnor1-1*, *atgsnor1-3* and *sid2*).

Through the analysis of the microarray data, pathogen-induced genes that are directly regulated by SNO levels could be identified by eliminating genes that were controlled by SA accumulation.

S-nitrosylation is known to regulate both SA signalling and accumulation (Feechan et al., 2005). Therefore, pathogen-induced genes differentially expressed in *sid2* mutants, which are defective in SA accumulation, were removed from the analysis. Following the analysis, one gene, *At4g14365*, was strikingly differentially regulated, consequently this gene was selected for further study. In this chapter, the rationale for choosing *At4g14365* will be explained. Furthermore, unpublished works from a previous lab member, Jeum-kyu Hong, has been included in this chapter to provide supporting data in addition to the presented *in silico* analysis.

3.2 The *RAP1* (*REDOX-ASSOCIATED PROTEIN 1*) Gene in *Arabidopsis*

Identification of *At4g14365* was based on the Affymetrix microarray data through the analysis of the transcript levels of genes in *Arabidopsis* genome upon avirulent pathogen *Pst*DC3000(*avrB*) inoculation. Microarray data for four plant lines; wild-type Columbia (WT, Col-0), the *GSNOR* overexpression mutant (*atgsnor1-1*), the *GSNOR* knock out mutant (*atgsnor1-3*) and the SA-biosynthesis impaired mutant (*sid2*) were analysed. *GSNOR* transcripts were accumulated in *atgsnor1-1* plants due to the T-DNA insertion in the *GSNOR* promoter (probably disrupting the repressor binding site), whereas no *GSNOR* transcripts was detected in *atgsnor1-3* plants as T-DNA was inserted in the exon just after the start codon (Feechan et al. 2005). The difference of the *GSNOR* transcript levels between *atgsnor1-1* and *atgsnor1-3* plants results in the variation in the SNO levels especially upon pathogen infection. Upon pathogen infection, excessive SNOs are normally removed by GSNOR, however loss of the *GSNOR* gene (i.e. *atgsnor1-3*) leads to the accumulation of GSNO and compromises defence responses. The SA-induction-deficient *sid2* has a mutation to a gene encoding isochorismate synthase (ICS1) which is an important enzyme in SA biosynthesis. The level of SA after infection in *sid2* mutants is only 5–10% of the wild-type levels and disease resistance is also compromised (Abreu and Munne-Bosch 2009).

The microarray analysis included 4 sets of experiments (Col-0, *atgsnor1-1*, *atgsnor1-3* and *sid2*) with duplication. Each set of the experiment detected the transcripts of a plant line during uninduced condition and pathogen-induced condition (6 hour *Pst*DC3000(*avrB*) treatment). Among the up-regulated genes upon *Pst*DC3000(*avrB*) treatment, only a small proportion of them were able to show the same extent of induction level in *sid2* mutant. Genes that showed reduced differential expression in the *sid2* mutant were regarded as SA-dependent, while genes that were still differentially regulated regardless of SA could be controlled by other signalling pathways. Table 3.1 shows genes that were sorted according to the fold induction in the *sid2* background. Expression of a gene with unknown function (*At1g19020*) increased dramatically both in *atgsnor1-3* (136.2 fold) and *sid2* (80.1 fold), while a putative aminotransferase (*At2g24850*) shows 38.9 fold induction in *atgsnor1-3* and 72.7 fold in *sid2*, a plastocyanin-like domain-containing protein (*At5g20230*) shows 96.8 fold in *atgsnor1-3* and 59.5 fold in *sid2* and a heat shock cognate 70 kDa protein 2 (HSC70-2) (HSP70-2)(*At5g02490*) was upregulated 99.2 fold in *atgsnor1-3* and 44.5 fold in *sid2*. The last candidate among the top five is a zinc finger (C3HC4-type RING finger) family protein / ankyrin repeat family protein (*A4g14365*) which shows increased expression of 80.6 fold in *atgsnor1-3* and 34.8 fold the in *sid2*. This gene is named *RAP1 (REDOX-ASSOCIATED PROTEIN 1)* in this study. The five candidates showed significant up-regulated gene expression in the *sid2* mutant, suggesting the regulation of expression is fully/partially independent of SA. Coincidently, the basal expression of these genes in *atgsnor1-3* mutant (when comparing to WT) was highly suppressed, for instance, *RAP1* basal expression was 25.8 fold lower in *atgsnor1-3* mutant than in wildtype.

Due to this interesting expression pattern, the *RAP1* gene was selected for further analysis. The full genomic sequence of *RAP1* is 2302 bp including 9 introns to give a full cDNA of 1407 bp after splicing. The coding sequence of *RAP1* is 1131 bp that encoded a peptide with 376 amino acids. Two conserved domains are found in RAP1, which are ankyrin repeats in the N-terminus and a RING domain in the C-terminus (Figure 3.1a). A paralog of *RAP1* is also presented in the *Arabidopsis* genome which is named *RAP2* in this study (*At3g23280*). The full genomic sequence of *RAP2* is 3079 bp which gives two splicing variants *RAP2.1* and *RAP2.2* with coding sequence of 1389 bp (462aa) and 1317 bp (439bp) respectively. Both conserved domains of

RAP1 are found in RAP2, and significant sequence similarities are located at the N-terminal and C-terminal ends.

Table 3.1 shows the averaged raw microarray hybridisation signal values for comparing the expression of *Rap1*, *Rap2* and *Actin1*. The expression behaviour of *RAP2* was very different from *RAP1*. In this context, *RAP2* was constitutively expressed with similar levels in WT, *atgsnor1-1*, *atgsnor1-3* and *sid2* plants and in addition, *RAP2* was not induced by *Pst*DC3000(*avrB*) upon 6 hour treatment. On the other hand, *RAP1* was highly induced in all the tested plants with the similar maximum level of induction across WT, *atgsnor1-1* and *sid2*. The induced level was lower in *atgsnor1-3* plants, although the fold of induction was still the highest at 30 fold. It is also worth noting that the basal expression level of *RAP1* in *sid2* was also suppressed, while the induced level was similar to that in WT and *atgsnor1-1* plants.

Table 3.1 Normalised microarray hybridisation signal of selected candidates that displays strong transcript induction upon challenge with *Pst*DC3000 (*avrB*).

Data is sorted in descending order by the ratio of sid2 6hr/sid2 0hr.

GENE NAME	DESCRIPTION	Col-0 0h average	Col-0 6h average	ratio	*atgsnor 1-1* 0h average	*atgsnor1-1* 6h average	ratio	*atgsnor1-3* 0h average	*atgsnor1-3* 6h average	ratio	*sid2* 0h average	*sid2* 6h average	ratio
At1g19020	expressed protein	255.5	2177.1	8.5	132.4	2143.3	16.2	43.0	5861.0	136.2	59.5	4819.1	81.0
At2g24850	aminotransferase, putative	1646.3	7727.3	4.7	989.0	8732.5	8.8	52.2	2028.5	38.9	59.4	4319.1	72.7
At5g20230	plastocyanin-like domain-containing protein	1582.3	12130.8	7.7	709.9	11179.7	15.7	155.8	15084.8	96.8	224.1	13323.2	59.5
At5g02490	heat shock cognate 70 kDa protein 2 (HSC70-2) (HSP70-2)	381.8	3042.0	8.0	221.6	3235.1	14.6	29.0	2874.8	99.2	76.1	3385.9	44.5
At4g14365	zinc finger (C3HC4-type RING finger) family protein / ankyrin repeat family protein	1056.1	3868.2	3.7	736.3	3705.7	5.0	28.5	2296.1	80.6	153.9	5349.9	34.8
At3g50930	AAA-type ATPase family protein	216.5	673.1	3.1	138.2	688.3	5.0	23.6	1207.1	51.2	43.3	1298.3	30.0
At5g39050	transferase family protein	70.5	961.5	13.6	61.4	1092.0	17.8	35.9	1936.6	54.0	34.3	970.8	28.3
At4g20830	FAD-binding domain-containing protein	301.7	1960.3	6.5	181.7	2258.1	12.4	70.7	3652.2	51.6	111.7	2995.5	26.8
At4g33050	calmodulin-binding family protein	695.4	2259.0	3.2	470.0	2352.5	5.0	41.4	4411.1	106.6	123.7	3158.4	25.5
At3g01290	band 7 family protein	773.2	3344.6	4.3	624.0	3225.6	5.2	53.6	3120.8	58.2	174.1	3661.5	21.0
At4g01700	chitinase, putative	464.7	1245.0	2.7	200.7	1422.1	7.1	37.9	211.6	5.6	39.0	762.3	19.5
At3g50480	broad-spectrum mildew resistance RPW8 family protein	1949.6	6187.5	3.2	1492.0	6448.0	4.3	32.5	2559.4	78.7	196.7	3779.3	19.2
At2g38470	WRKY family transcription factor	187.5	808.2	4.3	124.7	674.2	5.4	24.4	2344.2	96.0	84.6	1442.3	17.0
At3g44720	prephenate dehydratase family protein	123.5	445.1	3.6	95.5	592.0	6.2	34.6	1084.6	31.3	47.2	779.3	16.5
At5g40780	lysine and histidine specific transporter, putative	1101.1	3240.3	2.9	795.9	4007.2	5.0	48.8	2798.1	57.3	178.4	2659.2	14.9
At5g13490	ADP, ATP carrier protein 2, mitochondrial / ADP/ATP translocase 2 / adenine nucleotide translocator 2 (ANT2)	99.9	742.5	7.4	71.2	503.8	7.1	52.9	2628.8	49.7	53.9	798.7	14.8
At5g64310	arabinogalactan-protein (AGP1)	63.2	463.1	7.3	53.1	332.9	6.3	49.1	2344.8	47.7	77.9	1093.5	14.0
At2g41100	touch-responsive protein / calmodulin-related protein 3, touch-induced (TCH3)	1831.9	6873.7	3.8	1656.5	6221.5	3.8	206.9	9637.4	46.6	760.4	9631.1	12.7
At1g72680	cinnamyl-alcohol dehydrogenase, putative	249.7	601.3	2.4	193.4	778.7	4.0	117.4	1070.9	9.1	39.9	483.2	12.1
At5g19240	expressed protein	1447.8	3916.0	2.7	774.5	5225.1	6.7	55.0	2457.7	44.7	240.2	2861.4	11.9
At3g48090	disease resistance protein (EDS1)	315.3	688.1	2.2	244.4	491.6	2.0	33.5	139.6	4.2	54.0	616.1	11.4
At4g34390	extra-large guanine nucleotide binding protein, putative / G-protein, putative	258.1	785.9	3.0	206.4	788.9	3.8	75.6	850.7	11.3	97.9	972.0	9.9
At2g38290	ammonium transporter 2 (AMT2)	144.0	651.4	4.5	132.9	497.6	3.7	46.7	969.4	20.8	85.5	819.8	9.6
At1g08940	phosphoglycerate/bisphosphoglycerate mutase family protein	26.9	229.4	8.5	26.6	166.2	6.2	29.0	523.2	18.0	23.9	217.9	9.1
At2g41410	calmodulin, putative	1022.0	2772.3	2.7	676.9	2256.6	3.3	158.7	2684.3	16.9	401.0	3554.3	8.9
At2g23810	senescence-associated family protein	652.8	1950.1	3.0	435.4	2273.3	5.2	180.2	4106.6	22.8	443.4	3792.9	8.6

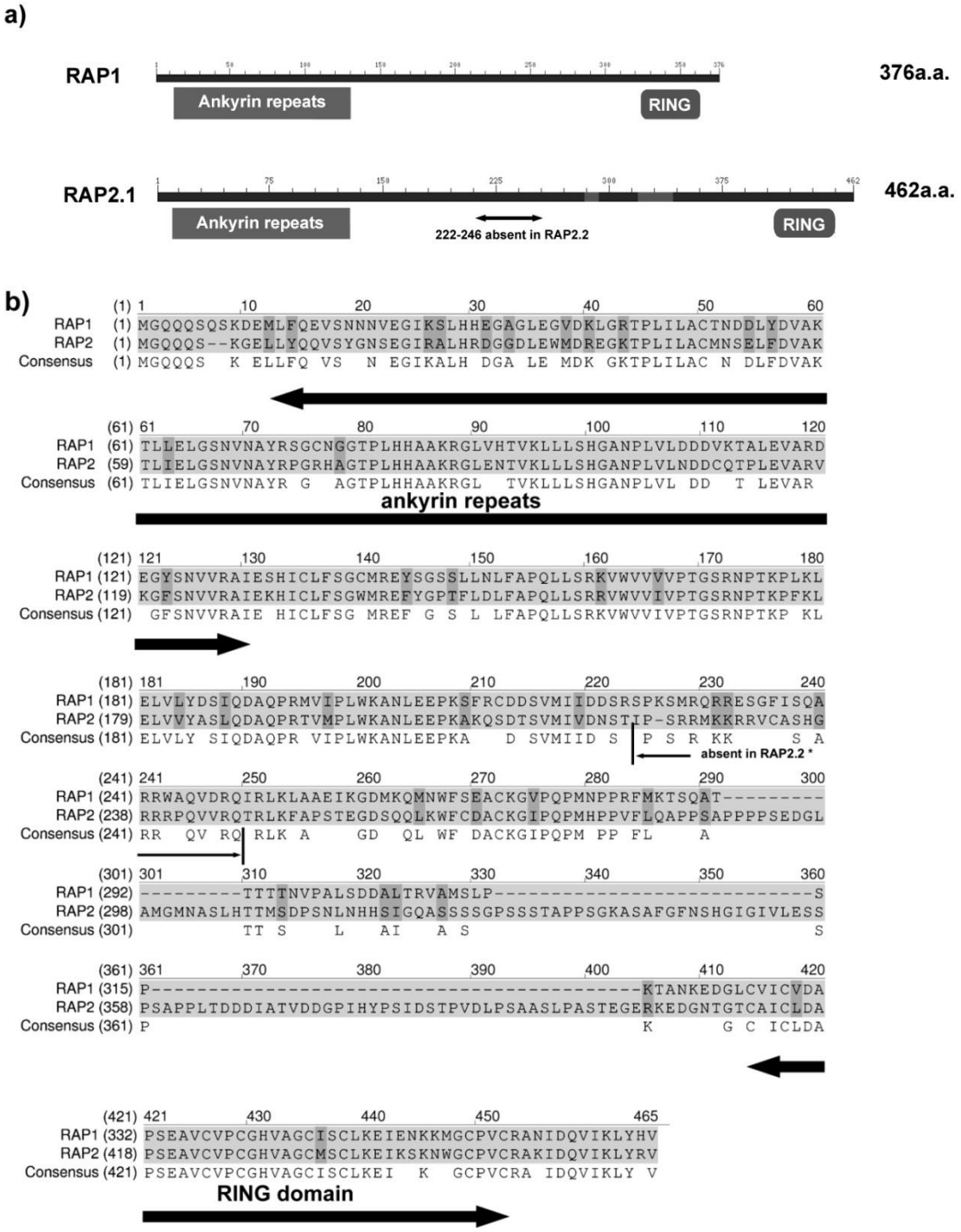

Figure 3.1 *In silico* analysis of RAP1 and RAP2 amino acid sequences.
(a) Two conserved domains are found in RAP1 and RAP2: Ankyrin (for protein binding) and RING (for E3 ligase activity). **(b)** sequence alignment of RAP1 and RAP2, wherein the peptide "IPSRRMKKRRVCASHGRRRPQVVRQ" is absent in RAP2.2.

3.3 Expression Profiling of *RAP1*

Analysis of microarray data suggests that *RAP1* is highly inducible upon *Pst*DC3000(*avrB*) infection. To verify this, the expression of *RAP1* was monitored by RT-PCR upon *Pst*DC3000(*avrB*) treatment. It was found that *RAP1* was induced after 2 hours treatment and reached a maximum at 6 hours, followed by the reduction of transcripts for 12 hours and 24 hours (Figure 3.2b). In the mock treatment, *RAP1* also up-regulated after 2 hours, however the levels of transcript returned to the basal level after 6 hours. This up-regulation in transcripts suggested due to a wounding effect by infiltration. On the other hand, the expression of both *RAP2s*, *RAP2.1* and *RAP2.2*, did not showed any significantly changes as *RAP1* in both mock and pathogen treated samples at all time-points.

RAP1 was induced in both *atgsnor1-3* and *sid2* plants in microarray data, suggesting the induction of *RAP1* might be independent of SA. Plant hormones such as jasmonic acid (JA), ethylene and abscisic acid (ABA) are known to be involved in plant defence; mutants that are insensitive to these hormones were used to determine whether expression of *RAP1* was also independent of these hormonal pathways. These mutants were *NONEXPRESSOR OF PATHOGENESIS-RELATED GENES 1*(*npr1-1*), *JASMONATE-INSENSITIVE1* (*jin1-1*), *ETHYLENE-INSENSITIVE 2* (*ein2*), A*BSCISIC ACID INSENSITIVE 3* (*aba3-1*) and *SALICYLIC ACID INDUCTION DEFICIENT 2* (*sid2*). Fig 3.3a shows that the expression of *RAP1* was induced by *Pst*DC3000(*avrB*) upon 6 hours in all these mutant backgrounds.

There is an intergenic region of 629bp between *RAP1* and the upstream gene (*At4g14368*) which should include the promoter of *RAP1* for regulation of expression. This DNA fragment was fused with a reported gene β-glucuronidase (GUS) and transformed into WT (Col-0) plants. GUS catalyses the substrate X-Gluc (5-bromo-4-chloro-3-indolyl-β-D-glucuronic acid) to blue precipitate of chloro-bromoindigo and colourless glucuronic acid. In Figure 3.2c, only a weak blue colour developed in Col-0 in untreated condition after X-Gluc staining, indicating that the GUS enzyme was expressed but in low extent. As the leaves were treated with cutting (wounding), a stronger blue colour was developed near the wounding sites. In addition, pathogen treatments with *Pst*DC3000(*avrB*) and *Blumeria graminis* f.sp. *tritici* (*Bgt*) were also

able to induce GUS expression in leaves which displayed a more intense colour than the untreated sample.

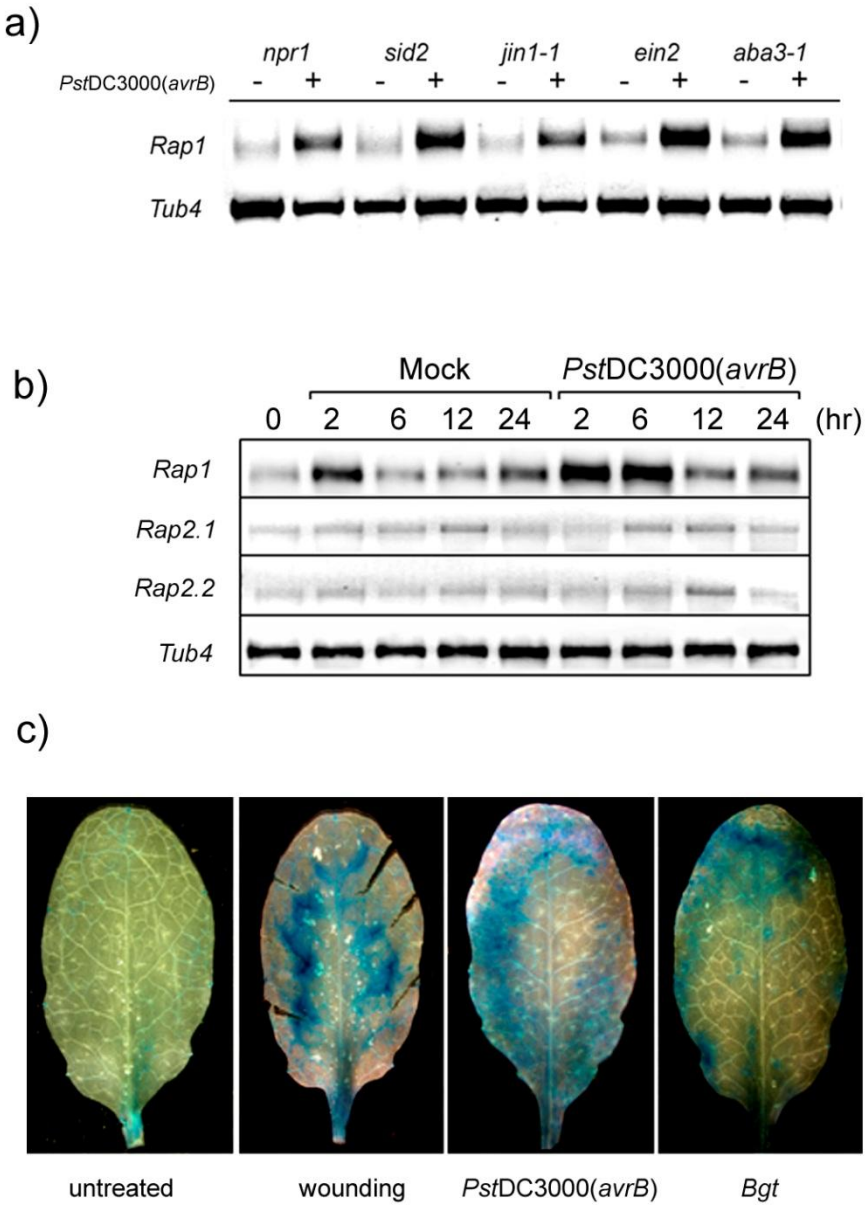

Figure 3.2 Transcriptional level of *RAP1* and *RAP2* after the infection by *Pst*3000 (*avrB*) as determined by RT-PCR and GUS.
a) In different genetic backgrounds; **b)** in Col-0 in different time points; and **c)** GUS staining of WT plants harbouring a construct of *Rap1* promoter-GUS. (Work of Jeum-Kyu Hong)

3.4 Bioinformatic Analysis of *RAP1*

Bioinformatic analysis is a powerful tool for studying a gene, especially if a gene has not been formerly characterized like *RAP1*. There are public microarray databases providing data of individual gene expression in various conditions such as developmental, biotic and abiotic stresses, hormone treatments and light exposure. In this study two databases were used, which are "The Bio-Array Resource for Plant Biology" (BAR) (http://esc4037-shemp.csb.utoronto.ca/welcome.htm) and "AtGenExpress Visualization Tool" (AVT) (http://jsp.weigelworld.org/expviz/expviz.jsp). BAR is a multifunctional database, which enables visualization of expression data in a graphical representation. For instance, the *Arabidopsis* eFP Browser is able to show the location of a particular gene expression projecting on a picture of an *Arabidopsis* plant (expression atlas) (Winter et al. 2007). Figure 3.3 shows the relative expression of *RAP1* and *RAP2* in different developmental stages. Referring to the expression atlas of *RAP1*, the basal expression was around signal 100-200, and the signal in some particular tissues was slightly higher (orange) such as in cotyledon, cauline leaves and mature flower. The expression of *RAP1* increased gradually during leaf development until leaf maturation (red) and then reduced to basal level but increased again during leaf senescence. *RAP2* shares a similar developmental expression pattern as *RAP1*, for instance, more signal in cotyledons, cauline leaves, and during leaf development. *RAP2* was also slightly up-regulated during embryo development.

Another available feature in BAR is Expression Angler, which allows comparison of expression profiles of all expressed genes in *Arabidopsis* and picking up genes that have similar pattern as the query gene (Toufighi et al. 2005) . When using *RAP1* as the query gene, the top 24 genes with similar expression to *RAP1* were identified in Expression Angler. The X-axis of Figure 3.4a shows the expression of these 25 genes in about 400 experiments, while the Y axis shows the gene IDs. From yellow to red, displays the increase in intensity of transcript signals. The 25 genes share a similar regulation pattern, suggesting their expression might be regulated by similar mechanisms. The identified genes can be divided into 5 categories which are ankyrin repeat, camodulin/calcium binding, defence-related, kinases and proteins with unknown function (Figure 3.4b). The majority of genes were placed in the defence-related category, suggesting that *RAP1* may be related to defence mechanisms.

To further understand the relationship of *RAP1* expression and defence, the AVT database was used to analyse *RAP1* expression upon treatments with a variety of pathogens and pathogen effectors (Figure 3.5). Similar induction patterns of *RAP1* expression are observed upon the treatments by $MgCl_2$, *Pst*DC3000 and *Pst*DC3000(*avrRpm1*), with signals increasing from 2 hours to 6 hours and decreasing at 12 hours. However, the overall level of *RAP1* expression in *Pst*DC3000(*avrRpm1*)-challenged plants was higher than the plants challenge with *Pst*DC3000(*avrB*) and induction lasted for 12 hours. Challenge with the *Pst*DC3000 *hrcC* deletion mutant or *Pseudomonas syringae* pv. *phaseolicola* (*Psp*) led to overall higher induction levels that lasted for 24 hours. The induction level *Psp* at 6 hours was among the highest in the whole set of experiments. *RAP1* expression was also induced following fungal infection by *Phytophthora infestans*.

Effectors and PAMPs could also induce *RAP1* expression, however the effects were diversified. In the experiment (Figure 3.5b), infiltration of either water or $MgCl_2$ solution only slightly induced the *RAP1* expression, while the *RAP1* expressions were significantly induced by HrpZ, NPP1 and Flg22 infiltrations. Induction by HrpZ and NPP1 infiltration could last for 4 hours while the detected signals of Flg22-induction was rapidly decreased at the fourth hour. In contrast, no induction of *RAP1* expression was observed by LPS-infiltration.

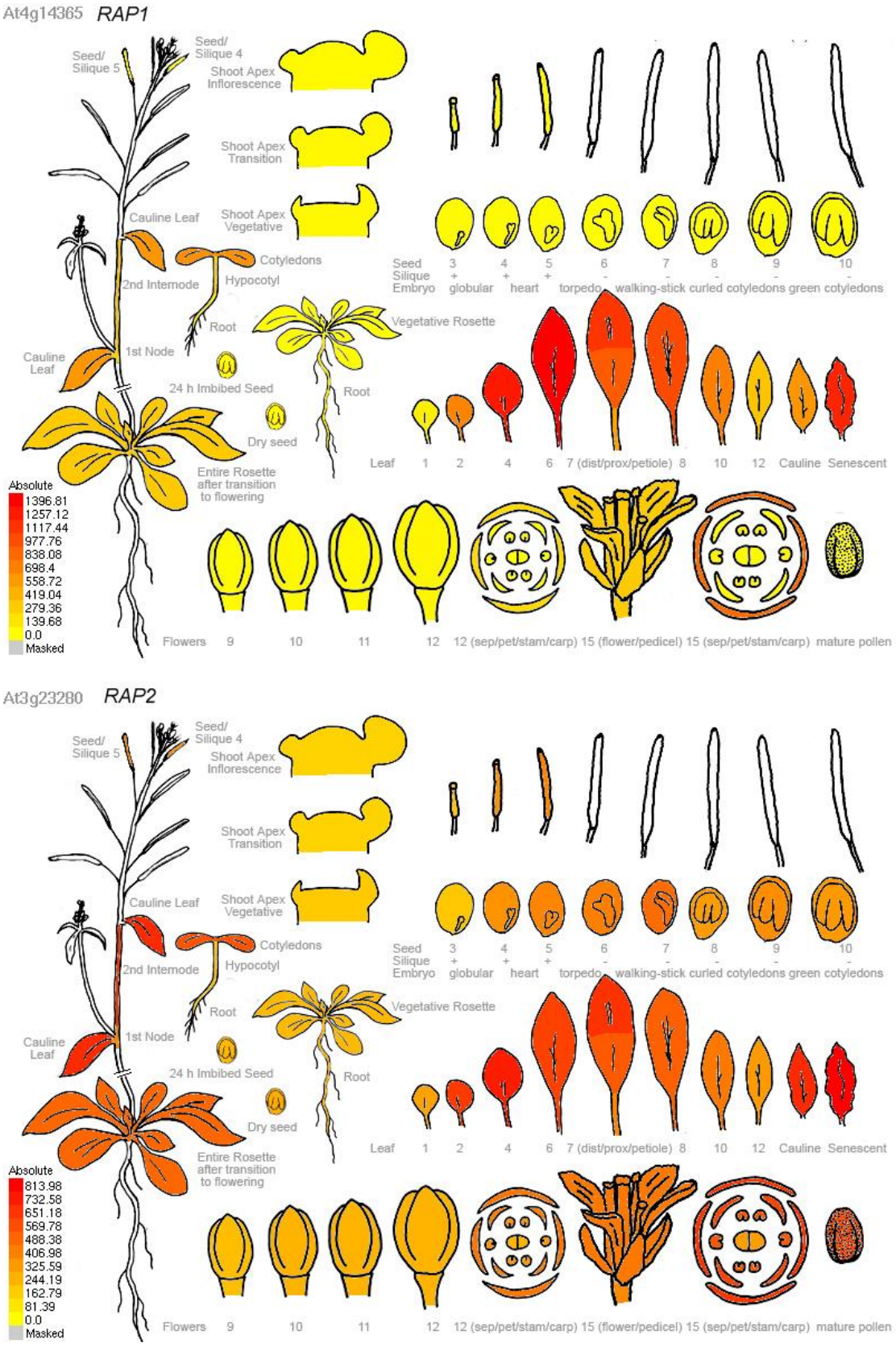

Figure 3.3 Relative expression of *RAP1* and *RAP2* in different stage of development as visualized in the *Arabidopsis* eFP Browser.

a)

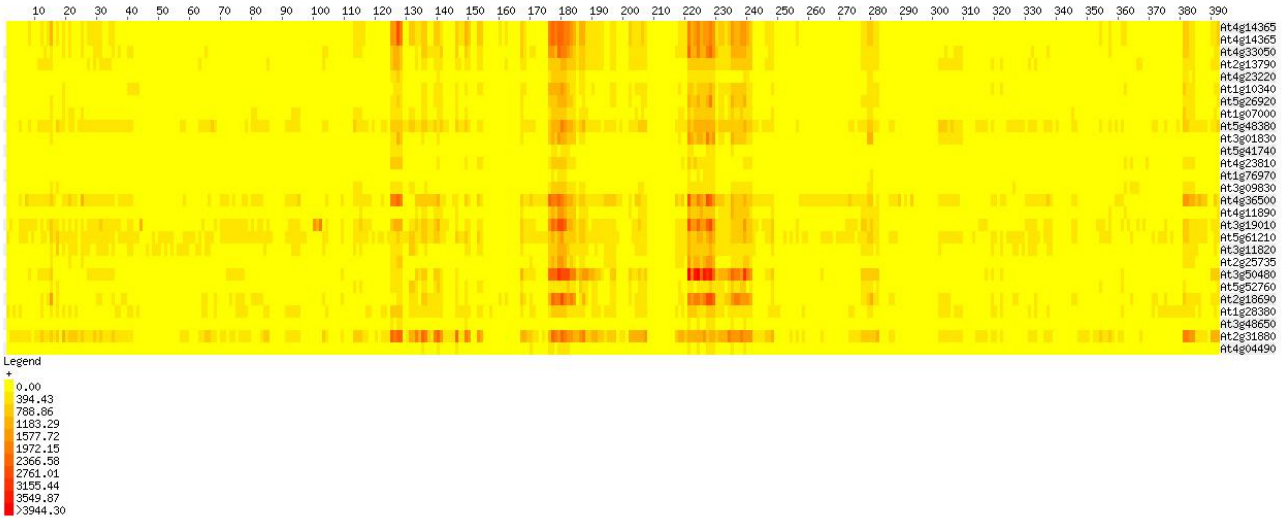

b)

	Ankyrin repeat	
At1g10340	cellular_component_unknown	ankyrin repeat family protein
	Camodulin/calcium binding	
At4g33050	calmodulin binding	EDA39 (embryo sac development arrest 39); calmodulin binding
At3g01830	calcium ion binding	calmodulin-related protein, putative
At5g26920	calmodulin binding	CBP60G (CAM-BINDING PROTEIN 60-LIKE.G); calmodulin binding
	Defence-related	
At5g48380	protein amino acid phosphorylation	leucine-rich repeat family protein / protein kinase family protein
At2g31880	protein amino acid phosphorylation	leucine-rich repeat transmembrane protein kinase, putative
At1g28380	biological_process_unknown	NSL1 (necrotic spotted lesions 1)
At5g41740	chloroplast	disease resistance protein (TIR-NBS-LRR class), putative
At2g13790	transmembrane receptor protein serine/threonine kinase activity	ATSERK4_BKK1__SERK4 (SOMATIC EMBRYOGENESIS RECEPTOR-LIKE KINASE 4); protein binding / protein kinase/ transmembrane receptor protein serine/threonine kinase
At3g11820	SNARE complex	AT-SYR1_ATSYP121_ATSYR1_PEN1_SYR1__SYP121 (SYNTAXIN OF PLANTS 121); SNAP receptor/ protein anchor
At5g61210	integral to membrane of membrane fraction	ATSNAP33_ATSNAP33B_SNP33__SNAP33 (SOLUBLE N-ETHYLMALEIMIDE-SENSITIVE FACTOR ADAPTOR PROTEIN 33); SNAP receptor/ protein binding
At4g23810	regulation of transcription, DNA-dependent	ATWRKY53__WRKY53; DNA binding / protein binding / transcription activator/ transcription factor
At3g50480	response to other organism	HR4 (HOMOLOG OF RPW8 4)
	Kinases	
At4g04490	protein amino acid phosphorylation	protein kinase family protein
At1g76970	protein amino acid phosphorylation	protein kinase, putative
At4g23220	cellular_component_unknown	kinase
At4g11890	kinase activity	protein kinase family protein
	Others / Unknown functions	
At3g19010	cellular_component_unknown	oxidoreductase, 2OG-Fe(II) oxygenase family protein
At5g52760	metal ion binding	heavy-metal-associated domain-containing protein
At1g07000	vesicle docking during exocytosis	ATEXO70B2 (exocyst subunit EXO70 family protein B2); protein binding
At1g76970	intracellular protein transport	VHS domain-containing protein / GAT domain-containing protein
At2g18690	biological_process_unknown	unknown protein
At4g36500	mitochondrion	unknown protein
At2g25735	molecular_function_unknown	unknown protein

Figure 3.4 Genes that share similar expression profile with *RAP1*.
a) Microarray analysis (from BAR database) to show the top 24 genes that were co-expressed with *RAP1*; **b)** Classification of identified genes according to their nature.

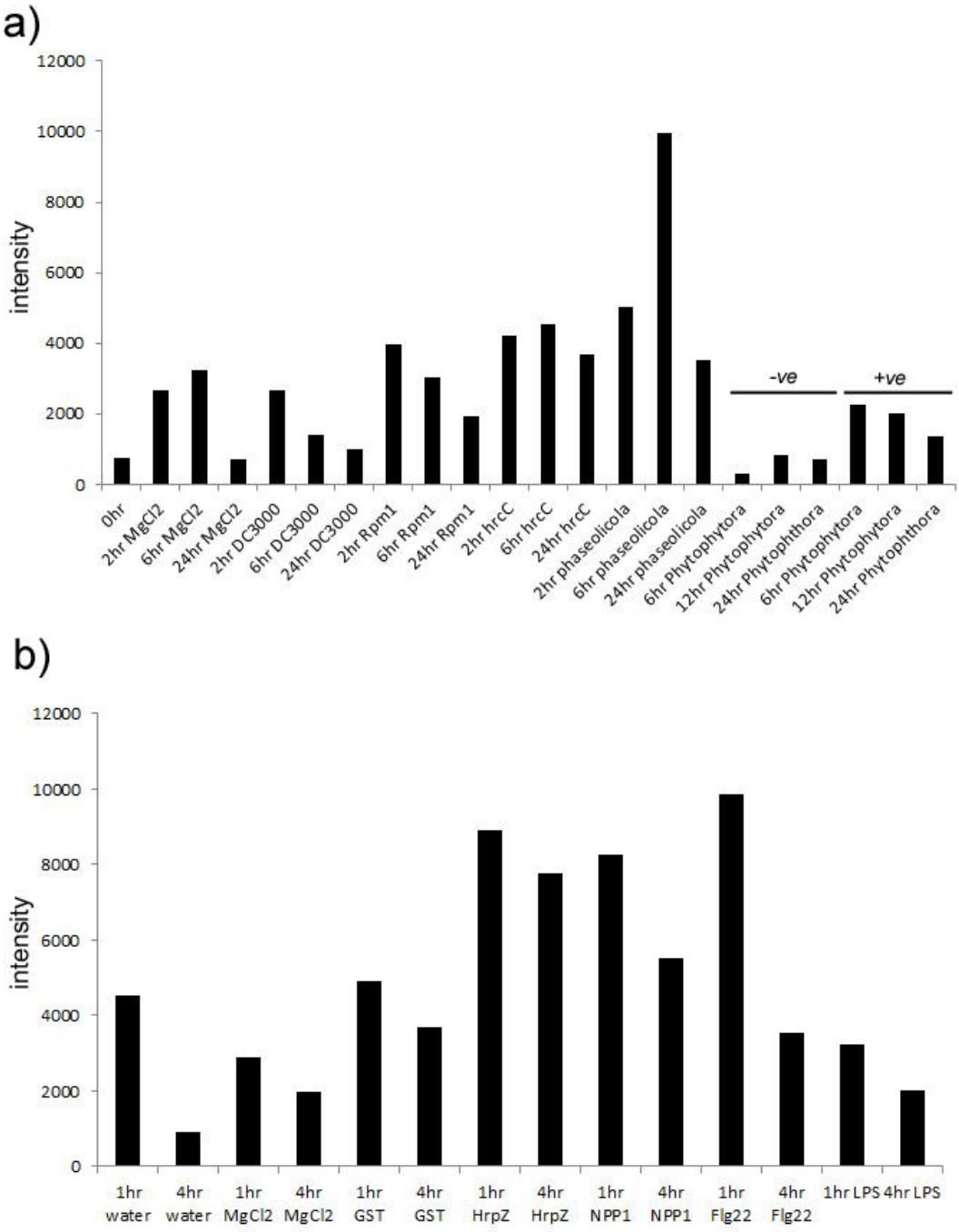

Figure 3.5 Expression of *RAP1* in response to various treatments.
a) Various pathogens and **b)** various effectors. With the exception of *Phytophthora*, inoculations were done by leaves infiltration. (Data from AVT database)

3.5 Discussion

Although there is emerging evidence that NO is taking part in many regulatory mechanisms, the component(s) of NO signalling have long been a missing link. NO production, S-nitrosylation and denitrosylation are all contributing to the homeostasis of NO as well as redox-based regulation, but it is still questionable whether a global regulator is present to coordinate NO signals. NO is actively involved in plant defence responses, and identification of GSNOR and its loss of function mutant *atgsnor1-3* has provided a platform to investigate the possible regulator(s) integral to control of nitrosative stress. Under unchallenged condition, loss of GSNOR activity does not have sufficient impact as cellular redox balance as NO production in healthy tissue is relatively low (although the developmental phenotype of *atgsnor1-3* is still very distinguishable). It has been reported that SNO levels are rapidly increased upon pathogen inoculation and this effect is even amplified in *atgsnor1-3* plants due to the absence of GSNOR (Feechan et al. 2005). The microarray data in Table 3.1 compares multiple gene expression in Col-0, *atgsnor1-1*, *atgsnor1-3* and *sid2* plants, and *RAP1* was selected based on its dynamic change of expression in *atgsnor1-3* and *sid2* plants. Although *RAP1* was inducible by pathogens in all tested plant lines, its transcriptions were lowered in *atgsnor1-3* and *sid2* than in wild-type. This suggests that high NO or low SA may down-regulate expression of *RAP1* and it could also be possible that suppression was due to the lowered SA content in *atgsnor1-3* plants (Feechan et al. 2005) rather than due to the elevated SNO level. However, the pathogen induction of *RAP1* is independent to SA, as the expression of *RAP1* in *sid2* plants could reach the maximum level seen in Col-0 and *atgsnor1-1* plants. This observation was also verified by RT-PCR of *RAP1* (Figure 3.2a). Furthermore, the induction in *npr1-1* also reveals that impairment of SA-signalling did not affect up-regulation of *RAP1* in response to pathogen challenge. Neither JA nor ethylene or abscisic acid had a significant effect in *RAP1* induction. Data from the *Arabidopsis* eFP Browser showed that *RAP1* was not induced by ACC (ethylene precursor), zeatin, IAA (auxin), ABA, MeJA and GA-3 but was slightly inducible by brassinolide (data not shown). In conclusion, *RAP1* may be involved in plant defence mechanisms that could be parallel but independent to other known defence pathways.

It is also clearly observable that *RAP1* is induced by wounding. Wounds caused by infiltration or cutting can activate *RAP1* expression (Figure 3.2b & c and Figure 3.4).

Infiltration is a common practice to allow effective contact between pathogens and host cells, however it will also lead to cell damage and leakage of electrolytes. According to previous research, electrolytes such as calcium ions can activate wounding-related gene expression in the adjacent cells (Dombrowski and Bergey 2007); from the co-expression data (Figure 3.4), three calmodulin/calcium binding genes share a similar expression pattern with *RAP1* that indicating *RAP1* may involve in wounding. In particular, CBP60g (*At5g26920*) is also related to disease resistance against *Pseudomonas syringae* and MAMP-induced SA accumulation (Wang et al. 2009a). Furthermore, a calmodulin-binding family protein (*At4g33050*) and a putative calmodulin (*At4g33050*) were arrayed together in Table 3.1. These two genes show significant induction in both *atgsnor1-3* and *sid2* plants after challeng by *Pst*DC3000(*avrB*). Especially *At4g33050* that is also known as *EDS39* (*EMBRYO SAC DEVELOPMENT ARREST 39*) was induced 106.6 fold and 25.5 fold in *atgsnor1-3* and *sid2* plants respectively. *EDS39* transcripts had a much lower basal level in *atgsnor1-3* than Col-0, and was placed in the top 24 gene candidates that share similar expression pattern with *RAP1* (Figure 3.4). This suggests there might be a close relationship between *EDS39* and *RAP1*.

Two predicted conserved domains are found in RAP1, which are ankyrin repeats and RING domain. Ankyrin repeats is one of the most widely existing protein motifs in nature, consists of 30−34 amino acid residues and exclusively functions to mediate protein−protein interactions. The intra- and inter-repeat hydrophobic and hydrogen bonding stabilizes the global structure of the repeat and the repetitive and elongated nature of ankyrin repeat proteins helps in protein stability, folding and unfolding, and determines binding specificity (Li et al. 2006). The RING domain was initially named after a newly discovered gene RING1 (really interesting new gene 1) and the RING finger motif can be defined simply as Cys-X_2-Cys-$X_{(9-39)}$-Cys-$X_{(1-3)}$-His-$X_{(2-3)}$-Cys-X_2-Cys-$X_{(4-48)}$-Cys-X_2-Cys, where X is any amino acid. The RING finger domain comprises 8 potential metal ligands that binds two zinc atoms with each zinc atom ligated tetrahedrally by either 3 or 4 Cys residues and a His residue (Borden and Freemont 1996). The RING domain proteins are classified as a sub-class of E3 ligases for specific recognition of target proteins leading to their 26S proteasome degradation. Therefore RAP1 may act as an E3 ligase to recognize target proteins for degradation. As expression of *RAP1* is upregulated during pathogen inoculation and wounding, the

potential target protein(s) could be a negative regulator in plant defence. Removal of this target protein may result in relieving the suppression of certain defence responses. For instance, *Arabidopsis* KEG (Keep on Going) is an E3 ligase which shows high similarity in peptide sequence with RAP1 and targets the degradation of ABI5 (ABSCISIC ACID-INSENSITIVE 5) which encodes an ABA-responsive transcription factor. KEG therefore regulates ABA-mediated signalling by controlling the amount of ABI5 in *Arabidopsis* (Stone et al. 2006).

RAP2 (At3g23280) is a paralog of *RAP1*. Both ankyrin repeats and the RING domain are found in RAP2 and a previous study has shown E3 ligase activity of RAP2 (Stone et al. 2005). An additional ~80 amino acids in RAP2 do not align with RAP1 and the expression behaviour between *RAP1* and *RAP2* is very different. The expression of *RAP2* across Col-0, *atgsnor1-1*, *atgsnor1-3* and *sid2* plants was consistent in the microarray data (data not shown). Also, *RAP2* expression seems to be independent of pathogen challenge, as no induction was detected by *Pst*DC3000(*avrB*) (Figure 3.2b). However, the expression atlas of *RAP1* and *RAP2* overlaps (Figure 3.3), suggesting that there could be some functional redundancy. Both *RAP1* and *RAP2* have been referred to the studies of *XBAT32* (Nodzon et al. 2004) and *KEG* (Stone et al. 2006) based on the homology in protein sequence. *Arabidopsis XBAT32* encodes an E3 ligase involved in lateral root development and like RAP1/RAP2, XBAT32 also contains an ankyrin repeat domain at the N-terminal half and a RING finger motif. *XBAT32* was expressed abundantly in the primary root but not in newly formed lateral roots, suggesting XBAT32 may degrade a key regulator during the initiation of the lateral root development. KEG also contains a RING domain and ankyrin repeats but with the addition of HERC-2 repeats in the N-terminus. Phylogenetic analysis showed that RAP1 and RAP2 share the most similar ankyrin repeats with KEG in *Arabidopsis*. KEG as an E3 ligase, targets transcription factor ABI5 for degradation and it could be possible that RAP1/RAP2 also regulate physiological effects by mediating degradation of certain transcription factors. *RAP1* is also one of the 25 most correlated expressed genes with *AtPNP-A* (Meier et al. 2008). PNPs (Plant natriuretic peptides) are a class of systemically mobile molecules distantly related to expansins. Ontology analysis of *AtPNP-A* and these 25 genes revealed a significant over representation of genes annotated as part of the systemic acquired resistance (SAR) pathway. These genes are also strongly inducible by SA or BTH and *AtPNP-A* expression is also

related to the SAR annotated transcription factor, WRKY 70, indicating *RAP1* may also take part in the SAR.

Further bioinformatics analysis revealed that *RAP1* is closely related to plant defence responses. The online analysis program Expression Angler in BAR picked up 24 genes that are showing the most similar expression profiles with *RAP1*. A large proportion of these 24 genes are defence-related, which includes three leucine-rich repeat (LRR) family proteins (At5g48380 (*BIR1*), At2g31880 and At5g41740), NSL1 (At1g28380), proteins involved in SNARE complex (At2g13790 and At3g11820), transcription factor WRKY53 (At4g23810), a homolog of RPW8 (At3g50480) and CBP60g (At5g26920), which functions in SA signalling (Wang et al. 2011). These proteins are important in pathogen-perception, signalling as well as defence gene activation. Interestingly, the LRR-protein BIR1, NSL1 and SNARE complex are associated with programmed-cell death (PCD) (Gao et al. 2009; Noutoshi et al. 2006; Zhang et al. 2007a), and NSL1, SNARE and RPW8 are related to defence against fungal pathogens (Dou et al. 2011; Eckardt 2009; Noutoshi et al. 2006), suggesting RAP1 may be involved in PCD during attempted fungal infection. Also, a number of kinases were co-expressed with *RAP1*, most of which are uncharacterized proteins. This suggests *RAP1* may be involved in other unidentified signalling pathway.

Induction of *RAP1* also carries certain specificity in response to various pathogens or effectors. As previously discussed, *RAP1* is wound (by cutting and infiltration) inducible, however the activation decreases after 6 hours. The same was found when plants were inoculated with *Pst*DC3000 and *Pst*DC3000(*avrRpm1*) but not when they were inoculated with *Pst*DC3000 *hrcC*$^{-}$ (Figure 3.5a), suggesting the knockout of type III-secretion system is required for the suppression of *RAP1* expression. Further, strong and sustainable induction was also observed during *Pseudomonas syringae* pv. *phaseolicola* (*Psp*) and *Phytophthora infestans* infection. These results revealed that *RAP1* induction may function in non-host resistance. Thus, NPP1 (necrosis-inducing *Phytophthora* protein 1) and HrpZ from *Psp* caused a longer lasting effect than Flg22, and LPS (Figure 3.5b).

Pathogen-related induction of *RAP1*is likely to be part of the early phase defence responses, as transcription occurs rapidly after 1-2 hour of pathogen/effector

inoculation. Early-production of RAP1 may be required for degradation of a negative regulator(s) to trigger defence responses.

In summary, this chapter identified an uncharacterized gene *RAP1* based on its specific expression behaviour towards high SNO levels (*atgsnor1-3* plants) and pathogen challenge. The expression profiles also show that *RAP1* may be involved in responses to wounding, pathogens and cell death. The presence of a putative RING domain has provided a functional hint that RAP1 could be an E3 ligase to mediate degradation of a negative regulator(s) in defence responses. *RAP1* may also be involved in redox-based signalling, as *RAP1* was strongly induced in high SNO levels.

Chapter 4

4 Molecular Characterisation of RAP1

4.1 Introduction

Two conserved domains are found in RAP1 protein, which are ankyrin repeats and RING finger motif. Ankyrin repeats are involved in protein binding and protein stability and RING finger is a key signature of an E3 ligase. E3 ligases cause the attachment of ubiquitin to a lysine on a target protein and also catalyse the polymerization of ubiquitin. Therefore RAP1 may function as an E3 ligase to recognize a target protein (substrate) for degradation through ubiquitin–proteasome systems (UPS). However, a previous comprehensive analysis of E3 ligases in *Arabidopsis* had stated that RAP1 did not have any E3 ligase activity. Interestingly, although RAP1 and RAP2 share high homology in protein sequence, RAP2 has been shown to carry E3 ligase activity (Stone et al. 2005). It is also worth noting that among the tested HCa type E3 ligases with 3.a.a between metal ligands 4 and 5, three out of five proteins could not demonstrate the E3 ligase activity, which is much higher than the total average 18 out of 64. Therefore, the E3 ligase activity assay for RAP1 might have to be optimized. Four proteins (E1, E2, E3 and ubiquitin) are essential for the assay. While E1 and ubiquitin are relatively conserved and universally reactive across species, alternative E2 enzymes could be used. It has been reported that E2s have specificity towards E3s (Kraft et al. 2005), so selection of a proper E2 for the activity assay could be critical. The use of an *Arabidopsis* E2 enzyme AtUBC1has been described in the activity assay of a disease related RING protein RIN2 (Kawasaki et al. 2005), therefore instead of UBC8 used in the previous study (Stone et al. 2005), UBC1 was used in this study for the activity assay of RAP1.

The cysteine-rich RING domain has been shown to be a reactive site for S-nitrosylation. For instance, E3 ligase XIAP in neuronal cells is S-nitrosylated at C450 in the RING domain and S-nitrosylation of the RING domain inhibits E3 ligase activity of XIAP (Nakamura et al. 2010). RAP1 could also be S-nitrosylated, as RAP1 contains 14 cysteine residues and 8 of them are located in the RING domain in the C-terminus (position 325-363). Furthermore, expression profiling suggests RAP1 is

highly related to S-nitrosylation and there could be a possibility that the activity of RAP1 is regulated by S-nitrosylation.

The *in vivo* E3 ligase activity of RAP1 (Figure 4.1) will be demonstrated in this chapter. RAP1 is shown to be S-nitrosylated and S-nitrosylation regulates the activity of RAP1.

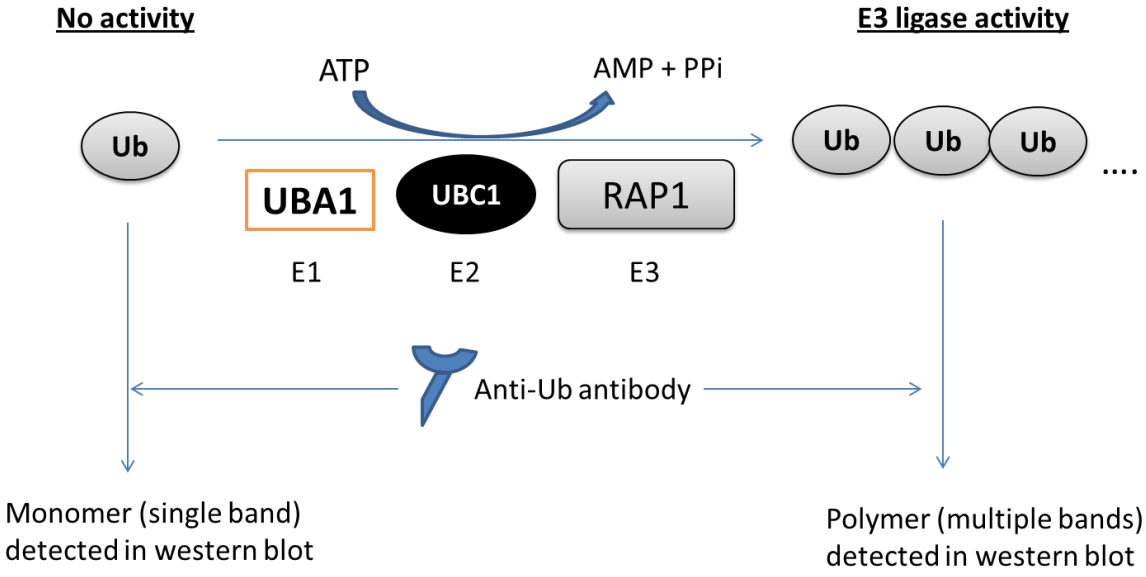

Figure 4.1 Schematic diagram shows the E3 ligase activity assay in this study. Monomer ubiquitins (Ub) are activated by E1 (UBA1), conjugated by E2 (UBC1) and polymerized by E3 to form a series of ubiquitin-polymers. The ubiquitin-polymers are then detected by anti-Ub antibody, while absence of any of the E1, E2 or E3 enzymes fails to polymerize ubiquitin and only single size monomer can be detected.

4.2 Expression and Purification of RAP1

Apart from RAP1, three other proteins E1, E2 and ubiquitin are essential to carry out the E3 ligase activity assay. The ubiquitin activating activity of E1 is found to be universal and compatible across species and human E1 has also been commonly used in *Arabidpsis*-based assays (Liu et al. 2011). The molecular size of E1 is relatively large, for instance, the cDNA of AtUBA1 is 3243 bp and encodes a protein of 120 kDa. In addition, ubiquitin is also highly conserved. In this study commercial available human E1 and ubiquitin were used. As previously discussed, a comprehensive E3 ligase activity study had demonstrated no E3 ligase activity for RAP1(Stone et al. 2005) using E2 (AtUBC8). Here, a disease related E2 (AtUBC1) was used instead. A RING E3 ligase, *Arabidopsis* COP1 interacting protein 8 (CIP8) (Hardtke et al. 2002) was employed as a positive control for the experiment.

The full coding cDNA fragments of *RAP1*, *RAP2*, *CIP8* and *Ubc1* were amplified by PCR from the cDNA library of WT plants (Col-0) with sizes of 1131 bp (*RAP1*), 1389 bp (*RAP2*), 459 bp (*Ubc1*) and 1005 bp (*CIP8*) (Figure 4.2). The fragments were then cloned into expression vector pGEX-4T1 for expression in *E. coli*. A fragment of glutathione-S-transferase (GST) is present at the 5'-end of the cloning sites to generate fusion proteins with GST at the N-terminus. The molecular size of GST is 28kDa, which leads to the expected fusion proteins size of GST-RAP1 (28kDa + 41.4kDa=69.4kDa), GST-RAP2 (28kDa+50kDa=78kDa), GST-CIP8 (28kDa + 37kDa=65kDa) and GST-UBC1 (28kDa+17.4kDa=41.4kDa). Figure 4.3 shows the expression of GST-UBC1, GST-RAP1 and GST-CIP8 in *E. coli* BL21(DE3). With the exception of GST-UBC1 extract, no dominant bands were observed in the total soluble extract, suggesting the expression level or solubility of GST-RAP1 and GST-CIP8 was much lower than that of GST-UBC1. The GST fusion proteins were then purified by Glutathione-Sepharose-4B (GSH-SE-4B) and eluted in elution buffer with glutathione. After elution, an intense and thick band of GST-UBC1 was observed between 30-46kDa, while weaker bands were observed in GST-RAP1 and GST-CIP8 eluents. However distinct bands were still present in the eluents of GST-RAP1 and GST-CIP8 between 58kDa-80kDa, which were likely to be the desired proteins.

As the efficiency of RAP1 purification was rather low, the protein identity had to be further confirmed. The distinct band in the GSH-SE-4B eluent of GST-RAP1

(arrowed in Figure 4.3) was excised and verified by mass spectrometry (MS). Figure 4.4a showed the peptide sequences that were identified by Mascot after the excised protein was digested by trypsin. Trypsin is a serine protease that specifically cleaves the carboxyl terminus of amino acid residues lysine (K) and arginine (R), resulting in digested peptides with K or R at the C-terminal ends. Masses of 28 peptides were found to match the predicted cleavage products of a zinc-finger (C3HC4-type RING finger) family protein (gi|18414200), which is RAP1 in *Arabidopsis*. Peptides with same sequence but with different masses were due to the modification during preparation. Methionine residues are normally oxidized to give two different masses, for example in peptides "GVPQPMNPPR" and "AIESHICLFGSCMR". Alkylation was required for effective identification of cysteine containing peptides and carbamidomethyl modifications were found in "CDDSVMIIDDSR", "AIESHICLFGSCMR" and "TPLILACTNDDLYDVAK". Figure 4.4b shows the coverage of identified peptides in RAP1 protein. The coverage was much better at the N-terminus which could be due to the ideal size of cleaved peptides for identification. Peptides that are either too big or too small are difficult to be picked up by MS, for instance "LYHV" (373-376) and "EDGLCVICVDAPSEAVCVPCGHVAGCISCLK" (321-351). However, there is still a significant coverage for the expressed GST-RAP1, suggesting RAP1 was properly expressed and purified. In addition, high coverage of peptides from GST were also found (data not shown) which indicates that the purification of RAP1 was due to the fusion to GST.

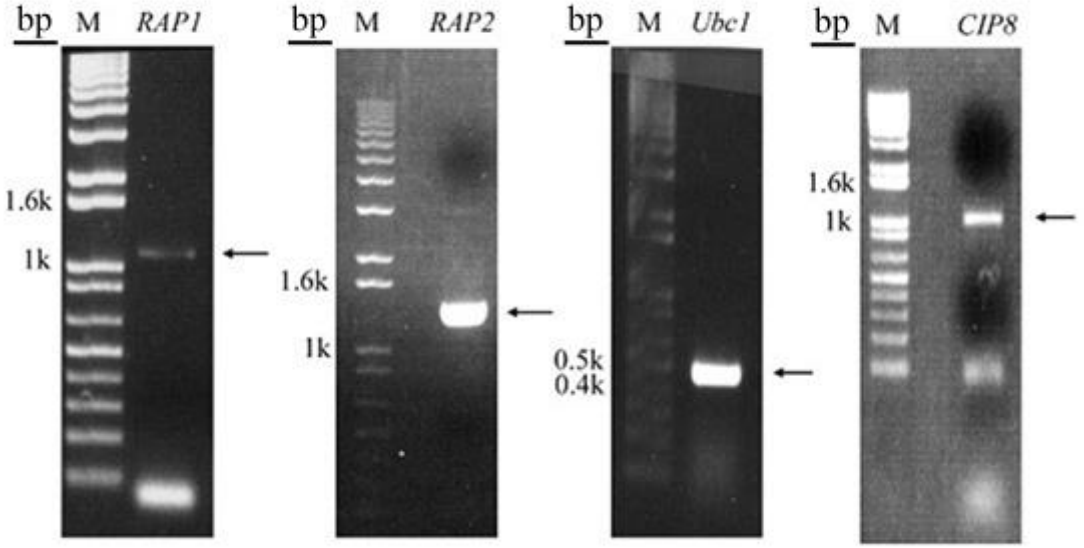

Figure 4.2 RT-PCR of full length cDNAs of *RAP1, RAP2, Ubc1* and *CIP8*.
Fragments were amplified by using proof-reading enzyme *Pfu* and subsequently cloned into expression vector pGEX-4T1.

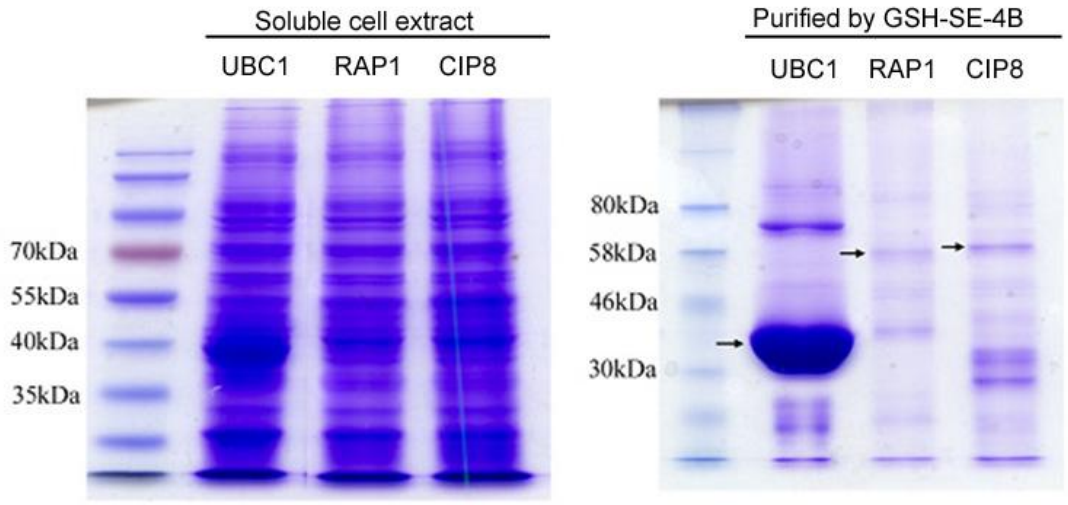

Figure 4.3 SDS-PAGE analysis for the expression of GST fused UBC1, RAP1 and CIP8 in *E. coli* BL21(DE3) cells.
Soluble cell extracts were extracted in PBS after cell bursting by sonication. Glutathione-sepharose 4B (GSH-SE-4B) was added to the extracts to bind GST fusion proteins and followed by elution in 10mM GSH. Arrowed bands indicate the desired proteins with expected sizes.

a)

zinc finger (C3HC4-type RING finger) family protein / ankyrin repeat family protein gi|18414200

Peptide Information

Calc. Mass	Obsrv. Mass	± da	± ppm	Start Seq.	End Seq.	Sequence	Ion Score	C. I. %	Modification	Rank	Result Type
900.5149	900.5342	0.0193	21	365	372	ANIDQVIK					Mascot
902.5168	902.564	0.0472	52	195	201	MVIPLWK			Oxidation (M)[1]		Mascot
930.4904	930.5341	0.0437	47	242	248	RWAQVDR					Mascot
994.4952	994.5547	0.0595	60	233	241	ESGFISQAR					Mascot
1038.4851	1038.5497	0.0646	62	120	128	DEGYSNVVR					Mascot
1092.5619	1092.6292	0.0673	62	274	283	GVPQPMNPPR					Mascot
1108.5568	1108.6212	0.0644	58	274	283	GVPQPMNPPR	14	0	Oxidation (M)[6]		Mascot
1108.5568	1108.6212	0.0644	58	274	283	GVPQPMNPPR			Oxidation (M)[6]		Mascot
1150.5963	1150.6812	0.0849	74	233	242	ESGFISQARR					Mascot
1198.6942	1198.7637	0.0695	58	162	172	VWVVVVPTGSR	62	99.03			Mascot
1198.6942	1198.7637	0.0695	58	162	172	VWVVVVPTGSR					Mascot
1326.7892	1326.8621	0.0729	55	161	172	KVWVVVVPTGSR	76	99.967			Mascot
1326.7892	1326.8621	0.0729	55	161	172	KVWVVVVPTGSR					Mascot
1441.5934	1441.6865	0.0931	65	212	223	CDDSVMIIDDSR			Carbamidomethyl (C)[1], Oxidation (M)[6]		Mascot
1448.7128	1448.7937	0.0809	56	27	40	SLHHEGAGLEGVDK					Mascot
1449.7697	1449.8483	0.0786	54	61	73	TLLELGSNVNAYR	69	99.842			Mascot
1449.7697	1449.8483	0.0786	54	61	73	TLLELGSNVNAYR					Mascot
1680.7655	1680.8638	0.0983	58	129	142	AIESHICLFSGCMR			Carbamidomethyl (C)[7,12]		Mascot
1696.7604	1696.8523	0.0919	54	129	142	AIESHICLFSGCMR			Carbamidomethyl (C)[7,12], Oxidation (M)[13]		Mascot
1759.9225	1760.0188	0.0963	55	180	194	LELVLYDSIQDAQPR	92	100			Mascot
1759.9225	1760.0188	0.0963	55	180	194	LELVLYDSIQDAQPR					Mascot
1778.9031	1778.9969	0.0938	53	113	128	TALEVARDEGYSNVVR					Mascot
1818.996	1819.0769	0.0809	44	96	112	LLLSHGANPLVLDDDVK					Mascot
1921.9575	1922.0721	0.1146	60	44	60	TPLILACTNDDLYDVAK			Carbamidomethyl (C)[7]		Mascot
1977.1643	1977.1656	0.0013	1	162	179	VWVVVVPTGSRNPTKPLK					Mascot
1995.0546	1995.1616	0.107	54	143	160	EYSGSSLLNLFAPQLLSR					Mascot
2164.0728	2164.1926	0.1198	55	287	307	TSQATTTTTNVPALSDDALTR					Mascot
2538.3926	2538.5298	0.1372	54	173	194	NPTKPLKLELVLYDSIQDAQPR					Mascot

b)

Figure 4.4 Mass spectrometry analysis of expressed GST-RAP1.
a) Result of identified peptides with predicted masses of trypsin cleaved RAP1. **b)** Alignment of the identified peptides to the RAP1 protein sequence.

4.3 E3 ligase activity assay of RAP1

E3 ligases catalyse the polymerization of ubiquitins (Figure 4.1) and leading to a mixture of ubiquitin chains with various numbers of ubiquitins. As the monomeric size of ubiquitin is 10kDa, so a "ladder" of bands with 10kDa differences are observed in a western blot if anti-ubiquitin antibody is used to detect ubiquitin. Figure 4.5a shows that the polymerization of ubiquitin occurred only if E1, E2 and E3 (RAP1 or CIP8) were present in the reaction mixture. Both RAP1 and CIP8 were able to demonstrate E3 ligase activity, which generated ladders of ubiquitin, but the activity of RAP1 was significantly lower than that of CIP8. The E3 ligase activity of RAP1 (polymerization of ubiquitin) could be demonstrated when the time of incubation was longer or more RAP1 was added into the reaction mixture (data no shown). As RING domains are found to be essential for E3 ligase activity (Lorick et al. 1999), mutation of the RING domain may abolish the E3 ligase activity of RAP1. To test this cysteine residue C340 in the RING domain of RAP1 was replaced by a serine residue (C340S). This resulted in no detectable RAP1 E3 ligase activity (Figure 4.5b), indicating that the E3 ligase activity of RAP1 is dependent on the RING domain.

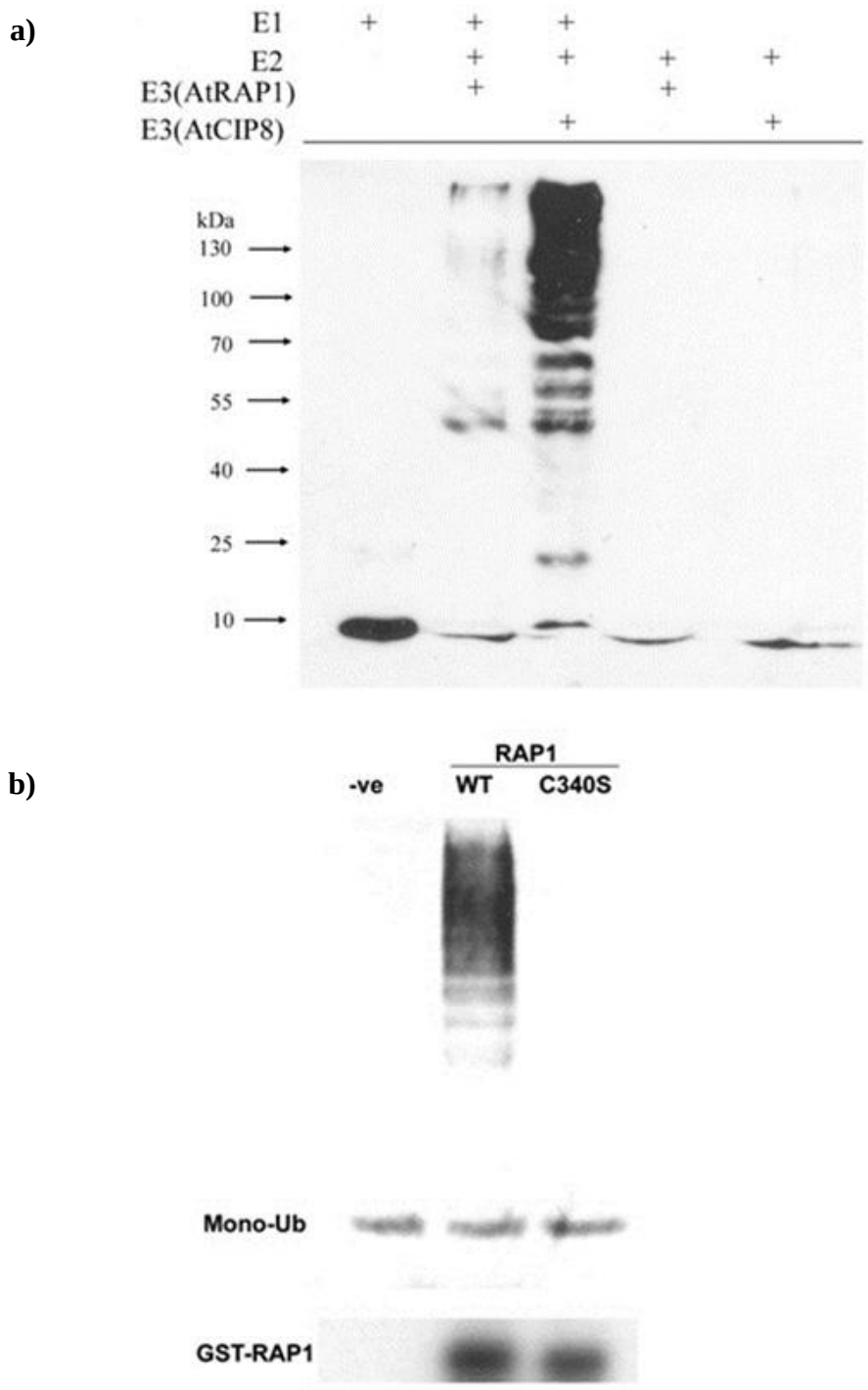

Figure 4.5 E3 ligase activity assay of RAP1.
a) Monomeric ubiquitin were mixed with E1 (HsUBA1), E2(AtUBC1) and E3 (AtCIP8 or AtRAP1) in the presence of ATP. Polymerization of ubiquitin was visualized via western-blot analysis using ubiquitin antibodies. **b)** RAP1 proteins with mutated RING domain (C340S) was expressed and included in an E3 ligase activity assay. Polymerization of ubiquitin occurred only when WT RAP1 was used and no activity was detected with the mutated RAP1(C340S).

4.4 Biotin-switch analysis of RAP1

The recombinant GST-RAP1 proteins were treated with the NO-donors (GSNO or CysNO) prior to the activity assay to explore the potential impact of NO on RAP1 E3 ligase activity. When a low concentration (0.1mM or 0.25mM) of GSNO was applied, no reduction of RAP1 activity was observed. However, when 1mM of GSNO was used, the polymerization of ubiquitin was significantly reduced, revealing that the E3 ligase activity was inhibited by a high GSNO concentration (Fig 4.6a). As GSNO is composed of glutathione (GSH), addition of GSH was utilised as a control to check for specificity (Dalle-Donne et al. 2009). In the presence of 1mM GSH, there was no damage of E3 ligase activity, suggesting NO might modulate the E3 ligase activity of RAP1. The idea was reinforced because 1mM CysNO (S-nitrosocysteine) also reduced the activity of RAP1 significantly.

To further study the relationship between NO and the E3 ligase activity of RAP1, different concentrations of CysNO were applied (Fig 4.6b). The activity was gradually reduced from as the concentration of applied CysNO increased from 0.25mM to 1mM, as less polymerization of ubiquitin was observed. The lowered activity is also reflected by the increased accumulation of monomeric ubiquitin (mono-Ub). Interestingly, the activity was slightly higher at a low CysNO concentration (0.1mM), an effect also observed at 0.1-0.25mM. The effects of GSNO and CysNO seem to be different, as applying GSNO at 0.25mM enhanced RAP1 E3 ligase activity, whereas in the presence of 0.25mM CysNO, the activity of RAP1 was gradually declining. Thus, CysNO is likely to be a more effective NO-donor than GSNO in these experiments.

The presence of NO-donor affected the E3 ligase activity of RAP1. It was speculated that the E3 ligase activity was regulated through the S-nitrosylation of reactive cysteine residues in RAP1 by the NO-donors. In the following contents, RAP1 was shown to be S-nitrosylated and the site of S-nitrosylation site in RAP1 was also identified.

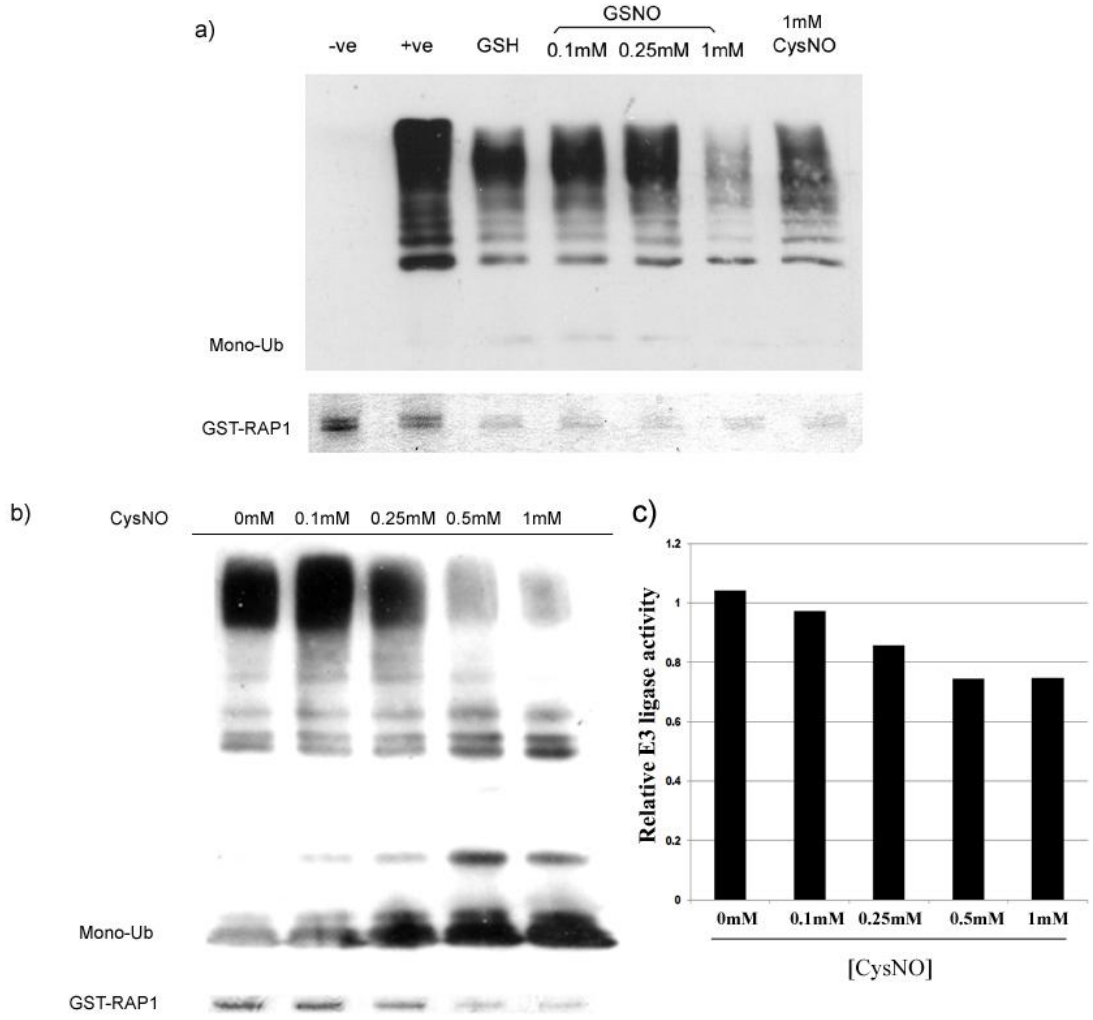

Figure 4.6 Effects of NO-donors on the E3 ligase activity of RAP1.
E3 ligase activity assay of: **a)** Purified GST-RAP1 that was pre-treated with GSH, GSNO (0.1mM, 0.25mM or 1mM) or CysNO (1mM). **b)** Similar to (a), GST-RAP1 was pre-treated with various concentrations of CysNO (0mM, 0.1mM, 0.25mM, 0.5mM and 1mM). Pre-treated GST-RAP1 proteins were purified by Zeba desalting columns and mixed with E1/E2/Ub. Polymerization of ubiquitin was detected by ubiquitin antibodies in a western blot. c) Relative E3 ligase activity after CysNO treatment. The relative activity was calculated by the signal of monomeric ubiquitin normalized with the signal of GST-RAP1.

4.5 Identification of S-nitrosylation sites of RAP1

Results in chapter 4.3 have shown that application of NO donors altered E3 ligase activity of RAP1. The impact of NO on RAP1 E3 ligase activity may be due to the S-nitrosylation of one or more cysteine residues in RAP1. To verify whether RAP1 is S-nitrosylated, a technique known as biotin-switch was used (Forrester et al. 2009) (Figure 4.7). Initially, RAP1 proteins were treated with NO donors (GSNO or SNO) which potentially can S-nitrosylate reactive cysteines. Application of methylmethane thiosulfonate (MMTS) blocked cysteine residues without S-nitrosylation and the S-NO group of S-nitrosylated cysteines were reduced by ascorbate and replaced by a biotin group that could be detected by anti-biotin antibodies or pulled-down by streptavidin.

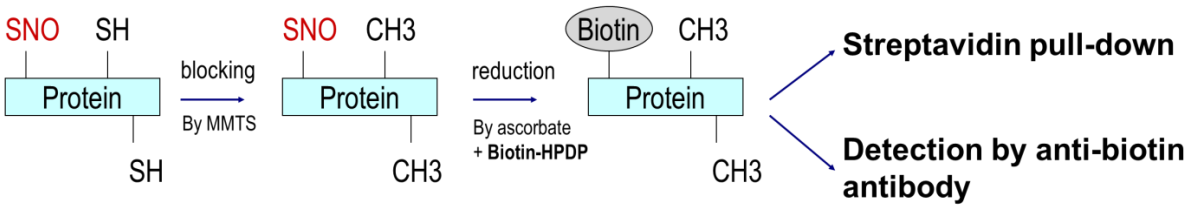

Figure 4.7 A schematic diagram to illustrate the mechansim of biotin-switch for detection of S-nitrosylation of proteins.

A strong signal was detected by anti-biotin antibody upon the application of GSNO to recombinant GST-RAP1, whereas a much weaker band was observed if no GSNO was added (Figure 4.8a). Cysteine-rich (29 Cys residues) bovine serum albumin (BSA) was also used as a control. BSA was S-nitrosylated, but it was less readily S-nitrosylated, as the intensity of signal was lower and more protein was required when comparing with GST-RAP1. The biotin-switched GST-RAP1 could also be pulled down by steptavidin and detected by anti-GST antibody (Figure 4.8b), indicating the signal detected by anti-biotin antibody in Fig 4.8a was from GST-RAP1. This result suggests that RAP1 is S-nitrosylated.

Due to the secondary structure of a protein, cysteine residues can be hindered and not readily be S-nitrosylated by NO donors. There are 14 cysteine residues in RAP1, in order to verify how easy of these residues are being accessed. SDS was applied to

relax the secondary structure of GST-RAP1 and expose all the cysteine residues to GSNO. Figure 4.8b showed that more GST-RAP1 was pulled down by steptavidin if SDS was added together with GSNO prior to the biotin-switch, indicating that some cysteine residues are obscured in native RAP1 proteins. Similarly, RAP1 was shown to be S-nitrosylated upon CysNO treatment and applying SDS also increased the intensity of signal (Figure 4.9a). As from the previous results (Fig 4.6b), increasing the applied concentration of CysNO altered the E3 ligase activity of RAP1. In order to explore if alternation in RAP1 E3 ligase activity following exposure to NO donors was due to S-nitrosylation of RAP1, various concentrations of CysNO were used to treat GST-RAP1 prior to the biotin-switch. It was observed that no signal was detected when 0mM or 0.1mM of CysNO was applied. The signal was gradually increasing with 0.25mM and 0.5mM CysNO applied and dramatically enhanced if 1mM CysNO was applied.

Treatment of SDS to RAP1 (Figure 4.8b & Figure 4.9a) indicated that not all cysteine residues in native RAP1 are exposed and readily S-nitrosylated. In order to identify the sites of S-nitrosylation, mass spectrometry was carried out. The sites of S-nitrosylation in RAP1 proteins were replaced by a biotin through the biotin-switch. The biotinylated RAP1 proteins were subsequently digested by trypsin into peptide fragments and peptides with increase of mass due to the addition of a biotin group could be detected by a mass spectrometer. Figure 4.10 shows the comparison of peptide coverage between untreated and CysNO-treated RAP1 and it was observed that the CysNO-treated samples had a reduced coverage from 87% to 77%. Most of the unidentified peptides were cysteine containing peptides which could be due to the lack of alkylation procedures by DTT and iodoacetamide. In addition, the key peptide, RING containing peptide "EDGLCVICVDAPSEAVCVPCGHVAGCISCLK" could be too heavy to be identified, and the situation would be even more challenging if more than one cysteine residue (total of 6 residues) were biotinylated. Several attempts with various adjustments including double-digestion with trypsin and LysC, use of lighter labelling method (MMTS/Iodoacetamide) (Chen et al. 2007) and use of truncated RAP1 protein were undertaken. However, the S-nitrosylated cysteine(s) could not be identified.

A truncated form of RAP1 (237 -376 a.a.) was expressed in *E. coli* which lacks of the ankyrin repeats but includes the RING domain with 8 cysteine residues. Comparing to the full-length RAP1, the expression level of the truncated RAP1 (RAP1-RING) was significantly improved (Figure 4.11a), suggesting the poor expression of full length RAP1 could be due to the N-terminal ankyrin repeats. Site-directed mutagenesis was carried out to generate four mutated proteins (RAP1-RING-C325H, RAP1-RING-C328H, RAP1-RING-C337H and RAP1-RING-C340H), each of which has a single replacement of a cysteine residue in the RING domain. The mutated proteins were expressed and purified with similar expression levels as the wild type RAP-RING protein (Figure 4.11b).

Biotin-switch analysis showed that the truncated RAP1 (GST-RAP1-RING) was S-nitrosylated and there was no significant difference in signals between the wild-type and mutated proteins, suggesting either the S-nitrosylated (target) cysteine might not have been mutated or multiple cysteine residues were S-nitrosylated. Mass spectrometry data suggested that some cysteine residues in the GST were also biotinylated (S-nitrosylated), therefore the GST part of the fusion proteins was removed. A thrombin cleavage site was located in between GST and RAP1-RING, so GST was removed by GSH-Sepharose-4B after thrombin digestion. Fig 4.12b showed the unbound proteins after thrombin digestion and incubation with GSH-Sepharose-4B, RAP1-RING proteins were purified with a size around 12kDa, which should be below the 25kDa marker band whereas the size of GST is 26kDa.

Collectively, the biotin-switch results showed that WT and all mutated RAP1-RING apart from C325H were S-nitrosylated (Fig 4.12c). Therefore, the site of SNO formation within RAP1 is C325 which is located in the RING domain. In addition, RAP1 C340 could also be another SNO site as the weak signal could be detected. Coincidently, the identified SNO site of RAP1 could be aligned with the SNO site of human XIAP (C450)(Nakamura et al. 2010).

A mutant form of RAP1 (C325H) was also expressed and purified with the replacement of the cysteine residue C325 with a histidine residue. As both cysteine and histidine are similar in chemical properties (Nakamura et al. 2010; Romero-Isart et al. 1999; Yi et al. 1999) but histidine cannot be S-nitrosylated due to the absence of a thiol group. The C325H mutant could be useful to study the role of C325 in protein

function *in vivo*. However, no E3 ligase activity was detected if C325 was replaced (Fig 4.13), suggesting the chemistry of cysteine for C325 is essential for the E3 ligase activity of RAP1.

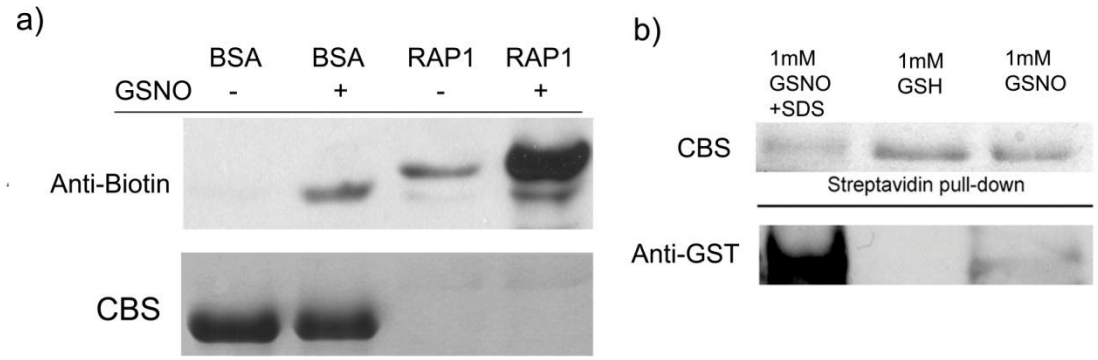

Figure 4.8 S-nitrosylation of RAP1 by GSNO.
a) BSA and GST-RAP1 were treated with GSNO and the S-nitrosylated sites were replaced by a biotin-group that was subsequently detected by anti-biotin antibodies. **b)** Biotinlyated GST-RAP1 protein were pulled down by streptavidin and detected by anti-GST antibody. CBS –Coomassie Blue Staining.

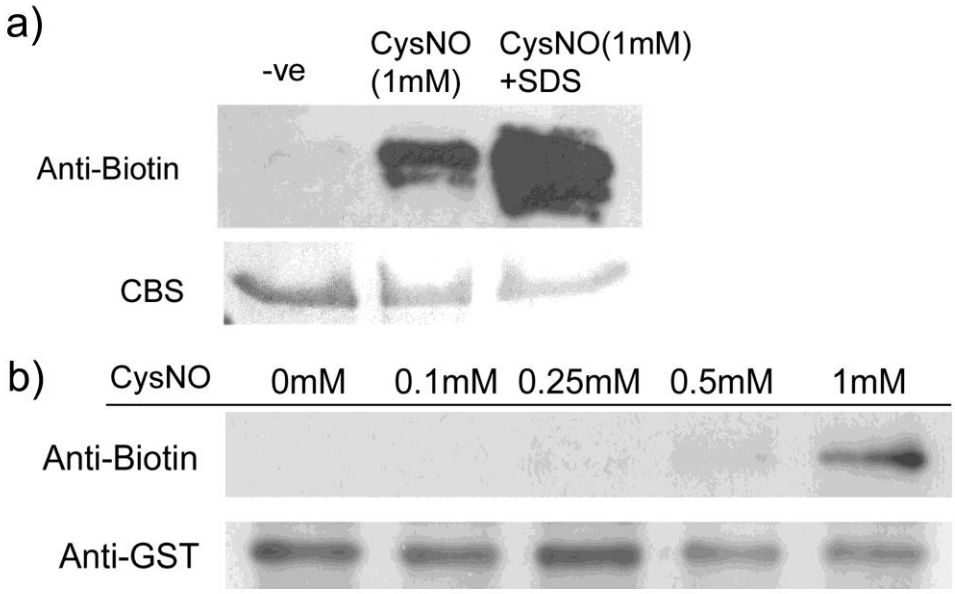

Figure 4.9 S-nitrosylation of RAP1 by CysNO.
a) GST-RAP1 proteins were shown to be S-nitrosylated by CysNO and proteins pretreated with SDS enhanced the level of S-nitrosylation. **b)** GST-RAP1 proteins were pretreated with various concentration of CysNO before Biotin-switch. Protein loading was detected by anti-GST antibodies.

untreated

Nominal mass (M_r): 68004; Calculated pI value: 6.94

Variable modifications: Biotin-HPDP (C),Oxidation (M)
Cleavage by Trypsin: cuts C-term side of KR unless next residue is P
Sequence Coverage: 87%

Matched peptides shown in Bold Red

```
  1 MSPILGYWKI KGLVQPTRLL LEYLEEKYEE HLYERDEGDK WRNKKFELGL
 51 EFPNLPYYID GDVKLTQSMA IIRYIADKHN MLGGCPKERA EISMLEGAVL
101 DIRYGVSRIA YSKDFETLKV DFLSKLPEML KMFEDRLCHK TYLNGDHVTH
151 PDFMLYDALD VVLYMDPMCL DAFPKLVCFK KRIEAIPQID KYLKSSKYIA
201 WPLQGWQATF GGGDHPPKSD LVPRGSPEFM GQQQSQSKDE MLFQEVSNNN
251 VEGIKSLHHE GAGLEGVDKL GRTPLILACT NDDLYDVAKT LLELGSNVNA
301 YRSGCNGGTP LHHAAKRGLV HTVKLLLSHG ANPLVLDDDV KTALEVARDE
351 GYSNVVRAIE SHICLFSGCM REYSGSSLLN LFAPQLLSRK VWVVVVPTGS
401 RNPTKPLKLE LVLYDSIQDA QPRMVIPLWK ANLEEPKSFR CDDSVMIIDD
451 SRSPKSMRQR RESGFISQAR RWAQVDRQIR LKLAAEIKGD MKQMNWFSEA
501 CKGVPQPMNP PRFMKTSQAT TTTTNVPALS DDALTRVAMS LPSPKTANKE
551 DGLCVICVDA PSEAVCVPCG HVAGCISCLK EIENKKMGCP VCRANIDQVI
601 KLYHV
```

CysNO treated

Nominal mass (M_r): 68004; Calculated pI value: 6.94

Variable modifications: Biotin-HPDP (C),Oxidation (M)
Cleavage by Trypsin: cuts C-term side of KR unless next residue is P
Sequence Coverage: 77%

Matched peptides shown in Bold Red

```
  1 MSPILGYWKI KGLVQPTRLL LEYLEEKYEE HLYERDEGDK WRNKKFELGL
 51 EFPNLPYYID GDVKLTQSMA IIRYIADKHN MLGGCPKERA EISMLEGAVL
101 DIRYGVSRIA YSKDFETLKV DFLSKLPEML KMFEDRLCHK TYLNGDHVTH
151 PDFMLYDALD VVLYMDPMCL DAFPKLVCFK KRIEAIPQID KYLKSSKYIA
201 WPLQGWQATF GGGDHPPKSD LVPRGSPEFM GQQQSQSKDE MLFQEVSNNN
251 VEGIKSLHHE GAGLEGVDKL GRTPLILACT NDDLYDVAKT LLELGSNVNA
301 YRSGCNGGTP LHHAAKRGLV HTVKLLLSHG ANPLVLDDDV KTALEVARDE
351 GYSNVVRAIE SHICLFSGCM REYSGSSLLN LFAPQLLSRK VWVVVVPTGS
401 RNPTKPLKLE LVLYDSIQDA QPRMVIPLWK ANLEEPKSFR CDDSVMIIDD
451 SRSPKSMRQR RESGFISQAR RWAQVDRQIR LKLAAEIKGD MKQMNWFSEA
501 CKGVPQPMNP PRFMKTSQAT TTTTNVPALS DDALTRVAMS LPSPKTANKE
551 DGLCVICVDA PSEAVCVPCG HVAGCISCLK EIENKKMGCP VCRANIDQVI
601 KLYHV
```

Figure 4.10 Mass spectrometry analysis of biotin-switched RAP1.
The upper result was the untreated sample and the below result was sample treated with CysNO. Both samples were biotin-switched and digested with trypsin.

a)

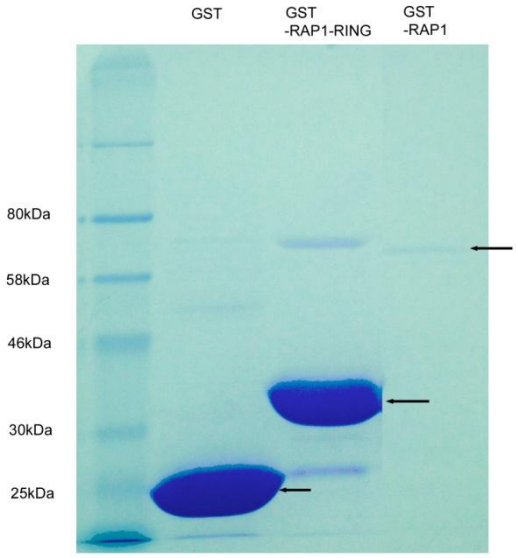

b)

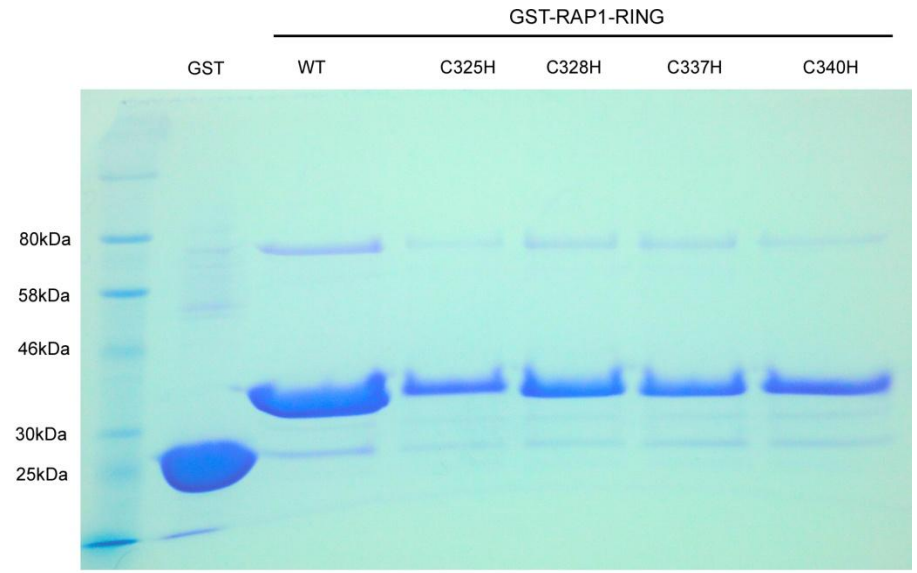

Figure 4.11 Expression of GST-RAP1-RING proteins.
a) A truncated form of RAP1 (C-terminal RING domain) was expressed and purified by GSH-Sepharose-4B (arrowed bands). **b)** A single cystenie residue in the RING domain of the GST-RAP1-RING protein was replaced by a histidine residue (C325H, C328H, C337H and C340H). These proteins were expressed in *E.coli* and purified.

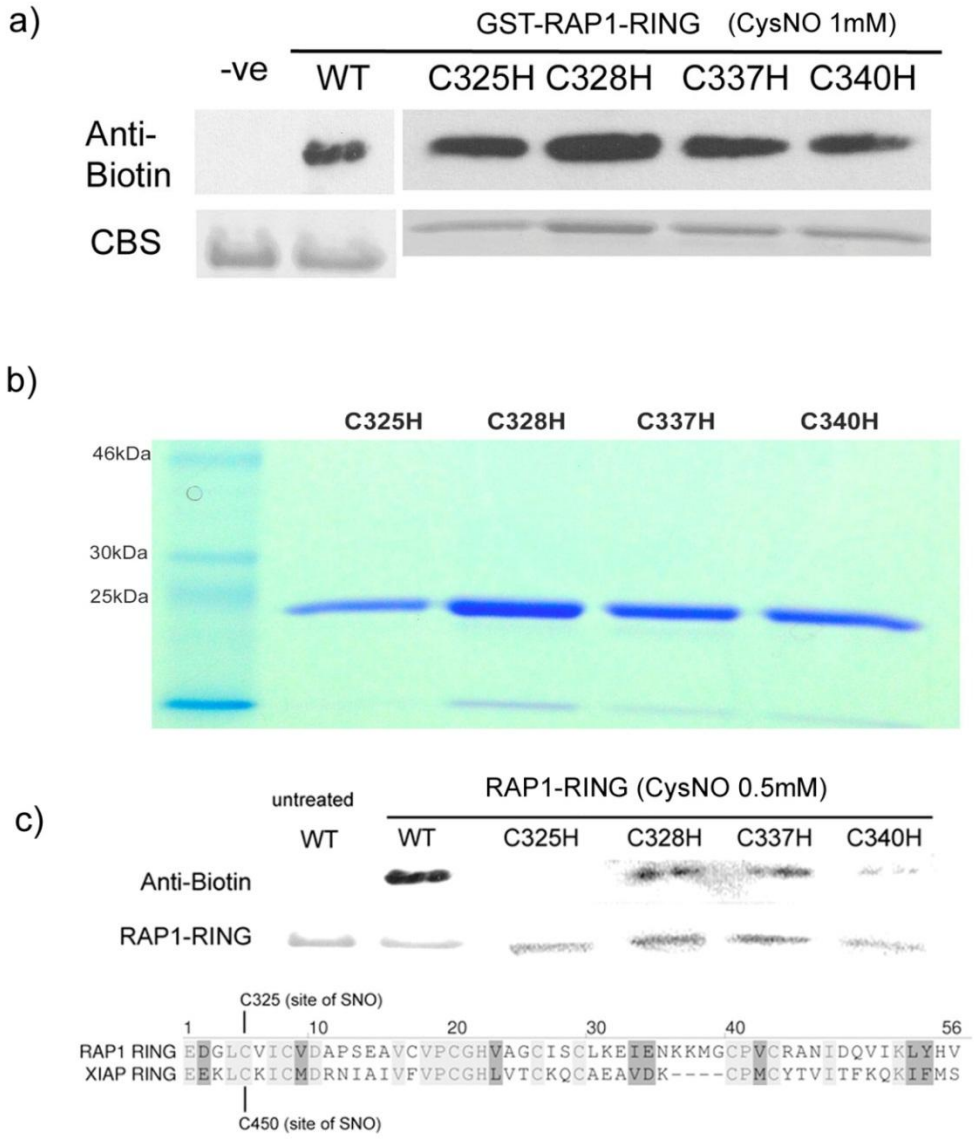

Figure 4.12 Biotin-switch analysis of the mutated RAP1-RING proteins.
a) Biotinlyated GST-RAP1-RING proteins were detected by anti-biotin antibodies. **b)** GST-tag of GST-RAP1-RING proteins were removed by cleavage of thrombin and RAP1-RING proteins were purified by exclusion from GSH-sepharose-4B. **c)** Biotin-switch of RAP1-RING proteins, no signal was detected in the mutant C325H, suggesting C325 is the site of S-nitrosylation. The C325 of RAP1 can be aligned with the C450 in human XIAP, which has shown to be S-nitrosylated.

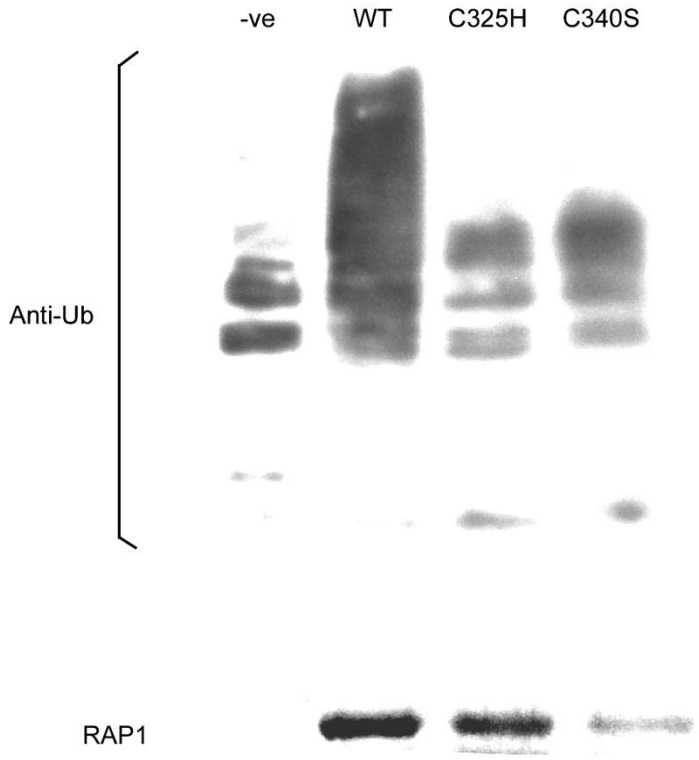

Figure 4.13 Replacement of the cysteine residue to histidine (C325H) abolished the E3 ligase activity of RAP1.
Full length RAP1 (WT, C325H and C340S) proteins were expressed, purified and mixed with E1/E2/Ub. Polymerization of ubiquitin was detected only in WT RAP1. The loading of RAP1 was shown by coomassie blue staining.

4.6 Discussion

Recombinant zinc-finger containing proteins are known to be recalcitrant to express (Casademunt et al. 1999; Geng and Carstens 2006) due to their poor solubility and their protein/DNA binding property may be toxic to host cells (e.g. *E. coli*). However RING proteins are zinc-finger E3 ligases, and the protein binding property of E3 ligases could also cause problems in expression. The *RAP1* cDNA was also fused to a His-tag sequence and attempted to be expressed in *E. coli*, but the outcome was unsatisfactory (data not shown). Glutathione S-transferase (GST) has been commonly used as a fusion protein to enhance solubility of zinc-finger/RING protein expression (Geng and Carstens 2006; Stone et al. 2005). Furthermore, GST-fusion proteins can be effectively purified by glutathione-conjugated-resin, which is more specific than His-tag based purification. GST fusion proteins of RAP1, RAP2 and CIP8 were successfully expressed and purified, but the levels of expression were much lower than those of GST alone or GST-UBC1 (Fig 4.3, 4.11a). Due to the poor expression, non-specific proteins were also purified by GSH-Sepharose-4B. Interestingly, the poor expression of RAP1 seems to be due to the presence of the ankyrin repeat rather than the zinc-finger containing RING domain, as the expression was much improved after removal of the ankyrin repeat. The ankyrin repeat is often associated with the binding of membrane proteins, for instance, *Arabidopsis* ankyrin repeat protein, AKR2A binds to the chloroplast outer envelope membrane (OEM) and functions as a cytosolic mediator for sorting and targeting of nascent chloroplast OEM proteins to the chloroplast (Bae et al. 2008). The ankyrin repeat of RAP1 may also bind to membrane proteins in *E. coli* which result in difficulty in extracting proteins from the cell. Mild extraction approaches (no detergent and reducing agent) were used in this study to minimize the damage of expressed proteins, therefore the amount of purified E3 proteins was relatively low. As the predicted band of RAP1 was not as strong as that of UBC1, in order to confirm the protein identity, the protein band was excised for mass spectrometry (MS). The MS result showed a high coverage of protein identity of RAP1, suggesting the RAP1 was properly expressed.

After optimization, the expressed RAP1 showed strong E3 ligase activity, confirming that RAP1 is a functional E3 ligase. This contradicts a previous study which had shown no E3 ligase activity for RAP1 (Stone et al. 2005). This might be due to the use of an alternative E2 enzyme AtUBC1, instead of AtUBC8 used in the previous

study. AtUBC1 has previously been successfully used in an E3 ligase assay for a disease-related RING protein RIN2 (Kawasaki et al. 2005). In addition, as AtUBC1 was strongly expressed, the resulting cell extract was directly used in the E3 ligase activity assay. It was observed that the activity of RAP1 was much better if cell extract was used rather than purified AtUBC1 (data not shown), suggesting cofactors or ions in the cell extract might be required for the activity of RAP1. In addition, no ubiquitin polymerization was detected in the absence of E1, E2 or E3 (RAP1), revealing that all three enzymes are essential for the RAP1-dependent E3 ligase activity, which is in line with findings of other E3 ligase studies.

The RING domain of RAP1 belongs to a class of RING-HCa C3HC4, which is composed of 8 cysteine residues. The characteristic of HCa type RING domain is the presence of a glycine (G341) residue just before the conserved histidine (H342) residue (Stone et al. 2005). Metal ligand (zinc-binding) residues of C3HC4 are the three cysteine residues in front of the H342 (C328, C337 and C340), H342 and the four cysteine residues after H342 (C346, C349, C360 and C363), therefore the first cysteine (C325) is probably not involved in zinc binding. A single mutation of C340 to a serine (C340S) abolished the E3 ligase activity of RAP1, which is probably due to the loss of zinc binding. This indicates that the E3 ligase activity of RAP1 is dependent on the RING domain.

The activity of RAP1 was also affected by NO donors. Prior to an activity assay, RAP1 was treated with GSNO or CysNO and the unreacted NO donors were removed by desalting columns. Results showed that the activity of RAP1 was significantly reduced if RAP1 was pre-treated with 1mM of GSNO or 0.5mM-1mM of CysNO. Application of NO donors may lead to S-nitrosylation of cysteine residues in RAP1, and studies in neuronal cells have demonstrated that nitrosative stress promotes S-nitrosylation of E3 ligases (Nakamura et al. 2010; Yao et al. 2004), which subsequently reduce the activity of these E3 ligases. Interestingly, a study of a Parkinson's disease related E3 ligase parkin has shown that S-nitrosylation initially led to a dramatic increase, followed by a decrease in the E3 ligase-ubiquitin-proteasome degradative pathway. The study claimed that the initial increase in parkin's E3 ubiquitin ligase activity could lead to autoubiquitination of parkin and subsequent inhibition of its activity. However, the observation in this study

demonstrates that pre-treatment of RAP1 with low concentration of GSNO (0.25mM) /CysNO (0.1mM) slightly increases E3 ligase activity (Fig 4.6). Biotin-switch data points out that RAP1 was only weakly S-nitrosylated at a low concentration of CysNO (0.1mM-0.25mM) (Figure 4.9b), suggesting RAP1 may also be S-nitrosylated at low concentrations but this may be was rather transient. However, S-nitrosylation could still lead to changes in protein structure, resulting in the increase in E3 ligase activity. On the other hand, the site of this transient S-nitrosylation could be different from the S-nitrosylated site (C325) under high CysNO concentration (1mM). These findings provide clues that RAP1 may be able to resist nitrosative stress at the early stage if the levels of reactive NO are not high enough to shut down the activity of RAP1 and hence RAP1 could function as a "buffer protein" of nitrosative stress. However, in the later stage of nitrosative stress, higher GSNO concentrations might abolish activity of RAP1 through the stable S-nitrosylation of cysteine residue C325 (Figure 4.12c).

The secondary structure of RAP1 also affects the efficiency of S-nitrosylation. Application of SDS tremendously promoted biotinlyation (S-nitrosylation) of RAP1 through GSNO (Figure 4.8b) and CysNO (Figure 4.9a). SDS exposed all cysteine residues where access of NO donors was used to be prohibited due to the hindrance of secondary structure, suggesting the difficulty of S-nitrosylation in low concentration of GSNO/CysNO could be due to the structure of native RAP1.

Although evidence clearly indicated that RAP1 is S-nitrosylated, the identification of the target site was a relatively a complicated task. Two similar studies for parkin (Yao et al. 2004) and XIAP (Nakamura et al. 2010) in neuronal cells used mass spectrometry (MS) to identify the sites of S-nitrosylation. However, the results of these studies were quite different. Five of seven cysteine residues in the RING I domain of parkin were candidates to be S-nitrosylated, but there was only one cysteine (C450) that was S-nitrosylated in XIAP. The methods used in these studies were direct detection of SNO-groups in the RING domains, but this requires relatively stable SNO formation because SNO-groups are routinely highly unstable and can be easily removed during trypsin digestion and protein purification. Therefore, instead of direct detection of the SNO-group, the S-nitrosylated site(s) of RAP1 were replaced by a more stable biotin group, which could also be detected by MS due to the mass

difference. Unfortunately, the tryptic peptide including all the important cysteines in the RING domain was too heavy to be detected and the problem increased further following biotinylation. In addition, it has been commonly observed that the peptide coverage of CysNO treated samples was lower which could be due to unknown modification of cysteines (e.g. disulphide bonds). Adjustments such as double digestion with LysC/Trypsin, use of truncated RAP1 or MMTS/IAM labelling method did not provide strong evidence to conclude which cysteine is S-nitrosylated, suggesting MS may not be an ideal approach to identify S-nitrosylation sites in RAP1.

As the cysteine residues of the RING domain are the potential target for S-nitrosylation, a truncated form of RAP1 (RAP1-RING) was expressed to exclude cysteines (6 out of 14) that were not in the RING domain. In addition, the individual cysteine residue in the RAP1-RING was replaced by a histidine residue and biotin-switched, the expressed protein with a mutated site for S-nitrosylation would therefore not be biotinylated. The biotin-switch data showed that all WT and mutated GST-RAP1-RING proteins were S-nitrosylated (Figure 4.12a), but MS data revealed that some of the cysteine residues in the GST-tag were also biotinylated upon treatment with 1mM CysNO. Therefore the GST-tagged the fusion proteins might not be able to reflect the actual situation. As a result, the GST-tag was removed by thrombin and further, a lower concentration of CysNO (0.5mM) was used to increase specificity towards the S-nitrosylation of the reactive cysteine. It can be clearly observed that the RAP1-RING mutant C325H was not biotinylated (Figure 4.12c), indicating that C325 could be the site of S-nitrosylation in RAP1. The C325 in RAP1 can also be aligned with the C450 of XIAP which is the site of S-nitrosylation in XIAP. NMR spectra revealed that formation of S-nitrosothiol on the RING domain of XIAP induced minor conformational perturbations to proximate amino acid residues (e.g., K448, L449, I458, and L468) but not unfolding of the RING domain (Nakamura et al. 2010). While L449 and L468 of XIAP match the position of L324 and V343 in RAP1, an identical region VPCGH is found and aligned in both RAP1 (338-342 a.a.) and XIAP (463-467 a.a.), suggesting RAP1 may also show similar shift as XIAP upon S-nitrosylation. In contrast, C450 of XIAP is involved in zinc binding but C325 of RAP1 may not bind zinc as it is the fourth cysteine in front of the conserved histidine (H342). However, the cysteine residue C337 of RAP1 may not be involved in zinc binding as it does not aligned with XIAP (F462). Thus, RAP1 could still have similar

chemical/structural properties as XIAP. In summary, the reduction in E3 ligase activity of both RAP1 and XIAP is probably due to the inhibition of zinc binding by S-nitrosylation at C325.

To study the effect of S-nitrosylation of C325 in RAP1 *in vivo* and *in vitro*, the C325 of full length RAP1 was replaced by a histidine residue. As histidine shares some similar properties with cysteine such as zinc coordination but cannot be modified by NO donor due to the absence of a thiol group, it was proposed that this mutant may be able to resist S-nitrosylation by CysNO at high concentration (1mM) and still be able to maintain its E3 ligase activity. However, no E3 ligase activity was detected in the mutant C325H, revealing that the chemistry of cysteine for C325 is critical for the activity. It would be therefore, be difficult to unveil the role of S-nitrosylation in the regulation of RAP1 E3 ligase function *in vivo*. Nonetheless, our results suggest that RAP1 is S-nitrosylated at residue C325 and that the E3 ligase activity of RAP1 is regulated by S-nitrosylation.

Chapter 5

5 Identification of *RAP1* and *RAP2* Mutant Lines

5.1 Introduction

The expression profiles of *RAP1* indicate that *RAP1*is related to wounding and defence. RAP1 can also be S-nitrosylated *in vitro* and its E3 ligase activity can be regulated by S-nitrosylation. However, the physiological importance of *RAP1* was yet to be defined. In order to study the physiological importance of *RAP1*, a knock-out mutant line of *RAP1* (*rap1*) was identified. In addition, as RAP2 is also very similar to RAP1 in protein sequence, the *RAP2* mutant (*rap2*) was also isolated. The T-DNA insertion sites of *rap1* and *rap2* were confirmed using gene-specific PCR reaction. Although the T-DNA insertion sites of *rap1* and *rap2* were both located in introns, no transcripts of *RAP1* or *RAP2* were detected. This suggested that the T-DNA insertions have knockout the target gene in the mutant lines. The confirmed *rap1* and *rap2* mutants were crossed to generate the *rap1/rap2* double mutants. Two double mutant lines (A14 and A91) were identified by genotyping PCR. In addition, *RAP1* was also overexpressed in a Col-0 background driven by a cauliflower mosaic virus 35S promoter (i.e. 35S::*RAP1*/Col-0). Lines with significantly elevated *RAP1* transcript levels were selected for further analysis.

5.2 Identification of the *RAP1* Mutant Line

Several T-DNA insertion lines of *RAP1* were found in the *Arabidopsis* Information Resource (TAIR), which were FLAG_357A03, ossowski_1161734, SALK_056294 and SAIL_395_E02 and GK-708C04-022874. SALK_056294 and GK-708C04-022874 were unlikely to be used as the insertions are located before and after the ORF respectively. As it has been reported that T-DNA insertion into an intron can also effectively knock-out the gene (Wang 2008), the three intron insertion lines (FLAG_357A03, ossowski_1161734 and SAIL_395_E02) could still be usable. FLAG_357A03 and ossowski_1161734 were lines where T-DNA had inserted into the 6th intron which could probably knock-out the RING domain but not the ankyrin repeat at the N-terminus. The SAIL_395_E02 line has an insertion in the second intron, which could terminate the transcription of a large proportion of the *RAP1* ORF.

Further, the SAIL_395_E02 line has been included in a recent study of lateral root development (Prasad et al. 2010), revealing the line is promising for further study. The line SAIL_395_E02 was selected for further analysis and disruption of *RAP1* in this line was through the insertion of a vector pCSA110. Two pairs of primers (LB1, LB3/QB1, QB3) were designed based on the sequence of pCSA110 which should be able to amplify DNA fragments by PCR when combined with the gene specific primers of *RAP1* (Start-F, 474R and 684R). DNA fragments with various sizes were amplified when using different combinations of pCSA110 and *RAP1* specific primers (Figure 5.1), in which fragments amplified by primer pairs Start-F/QB1, LB1/684R and LB3/474R were selected for further analysis. Sequencing results from the fragment LB1/684R (Figure 5.2) has identified the DNA sequences from both *RAP1* and pCSA110, the site of T-DNA insertion was found to be 397bp after ATG which was located in the second intron.

The parental line of SAIL_395_E02 is CS8846 (*qrt1-2*) which has a mutation in the gene At5g55590 by fast neurons. At5g55590 (*QRT*) encodes a protein with pectin methylesterase activity, which is required for pollen separation during normal development (Francis et al. 2006; Preuss et al. 1994). The line CS8846 does not have other significant phenotypes apart from the pollen grains are released as tetrads, therefore this genetic background should not affect the phenotypic study of *RAP1*. The homozygousity of T-DNA insertion was further proven by genotyping PCR. Figure 5.3a shows the PCR amplification of genomic DNA using *RAP1* gene specific primer pair Start-F/684R to give an expected size of 1377 bp. PCR reactions using genomic DNA of Col-0 and *qrt1-2* plants were able to show a band with expected size, while no PCR products were found in 4 out of 5 of the SAIL_395_E02 plants. This suggested that these 4 plants have T-DNA insertion in both copies of the gene (homozygous). Further, total RNA of the homozygous mutant plants was extracted for RT-PCR assay (Figure 5.3b). A pair of *RAP1* gene-specific primers (180F/831R) flanking the insertion site was able to amplify a fragment (651bp) from *qrt1-2* but not in all the tested insertion lines, indicating the T-DNA insertion was a successful knock-out of the *RAP1* gene and the homozygous line is named *rap1* in this study.

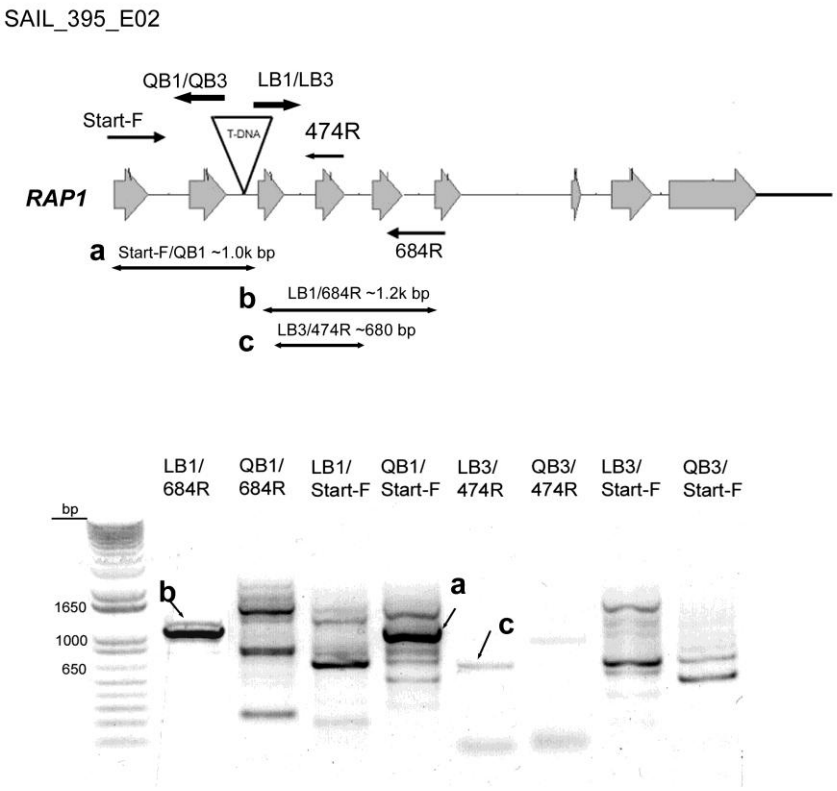

Figure 5.1 Identification of the T-DNA insertion site of SAIL_395_E02 (*rap1*). *RAP1* gene specific primers and pCSA110 specific primers were used to identify the site of T-DNA insertion in SAIL_395_E02 line. Genomic PCR reactions were carried out by using different combinations of the primers, which the positions of the primers were shown in the upper panel. The lower panel shows the results for agarose gel analysis of the PCR product, which the PCR products corresponded to the predicted size (a, b and c). The PCR products were further cloned and sequenced.

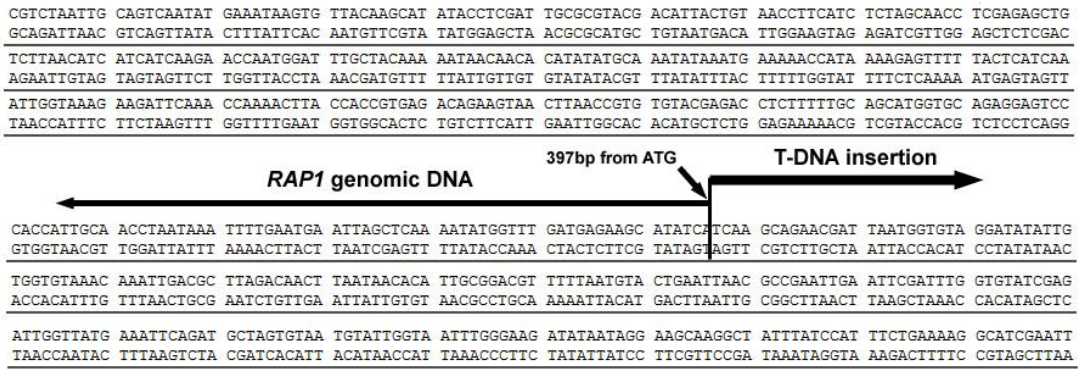

Figure 5.2 Sequencing result of the PCR fragment amplified by LB1/684R. The size of the DNA fragment amplified by LB1/684R (as "b" in Fig 5.1) is ~1.2 kb. T-DNA insertion site was found to be 397bp after the start codon (ATG) of RAP1.

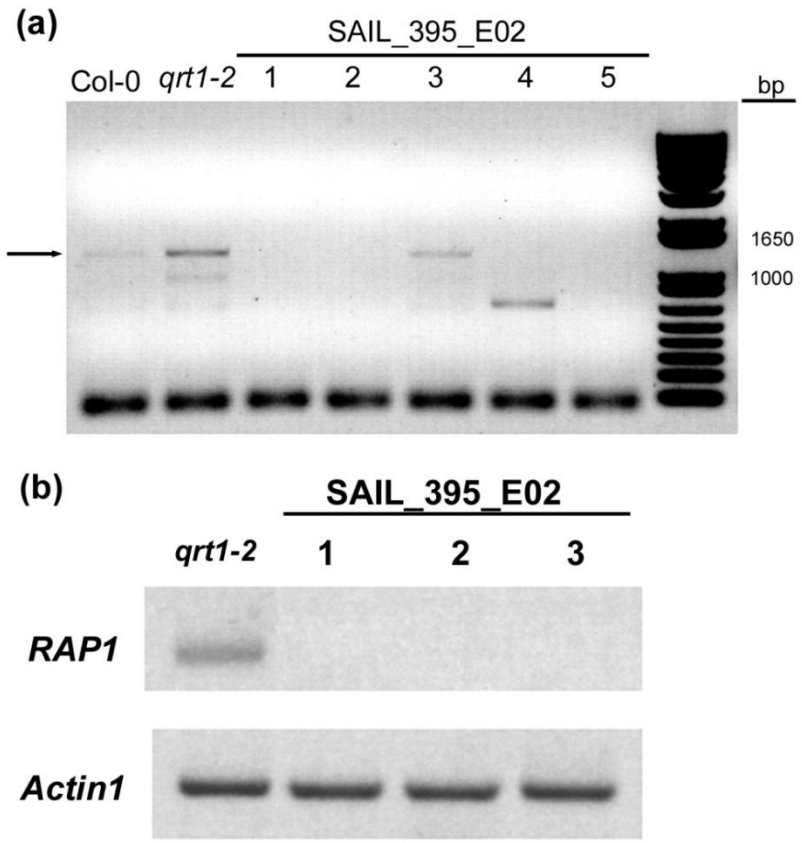

Figure 5.3 Confirmation of *RAP1* T-DNA insertion by genomic PCR and RT-PCR.
a) Genomic PCR results of Col-0, *qrt1-2* and the T-DNA insertion line SAIL_E395_E02. **b)** RT-PCR to detect RAP1 transcripts in *qrt1-2* and SAIL_395_E02 homozygous plants.

5.3 Identification of the *RAP2* Mutant Line

Similarly, identification of *RAP2* knock-out line was based on the information in TAIR and SALK Institute Genomic Analysis Laboratory (SIGnAL). Only two potential lines have the T-DNA insertion in the ORF region, which are GK-407F09-017953 and SALK_104813. The insertion site of GK-407F09-017953 is located in the third intron of *RAP2*, which should disrupt a large proportion of the downstream region of the gene. However, instead of the intron insertion line GK-407F09-017953, SALK_104813 was preferred due to the predicted exon insertion site. The line SALK_104813 has a predicted insertion site in the last exon which could knock-out the important RING domain of RAP2. In addition, as *RAP2* has an alternative transcript (*RAP2.2*), this insertion was likely to disrupt both transcript forms. The T-DNA insertion plasmid for SALK_104813 was pROK2. Specific primers of pROK2 (LB1b/RB1) were used to determine the location and orientation of the insertion. The *RAP2* gene specific primer Rap2F was only able to amplify a band with LB1b, suggesting the orientation of LB1b is towards the 5'-end of the gene (Figure 5.4). Some non-specific bands were amplified in common between *rap1* and *rap2* lines by using this pair of primers, but the specific band about 650 bp was missing in the *rap1* samples. The sequencing result of this 650 bp fragment revealed that the insertion was located at 1883 bp downstream of start codon "ATG" of *RAP2* gene. However, instead of the last exon as expected, the actual T-DNA insertion site was located in the last intron. Nonetheless, the homozygous insertion was still effectively knocking out the *RAP2* gene in the RT-PCR result (Figure 5.10a) and the line is named *rap2* in this study.

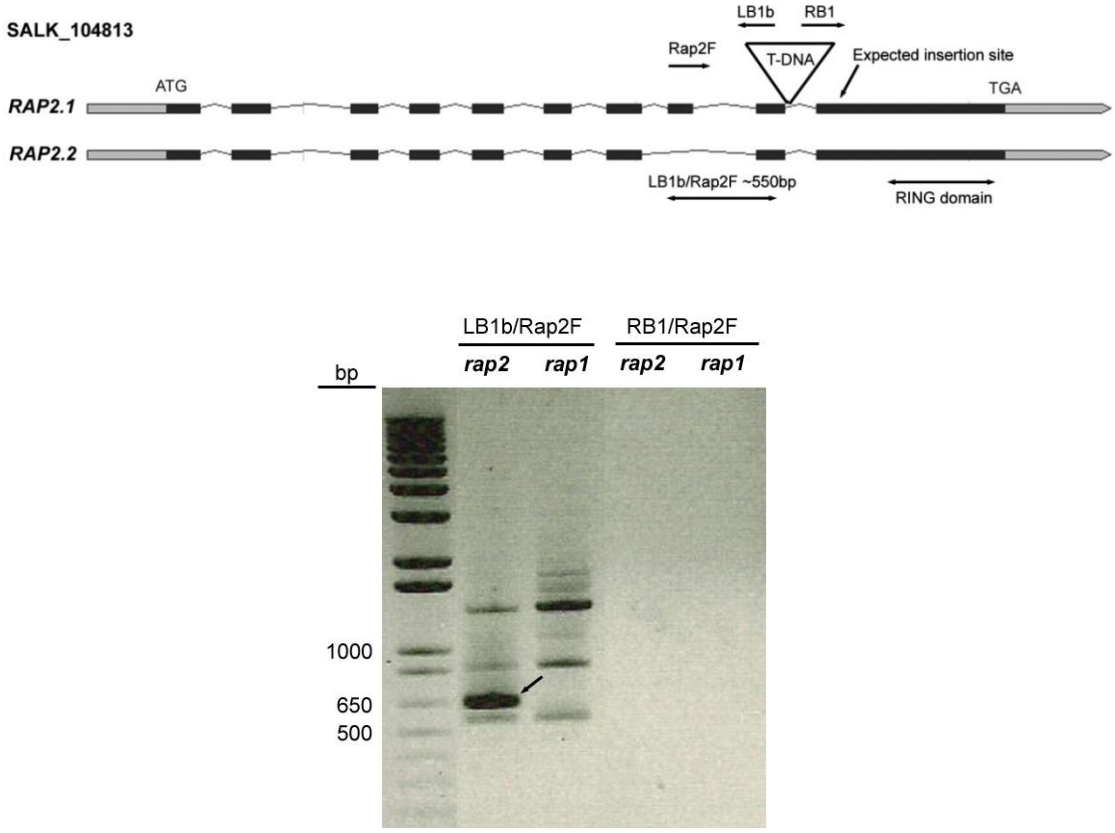

Figure 5.4 Identification of the T-DNA insertion site of SALK_104813 (*rap2*).
A 650 bp fragment was amplified in the *rap2* mutant with primer pair (Rap2F and LB1b) but not in the *rap1* mutant.

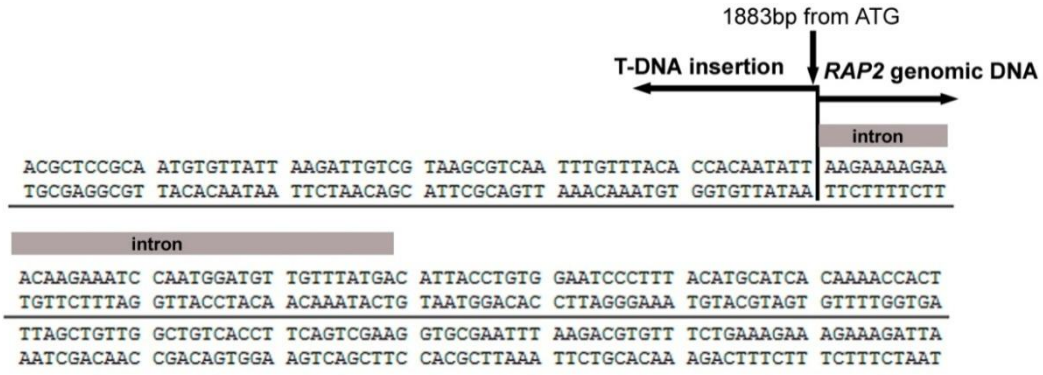

Figure 5.5 Sequencing result of the PCR fragment amplified by LB1b/Rap2F.
The T-DNA insertion site was found to be 1883 bp after the start codon (ATG) of *RAP2* gene.

5.4 Generation of the *rap1/rap2* Double Mutant Lines

The *rap1* and *rap2* single mutants were crossed to generate the *rap1/rap2* double mutant. The *rap1* line was employed as a pollen donor to *rap2* plants and hence the next generation will acquire the *RAP1* insertion as well as basta resistance from the T-DNA of *rap1*. The *rap1* and *rap2* heterozygous plants (i.e. *rap1* +/-; *rap2* +/-) were screened by spraying basta and the resistance plants were further verified by genotyping PCR. Figure 5.6 showed that both the T-DNA insertion from *rap1* and *rap2* were found in the heterozygous *rap1/rap2* mutant as both the specific bands from *RAP1*-pCSA110 (LB1/474R) and *RAP2*-pROK2 (LB1b/Rap2F) were observed. In contrast, only one of the bands was amplified from the single knock-out mutant (*rap1* or *rap2*). The heterozygous *rap1/rap2* plants were self-pollinated and the F2 generation should have a chance of 1/16 for homozygous *rap1/rap2*. Genomic DNA of about a hundred plants were tested by PCR, samples that were unable to show both *RAP1* and *RAP2* bands were suggested to be homozygous *rap1/rap2* plants (Figure 5.7). Three plants (A14, A91 and B41) were found to show the absence of both bands and were isolated for further analysis.

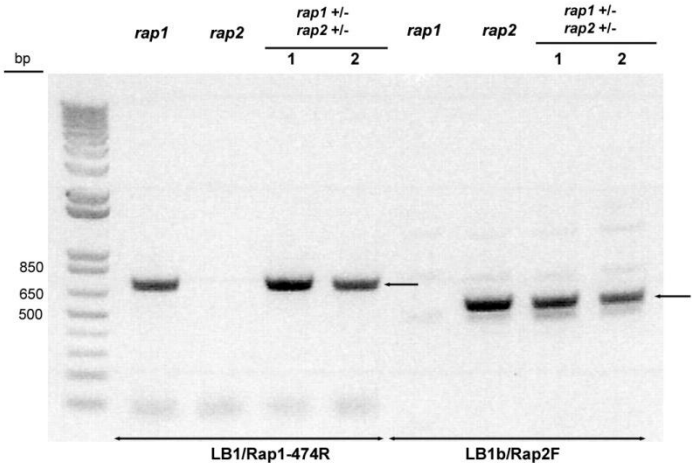

Figure 5.6 Genomic PCR of the *rap1*, *rap2* and the heterozygous *rap1/rap2* lines
The T-DNA insertion in *RAP1* gene *and* RAP2 gene was verified by primer pair LB1/Rap1-474R or LB1b/Rap2F respectively.

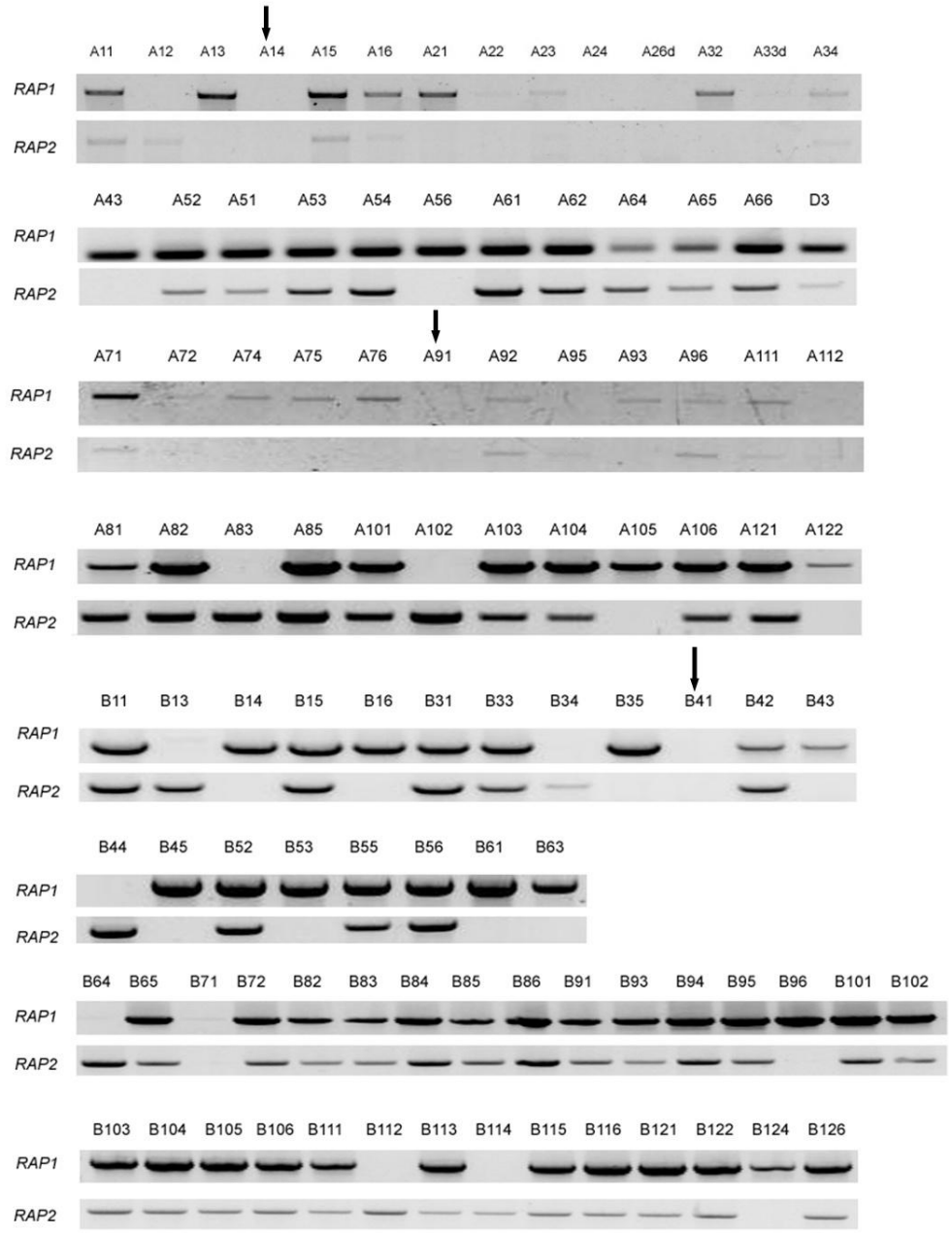

Figure 5.7 Screening for homozygous *rap1/rap2* plants.
Gene specific primers of *RAP1* and *RAP2* flanking the T-DNA insertion sites were used. Plants A14, A91 and B41 showed absence of both *RAP1* and *RAP2* bands (arrowed), indicating that they were the homozygous *rap1/rap2* double mutant.

5.5 Screening of *RAP1* Overexpression Lines

The full length *RAP1* gene was also fused with a strong constitutive CaMV *35S* promoter and transformed into wild-type *Arabidopsis* plants (Col-0) (i.e. 35S::*RAP1*/Col-0). The T-DNA insertion plasmid pGreen0229 was used to confer basta resistance in the transformed plants. There were 17 lines with basta resistance and seed were collected and sowed (work of Jeum-Kyu Hong). Expression of *RAP1* in these plants was tested by RT-PCR (Figure 5.8a), five lines (#1-1, #2-1, #3-1, #5-1 and #11-1) showed strong expression of *RAP1* and were selected for further analysis. Subsequently, two lines #1 and #3 have demonstrated stable transformation and strong *RAP1* expression. Genomic PCR reaction using *RAP1* specific primers (103F/831R) amplified two specific bands from genomic DNA (1531 bp) and from cDNA (729bp). Figure 5.8b showed that all tested *35S*::*RAP1*/Col-0 #1 and #3 plants were able to show two PCR products, while WT (Col-0) only gave the genomic PCR product.

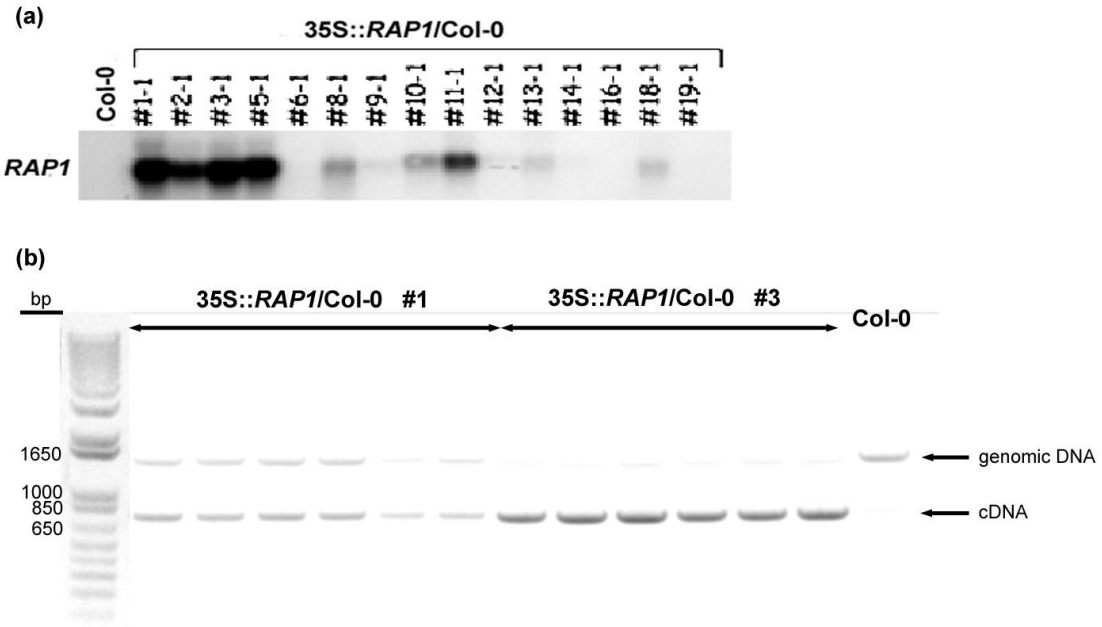

Figure 5.8 Screening for *RAP1* overexpression line.
a) RT-PCR of *RAP1* transcripts for plants that were resistance to basta after transformation of the plasmid pGreen0229-35S::*RAP1* into WT plants (Col-0). **b)** Genomic PCR of two lines 35S::*RAP1*/Col-0 #1 and #3 using the *RAP1* specific primer pair (103F/831R).

5.6 Molecular Characterization of *rap1* and *RAP1* Overexpression Lines

The genetically verified plant lines (*rap1, rap2, rap1/rap2* and 35S::*RAP1*/Col-0) were further analysed with molecular approaches. Anti-RAP1 antiserum was produced from rabbit to detect the RAP1 protein *in vivo*. However, only a very weak signal at the expected size (41kDA) was detected in unchallenged Col-0 plants (Figure 5.9a). Interestingly, strong signals were detected in high molecular size of *Arabidopsis* powdery mildew (*Erysiphe cichoracearum*) infected Col-0 and *atgsnor1-3* leaves, but this was significantly reduced in the *rap1* mutant. This suggested that the T-DNA insertion in *rap1* also disrupted RAP1 protein synthesis and accumulation. However, a weak signal was also detected in the *rap1* (infected) samples, which could be due to the cross activity of RAP1 antibody or the intron-insertion in *rap1* did not completely remove the transcripts of *RAP1*.

The transcript levels of *RAP1* and *RAP2* were verified in the *rap1/rap2* double mutant and *RAP1* overexpression (*35S*::*RAP1*/Col) lines. Figure 5.10a showed that neither *RAP1* nor *RAP2* transcripts were detected in the *rap1/rap2* double mutant. Conversely, the 35S::*RAP1*/Col (R#3) showed a significant increase of *RAP1* transcripts. In addition, the expression levels of *GSNOR* and *PR-1* in the *RAP1* overexpression line were tested (Figure 5.10b). The expression of *GSNOR* gene increased dramatically in the *RAP1* overexpression line and *PR-1* expression was also increased. The increase of *GSNOR* transcript levels in R#3, however did not extend to an increase of GSNOR protein or activity as determined by western blot analysis and GSNOR in-gel activity assay (Figure 5.11). Accumulation of GSNOR signals at a high molecular weight in Col-0 was observed, while the signals were significantly reduced in *atgsnor1-3* and R#3.

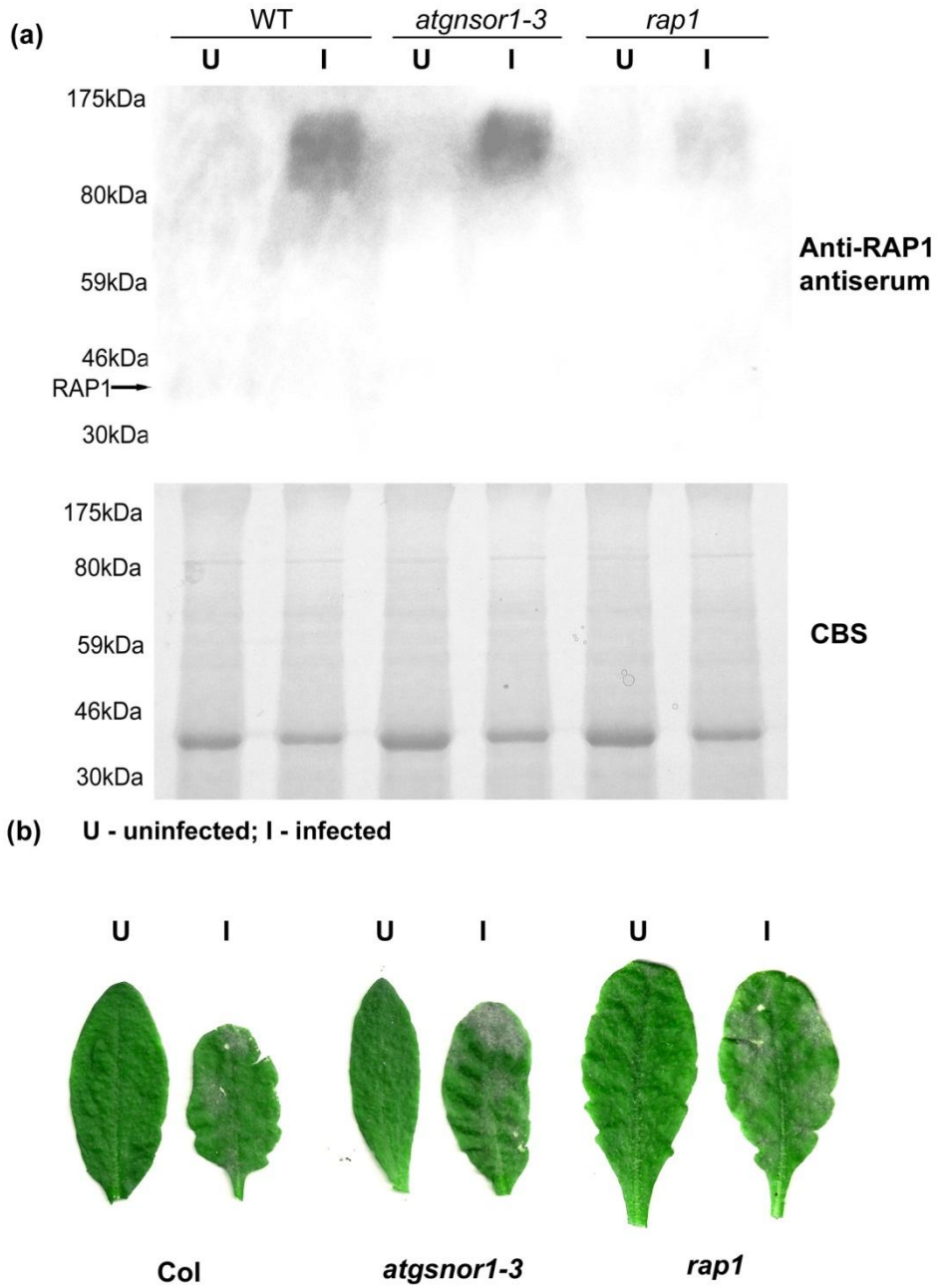

Figure 5.9 Accumulation of RAP1 proteins as a high molecular form upon *Arabidopsis* powdery mildew (*Erysiphe cichoracearum*) infection.
a) Western blot analysis by using anti-RAP1 antiserum, arrow indicates the monomeric size of RAP1. **b)** Appearance of leaves that were uninfected (U) or infected (I) by *Erysiphe cichoracearum*.

a)

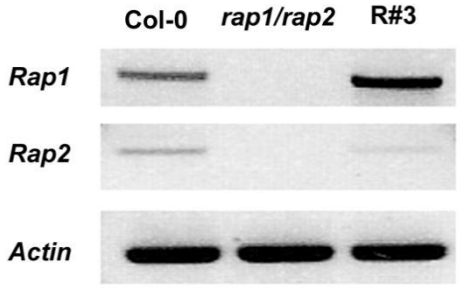

b)

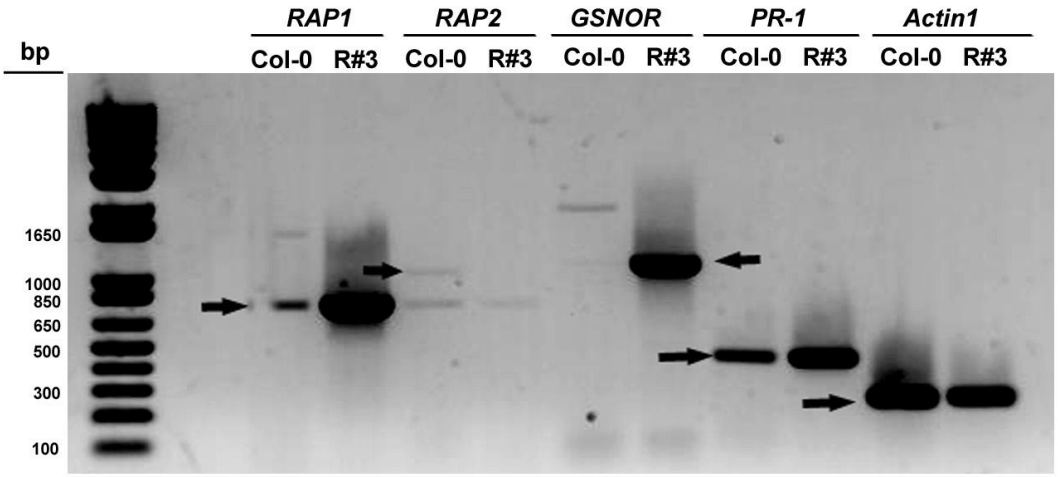

Figure 5.10 Overexpressing *RAP1* induced *GSNOR* and *PR-1* expression in *Arabidopsis* leaves.
a) Expression of *RAP1* and *RAP2* in WT (Col-0), the *rap1/rap2* double knockout mutant and the *RAP1* overexpressor *35S*::*RAP1*/Col-0 (R#3). **b)** Expression of *RAP1*, *RAP2*, *GSNOR*, *PR-1* and *ACTIN1* in Col-0 and the *RAP1* overexpressor (R#3)(arrows indicated the expected size of PCR products).

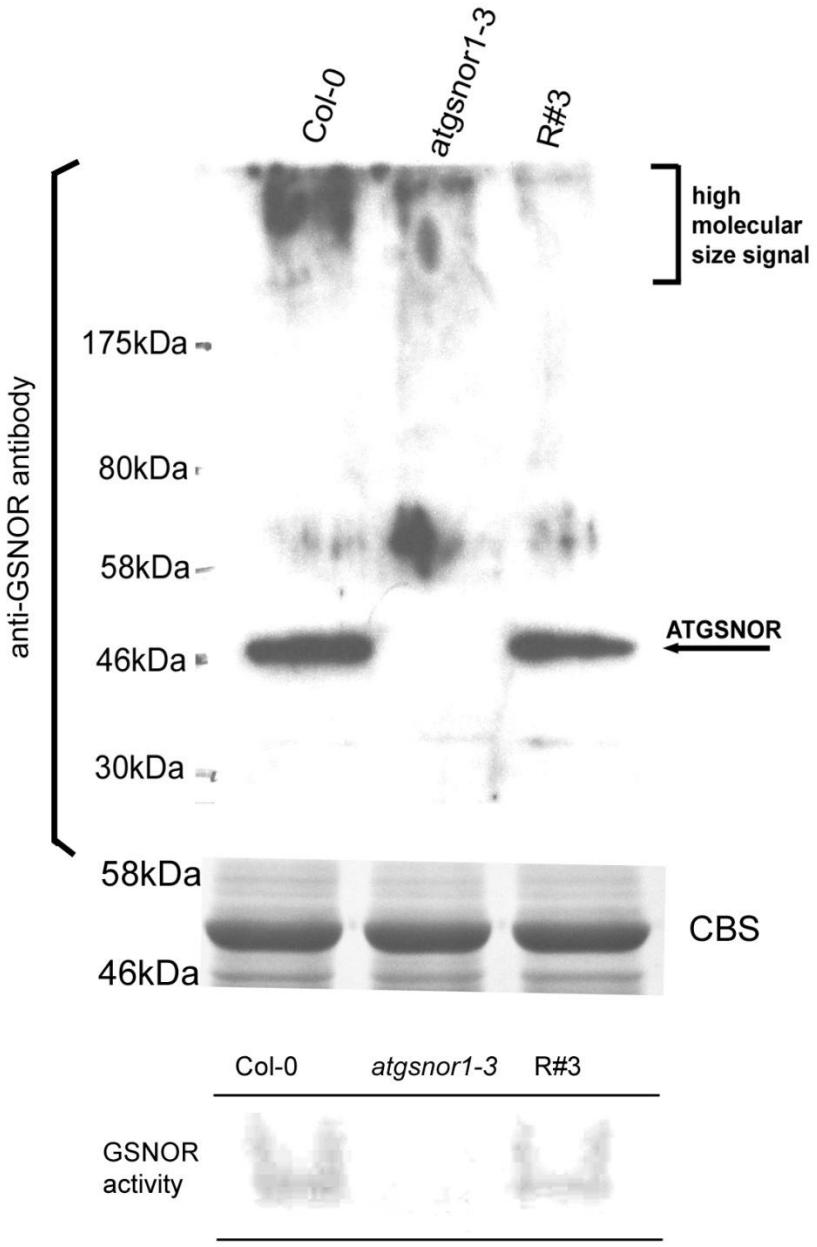

Figure 5.11 Overexpressing *RAP1* did not accumulate GSNOR proteins in *Arabidopsis* leaves.
Western blot and GSNOR activity assay of Col-0, *atgsnor1-3* and the *RAP1* overexpressor 35S::*RAP1*/Col-0 (R#3) plants. GSNOR proteins were detected by anti-GSNOR antibody; and the enzymatic GSNOR activity was detected by the UV-luminance after treatment of NADH/GSNO in a native gel.

5.7 Discussion

In order to study the physiological roles of *RAP1*, obtaining a good *RAP1* knockout/knockdown mutant line would be essential. Although there are several T-DNA insertion lines available in the public seed stocks (e.g. SALK, SAIL and INRA), none of them were shown to have insertion into the exon of *RAP1*. A report has shown that insertion in an intron could still effectively knock out a gene, where only 0.7% (2/263) of intron insertion did not affect gene transcription which is comparable with exon insertion of 1.1% (7/609). In addition, 82% of intron insertions have no protein expression (Wang 2008). Therefore, a T-DNA insertion line of *RAP1* (SAIL_E395_E02) was chosen, which has an insertion in the third intron. A homozygous *RAP1* insertion line (*rap1*) was isolated and verified by RT-PCR which showed no detectable *RAP1* transcript (Figure 5.3). Furthermore, a significant reduction of RAP1 protein signal was observed in the *E. cichoracearum* infected leaves (Figure 5.9) and the same T-DNA line has been used in a recent publication (Prasad et al. 2010). These results showed that the *rap1* plant line would be reliable for further analysis.

However, the *rap1* plants did not show any obvious developmental phenotype. Two individual reports have already mentioned that *RAP1* is associated with four other family genes (Nodzon et al. 2004; Stone et al. 2006), in which *RAP1* and one of the genes At3g23280 (*RAP2*) was clustered together due to the similarities in amino acid sequence and gene structure (Figure 3.1). A T-DNA insertion line of *RAP2* (SALK_104813) was identified and the homozygous *RAP2* insertion line (*rap2*) was isolated. However, sequencing results indicated that the T-DNA was inserted into the last intron of *RAP2* (Figure 5.5). Nonetheless, the *rap2* plant line was also found to have no full-length transcript of *RAP2* and was included for further analysis.

Similarly, *rap2* plants did not show obvious developmental phenotype. Therefore, the *rap1* and *rap2* mutant lines were crossed to generate the double knockout mutant. The F1 was found to carry both of the T-DNA insertions of *RAP1* and *RAP2* (heterozygous *rap1/rap2*) (Figure 5.6) and were self-pollinated. The seeds of F2 were collected and sowed. Since *RAP1* and *RAP2* are located on different chromosomes, the expected ratio of segregation to obtain homozygous *rap1/rap2* double mutant should be 1:16. PCR results showed that among the tested ~100 plants, only two of

them appeared to be homozygous double mutants (Figure 5.7), which was lower than the expected segregation ratio (1:16). The realistic ratio (~2/100) was lower than expected, which could be due to the reduced in germination rate and poor growth of seedlings (data not shown) The bioinformatic data also showed that *RAP1* and *RAP2* expression were increased in hypocotyl and cotyledons (Figure 3.3). These suggested that knocking out both *RAP1* and *RAP2* could be unfavourable in the early stage of development.

In the previous chapter (Chapter 4.3), RAP1 was shown to be a functional E3 ligase. Theoretically, overexpression of RAP1 could significantly reduce the amount of substrate (target protein) through proteasomic degradation. A transgenic line harbouring the *RAP1* overexpression construct (35S::*RAP1*) in WT (Col-0) was generated. It has been shown that overexpression of *RAP1* increased the expression of *GSNOR* (Figure 5.10b), suggesting *RAP1* may be involved in regulating of *GSNOR* expression. However, although higher amount of *GSNOR* transcripts in *35S*::*RAP1*/Col-0 was detected, there was no significant increase in the amount of GSNOR proteins nor GSNOR activity between Col-0 and *35S*::*RAP1*/Col-0 (Figure 5.11). Perhaps the overproduced GSNOR proteins have been rapidly degraded in *35S*::*RAP1*/Col-0 plants. RAP1 may induce the mechanism for degradation of GSNOR possibly through the 26S proteasome. *PR-1* expression was increased in *35S*::*RAP1*/Col-0. Increased *PR-1* expression is an indicator of enhanced disease resistance, suggesting that *RAP1* could be a positive regulator in defence responses. Nonetheless, the basic molecular data has already revealed that *RAP1* may be involved in a complicated gene expression network (Figure 5.12).

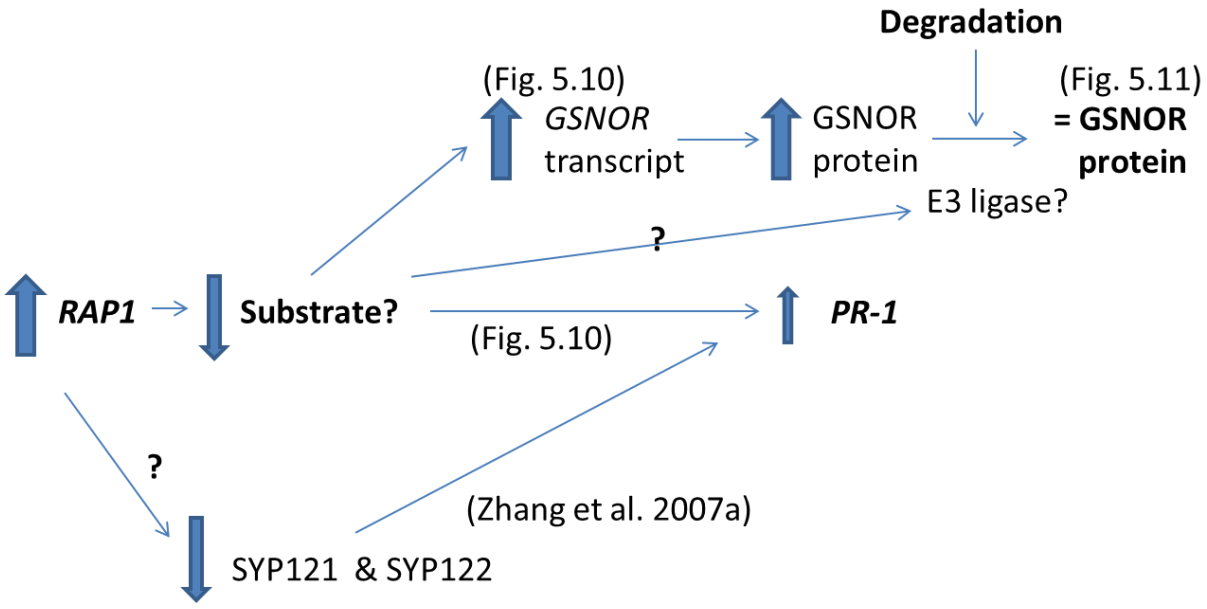

Figure 5.12 A schematic diagram to show the gene regulation network in 35S::*RAP1*/Col-0 line.
Overexpression of *RAP1* induced the expression of *GSNOR* and *PR-1*. However, no significant increase of GSNOR protein was detected, which was probably due to the enhanced proteasomic degradation of GSNOR. Furthermore, double mutation of *SNARE* genes *syp121/syp122* enhanced *PR-1* expression (Zhang et al. 2007a). *SYP121* was co-expressed with *RAP1* in microarray data, which *RAP1* may be involved in the downregulation of *SYP121* or/and *SYP122*.

Chapter 6

6 Phenotypic analysis of *RAP1* and *RAP2* Mutants

6.1 Development Phenotypes

6.1.1 Introduction

Knocking out *RAP1* or *RAP2* individually did not show any significant development phenotype. As RAP1 and RAP2 are very similar in protein sequence (93% coverage and 72% identity), knocking out both *RAP1* and *RAP2* could be an essential approach to display the physiological importance of *RAP1* and *RAP2* in growth and development. In chapter 5.4, three plants (A14, A91 and B41) have been isolated due to the genomic screening results. Further confirmation has shown that only A14 and A91 were homozygous *RAP1* and *RAP2* double knockout lines (*rap1/rap2*), while B41 is a heterozygous *RAP1* and homozygous *RAP2* knockout (*rap1+/-, rap2-/-)*(data not shown). The double mutants (A14 and A91) have demonstrated delay in emergence of primary bolt and flowering. This supported the expectation of functional redundancy between RAP1 and RAP2. In addition, overexpression of full length and truncated *RAP1* had direct impacts on root and secondary bolt development respectively.

6.1.2 Delayed Flowering in the *rap1/rap2* Double Mutant Plants

The F2 homozygous *rap1/rap2* double mutant lines (A14/A91) showed delay in flowering, while the heterozygous *rap1* and homozygous *rap2* plant (*rap1 +/-; rap2 -/-*) (B41) as well as *rap1* and *rap2* plants displayed similar flowering behaviour as WT (Col-0) (Fig 6.1a & c). Flowering time can be measured by the number of leaves developed at flowering (Teper-Bamnolker and Samach 2005). Figure 6.1b showed the comparison of Col-0 and *rap1/rap2*. The number of leaves in *rap1/rap2* was significantly more than Col-0, revealing that the initiation of flowering in *rap1/rap2* plants was delayed. Also, there was a reduction of bolt height and number of bolts in the later stage of development in *rap1/rap2* plants (Figure 6.1d).

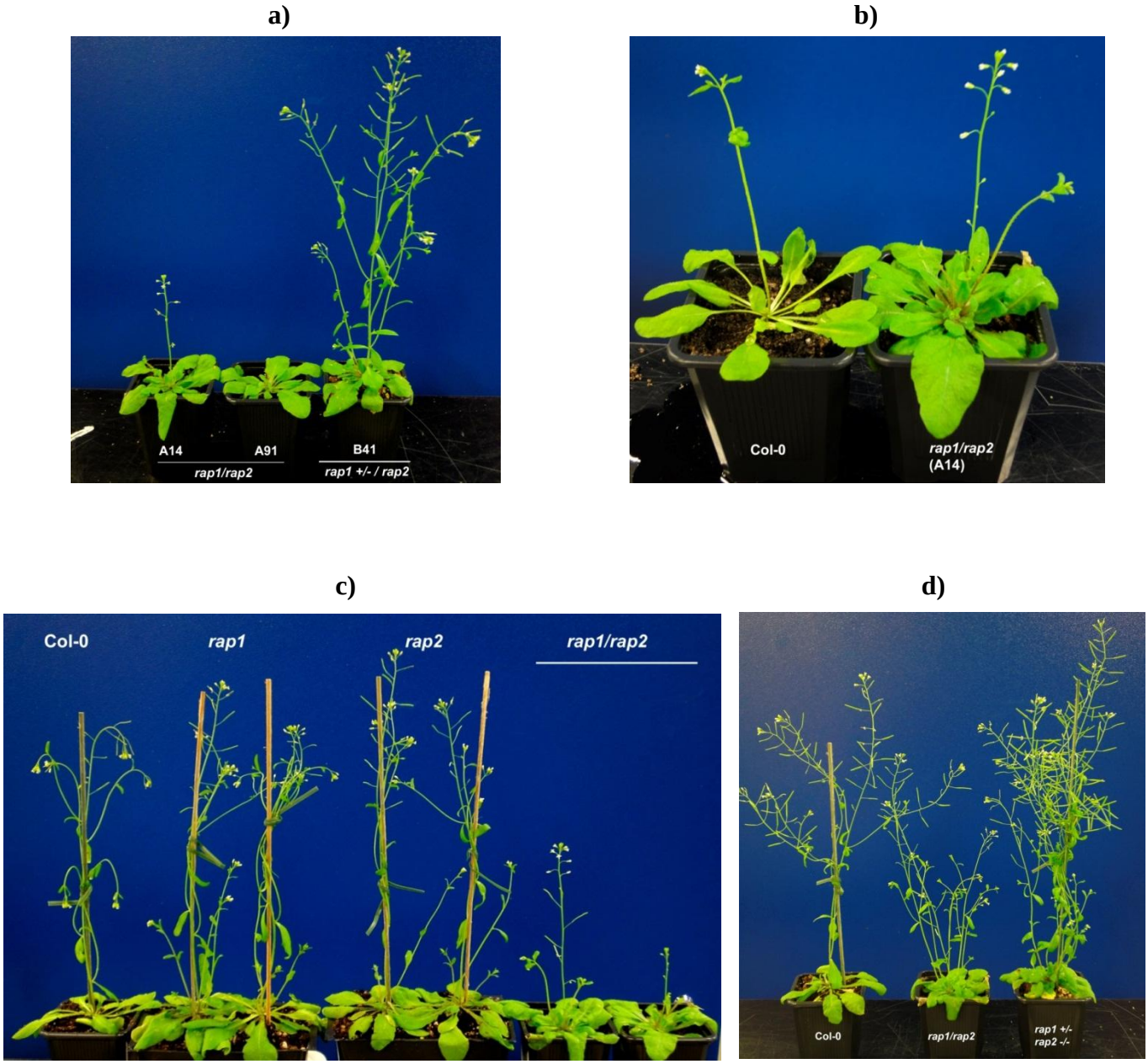

Figure 6.1 Delay in flowering in the F2 *rap1/rap2* double mutant plants.
a) Heterozygous *RAP1* knockout in *rap2* background (B41) did not show delay in flowering. **b)** Increased numbers of leaves during flowering in the *rap1/rap2* double mutant plant. **c)** Knocking out of *RAP1* or *RAP2* did not show delay in flowering. **d)** The *rap1/rap2* double mutant showed reduced height and number of bolts at later stages of development.

6.1.3 Loss of Apical Dominance in Lateral Bolts of *35S*::*RAP1ΔRING* Mutant Line

A truncated form of RAP1 (RAP1ΔRING) was overexpressed in WT (Col-0). The RING domain was removed so that the expressed proteins might be able to compete with endogenous RAP1 protein, but could not express E3 ligase activity. There were 17 transgenic lines generated, in which 6 lines had demonstrated alternation in phenotypes. Among the tested lines, line #16 showed the highest expression level of *RAP1* transcripts (WT *RAP1* expression is suppressed in unchallenged condition). Line 16 has showed WT timing of primary bolt formation but the growth of secondary bolts was affected. The secondary (lateral) bolts were shorter (dwarf) and there was a loss of apical dominance relative to wild type plants (Figure 6.2).

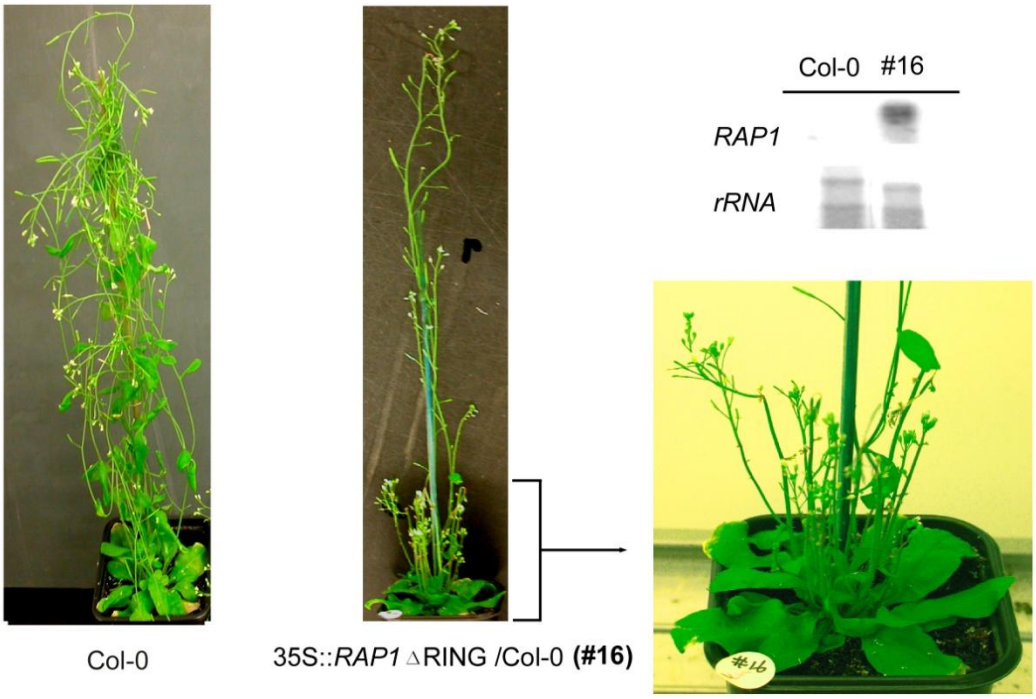

Figure 6.2 Phenotypes of mutant with the overexpression of truncated RAP1 proteins.
Overexpression of truncated RAP1 proteins (RAP1ΔRING) in WT plants affected the growth of secondary bolts. (Work of Jeum-Kyu Hong).

6.1.4 Enhanced Branching of Roots in the *35S*::*RAP1* Mutant Line

It has also been reported that, *XBAT32*, a gene in the same E3 ligase clade to *RAP1* and *RAP2*, has been implicated in lateral root development (Nodzon et al. 2004). Therefore, root development was also assessed in *rap1* lines. There was no significant difference in root morphology in Col-0, *rap1*, *rap2* and *rap/rap2* lines (data not shown). However, a distinguishable variation in root development was observed in *35S*::*RAP1*/Col-0 seedlings. Roots in this line were more branched from the origin of the primary root and in addition the branched roots were also longer than those of Col-0 (Figure 6.3).

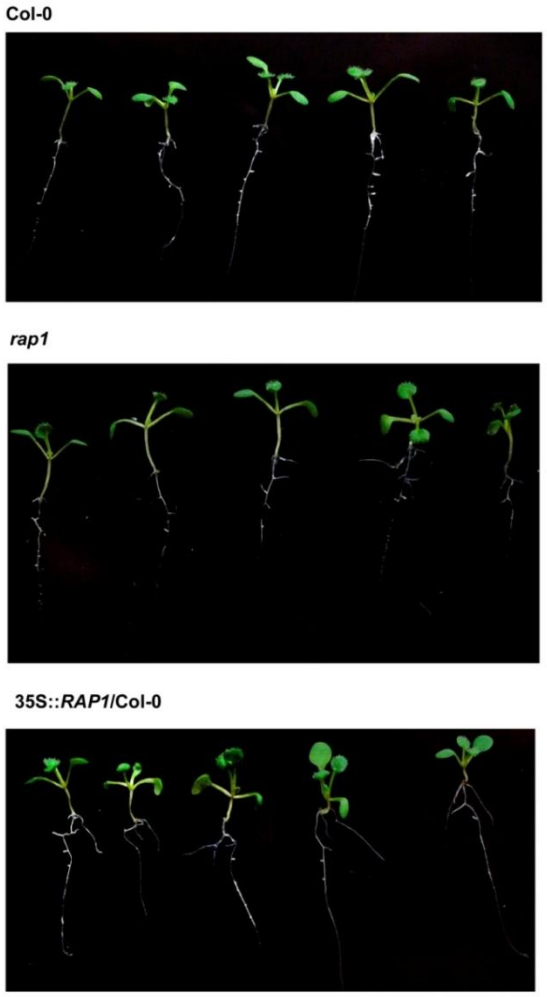

Figure 6.3 Overexpression of *RAP1* enhanced lateral root development in young seedlings.
10 days old seedlings were grown in half-strength MS agar plates. A single main root was developed in wild type Col-0 and *rap1* seedlings, while two main roots developed in 35S::*RAP1/*Col-0 seedlings, which were branched from the proximal zone of the primary root.

6.1.5 Discussion: Developmental Phenotypes

It has been commonly observed that knock out of a single member of a gene family often does not produced a strong phenotype. Similarly, no obvious developmental phenotype was identified if *RAP1* or *RAP2* were knocked out individually. Due to time constrains, the *RAP1*-related developmental phenotype has not been well-studied in this study. Nonetheless, preliminary data has shown three observable effects due to the alternation of *RAP1* expression or overproduction of truncated RAP1: (1) the flowering time was delayed in *rap1/rap2* plants (Fig 6.1). (2) Overexpression of a truncated RAP1 protein (RAP1ΔRING) led to a loss of apical dominance (Figure 6.2). (3) And, the *RAP1* overexpressor (35S::RAP1/Col-0) affected root development (Figure 6.3).

There is still insufficient data to discuss the roles of *RAP1* or *RAP2* during plant development and growth. The tissue expression profiles (Figure 3.3) have indicated high expression of *RAP1* and *RAP2* in first node and cauline leaves, suggesting *RAP1* and *RAP2* may take part in the initiation of the primary bolt. Either knocking out *RAP1/RAP2* or overproducing the truncated RAP1 proteins (RAP△RING) may lead to the accumulation of RAP1-substrate proteins. This suggests that the substrate protein(s) could be a potential negative regulator of bolt development.

It is worth noting that the findings were in line with a report of *XBAT32* (a *RAP1* family gene) (Figure 6.4). *XBAT32* was shown to affect lateral root development (Nodzon et al. 2004; Prasad et al. 2010; Prasad and Stone 2010). XBAT32 has been shown to interact with the ethylene biosynthesis enzymes AMINOCYCLOPROPANE-1-CARBOXYLIC ACID SYNTHASE4 (ACS4) and ACS7 *in vitro*. Loss of *XBAT32* may promote the stabilization of ACSs and lead to increased ethylene synthesis and suppression of lateral root formation (Prasad et al. 2010). It is speculated that RAP1 and RAP2 may not be the key players in root development. However, due to the sequence similarity between RAP1/RAP2 and XBAT32, overexpression of *RAP1* promoted lateral root development which is similar to the inhibition effect of lateral root development in *XBAT32* knockout mutant. In summary, the *RAP1* and *RAP2* could be involved in plant growth and development. There are also function overlaps between individual members in the gene family.

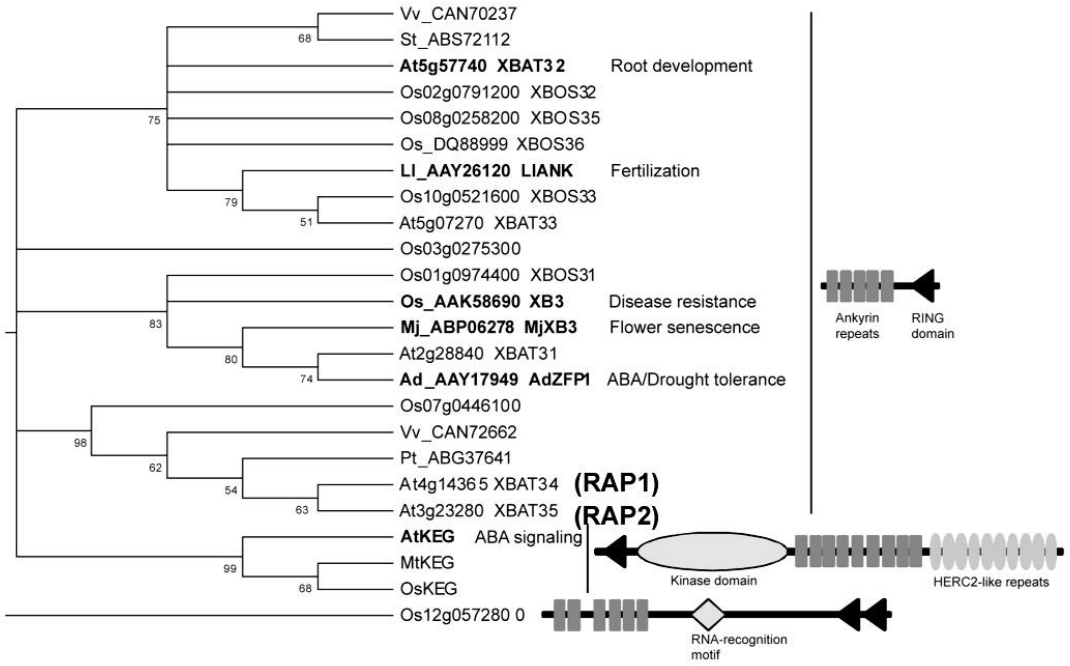

Figure 6.4 The *RAP1* family genes (*RAP1, RAP2, XBAT31, XBAT32* and *XBAT33*) in *Arabidopsis*.
Homologs sharing similar protein structure (ankyrin repeats and RING domain) were identified in different plant species and found to be involved in various physiological responses. (Adapted from Prasad & Stone 2010)

6.2 Defence-Related Phenotypes

Expression profiles indicated that *RAP1* may be actively involved in the defence mechanism. In order to verify the role of *RAP1* in defence, the *RAP1*-related mutant plants (*rap1*, *rap2*, *rap1/rap2* and *35S*::*RAP1*/Col-0) were challenged with different type of pathogens: avirulent *Pseudomonas syringae* pv tomato (*Pst*)DC3000 (*avrB*), virulent *Pst*DC3000 and obligate biotrophic (*E. cichoracearum*). In addition, the *atgsnor1-3* plants were known to show enhanced disease susceptibility to various pathogens and therefore were included in the experiments as a positive control.

6.2.1 Hypersensitive Response Towards *Pst*DC3000 (*avrB*)

The leaves of the various plant lines were inoculated with avirulent *Pst*DC3000(*avrB*). This pathogen injects effectors into the host cells through type III secretion system, leading to the induction of the hypersensitive response (HR). HR is a form of cell death which might limit the further spread of pathogens. HR-induced cell death was stained by trypan blue, which marks dead or dying cell blue (Figure 6.5). The *atgsnor1-3* (Feechan et al. 2005) showed more severe and rapid cell death upon *Pst*DC3000(*avrB*) treatment than wild type (Yun et al. 2011). Leaves of wild-type Col-0 developed HR but staining was less intense than in *atgsnor1-3* plants. The *rap1/rap2* double mutant (A14/A91) and *35S*::*RAP1*/Col-0 showed similar results as Col-0. The HR in the *rap1* and *rap2* single mutants might be slightly upregulated, but the results were rather ambiguous and therefore no conclusion could be drawn to suggest the role of *RAP1* or *RAP2* in the HR.

a)

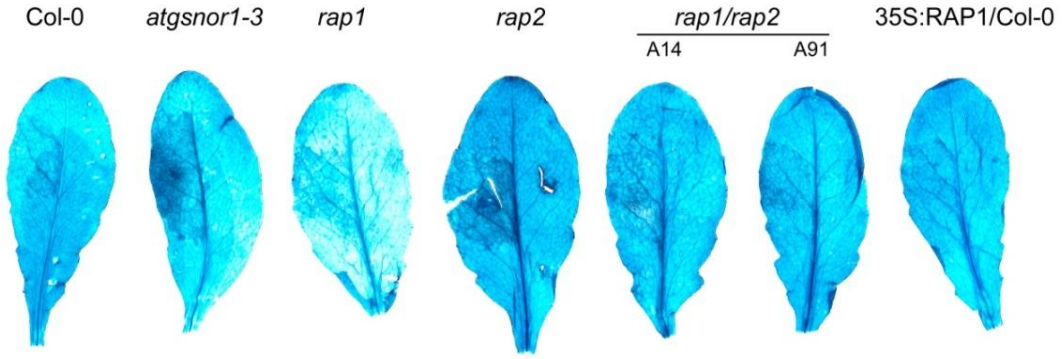

b)

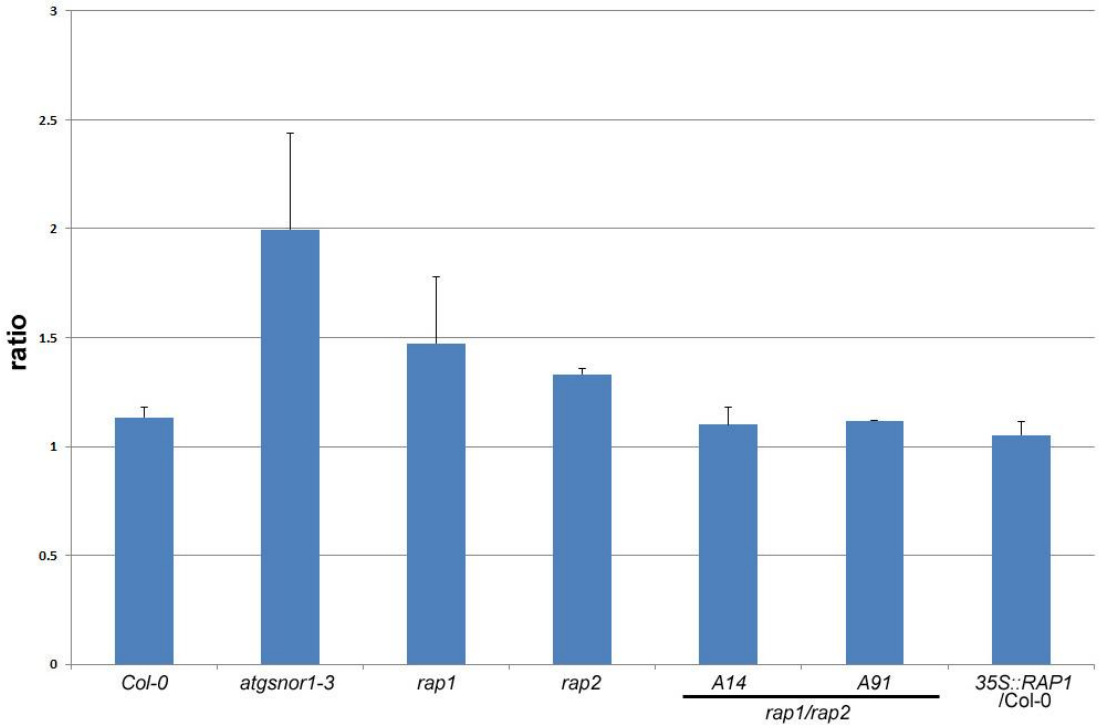

Figure 6.5 Hypersensitive response (HR) analysis after infection of avirulent *Pst*DC3000(*avrB*).
Cell death was determined by trypan blue staining upon treatment of *Pst*DC3000(*avrB*) at OD_{600}=0.002 for 72 hours. **a)** Appearance of trypan blue stained leaves. **b)** Ratio of trypan blue intensity of treated over untreated leaf area, average of two individual trials.

6.2.2 Enhanced Susceptibility towards *Pst*DC3000 in *RAP1* and *RAP2* Mutants

The *rap1* and *rap2* lines were challenged with virulent *Pst*DC3000 and leaf extracts were collected 3 days after inoculation. Diluted leaf extracts were then spread on agar plates and bacterial growth determined from the numbers of colonies on the agar plates. The *atgsnor1-3* line was known to be very susceptible to *Pst*DC3000 (Feechan et al. 2005), and accordingly showed a significant increase bacterial growth relative to wild-type (Figure 6.6a). At 3 days post inoculation (dpi), enhanced susceptibility to this pathogen was found in the *rap1* and *rap2* single mutants. The phenotype was further amplified in *rap1/rap2* double mutants (A14/A91). At 5 dpi, the difference in susceptibility was further increased, leading to a large increase in the number of colonies found in the *rap1, rap2* and *rap1/rap2* compared to Col-0. Similar to the results at 3 dpi, the *rap1/rap2* mutants were more susceptible than the single mutants. The reliability of the data was also verified by a Student's t-test as the enhanced in susceptibility in *rap1 and rap2* mutants was not as obvious as the *atgsnor1-3* mutant. The p-value of the averages between Col-0 and the *atgsnor1-3* mutant (3 dpi and 5 dpi) were well below 0.05, indicating that the *atgsnor1-3* mutant was significantly more susceptible towards *Pst*DC3000. The p-values of the *rap1, rap2* and *rap1/rap2* mutants at 3 dpi failed to reject the null hypothesis, suggesting the early resistance of these mutant lines was only slightly compromised. On the other hand, the p-values at 5dpi showed that the *rap1* and *rap1/rap2* (A14) mutants were significantly more susceptible than Col-0.

The variation of resistance in the plant lines could also be reflected in the appearance of the leaves (Figure 6.6b). The most susceptible *atgsnor1-3* plants showed complete leaf chlorosis. Leaves of the *rap1/rap2* double mutant (A14/A91) also became chlorotic. The *rap1* and *rap2* single mutants were also more susceptible than Col-0 as chlorosis also developed in their leaves.

a)

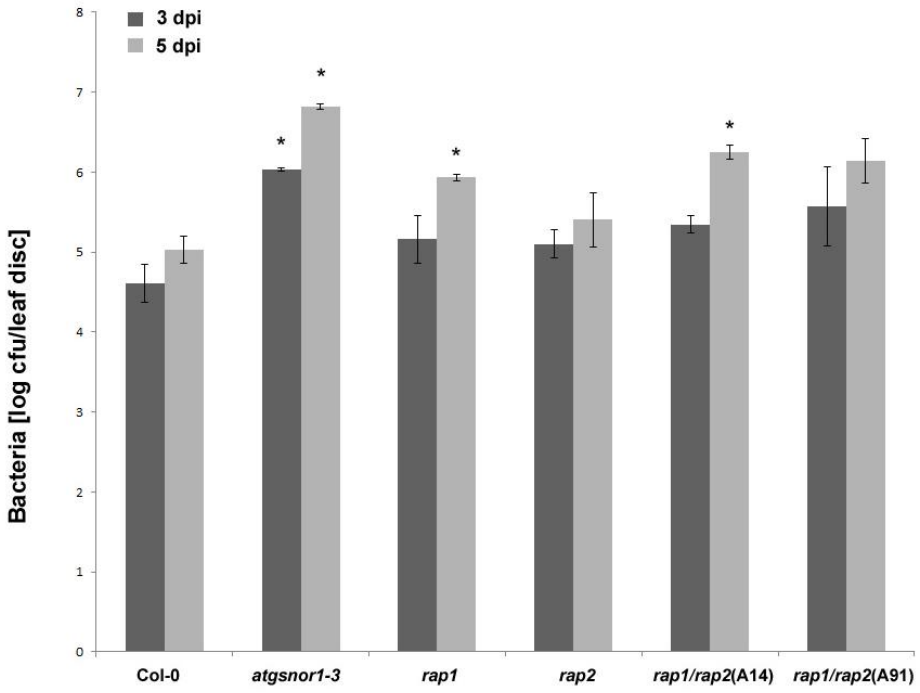

Student's t-test

Col-0 :	*atgsnor1-3*	*rap1*	*rap2*	*rap1/rap2* A14	*rap1/rap2* A91
3 dpi	* 0.001	0.210	0.172	0.092	0.280
5 dpi	* 0.003	* 0.034	0.514	* 0.050	0.129

** p-value<0.05 rejects null hypothesis, suggesting the averages of the two samples are significantly different.*

b)

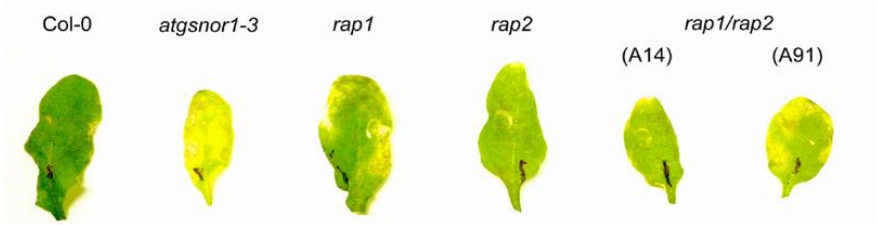

Figure 6.6 Pathogenicity test of infection with *Pst*DC3000.
a) Number of colonies recorded upon 3 days and 5 days post inoculation (dpi). A Student's t-test was used to compare the average values between Col-0 and the mutants. **b)** Appearance of leaves after 5 days of inoculation.

6.2.3 Enhanced Susceptibility towards *Arabidopsis* Powdery Mildew in *RAP1* and *RAP2* Mutants

Previous results have shown that RAP1 proteins were accumulated upon infection of *Arabidopsis* powdery mildew (*Erysiphe cichoracearum*)(Figure 5.9), therefore the plant lines were challenged with *Arabidopsis* powdery mildew. The time after inoculation was shortened to 3 days to allow the observation of early stage resistance in different plant lines. The infected leaves were then stained with trypan blue for visualising the fungal structures (Figure 6.7). Identification of spores was the first approach to assay fungal development, as non-germinated spores were usually washed away during the boiling procedure in staining. After 3 days of inoculation, no spores could be found on the leaf surface of wild-type Col-0, *atgsnor1-3* and *35S*::*RAP1*/Col-0, whereas spores were found in the *rap1* mutant. The *rap2* mutant was shown to be more susceptible to *E. cichoracearum*, which secondary structures such as hyphae was identified. There was an additional effect in the *rap1/rap2* double mutants (A14 and A91), where most of the early fungal structure (i.e. primary germtube, conidia) were developed into mature structures. Networks of hyphae were well-developed in the A14 line.

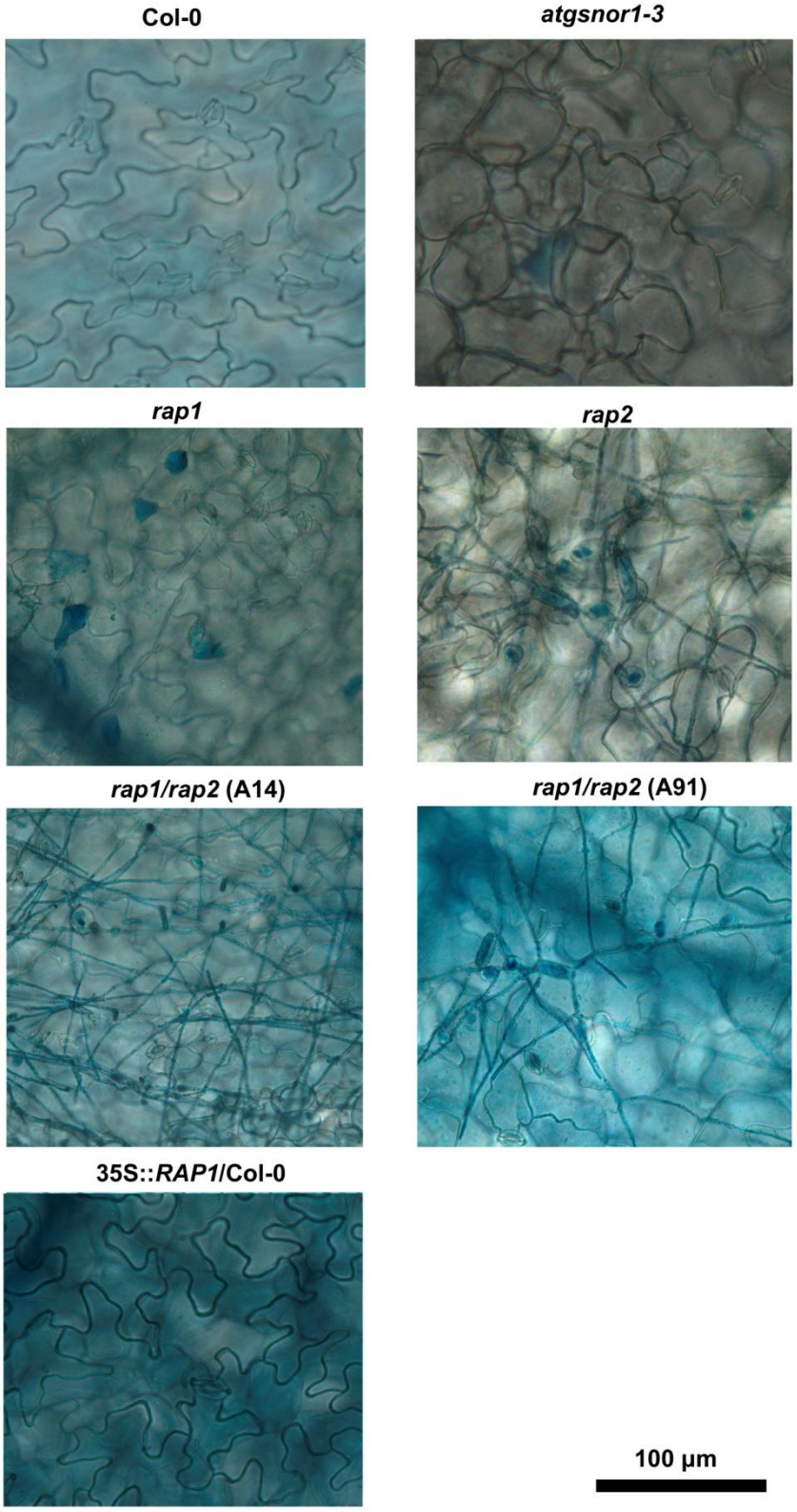

Figure 6.7 Inoculation with *Erysiphe cichoracearum*.
Four week old leaves were infected with *Arabidopsis* powdery mildew via rubbing of infected leaves and inoculated for 3 days. Fungus structure was stained with trypan blue. Images were taken in 200 x magnification under a light microscope.

6.2.4 Discussion: Defence-Related Phenotypes

The disease-related phenotype of *RAP1* was one of the key interests in this study, as *RAP1* was identified based on the SA-independent induction follow *Pst*DC300(*avrB*) treatment. In addition, *RAP1* was found to be co-expressed with many disease-related genes (Figure 3.4) that were highly inducible by pathogens (Figure 3.1 and Figure 3.5). The *RAP1* promoter was responsive to pathogen/wounding induction (Figure 3.2) and RAP1 proteins accumulated follow infection by *Erysiphe cichoracearum* (Figure 5.9). In, addition, the RAP1 related protein XB3 in rice (*Oryza sativa*) (Figure 6.4) interacts with a receptor-like kinase XA21 that confers gene-for-gene resistance to *Xanthomonas oryzae* pv *oryzae*. Reduced expression of the *Xb3* gene compromised resistance to *X. oryzae* pv *oryzae* (Wang et al. 2006).

In order to analyse the role of *RAP1* in plant defence, the *RAP1* mutant lines were challenged with avirulent (Figure 6.5) and virulent (Figure 6.6) *Pseudomonas syringae* pv *tomato* (*Pst*) DC3000 strain and the biotrophic pathogen mildew *Erysiphe cichoracearum* (Figure 6.7). Inoculation of avirulent strain *Pst*DC3000 (*avrB*) induces hypersensitive response (HR) which leads to local cell death proximal to the inoculation site. HR is a key defence response to limit pathogen growth and defence-compromised plant lines are often shown to have reduction in HR (Brodersen et al. 2005). It was speculated that *RAP1* could be involved in programmed-cell death (PCD). *RAP1* was co-expressed with PCD related genes such as LRR-protein *BIR1*, *NSL1* and *SNARE* complex (Figure 3.4). Knocking out *BIR1* leads to extensive cell death and activation of constitutive defence responses (Gao et al. 2009). As *RAP1* is co-expressed with *BIR1*, knocking out *RAP1* might impact PCD. HR in the *rap1* and *rap2* mutant was enhanced but no obvious difference was observed in the *rap1/rap2* and *35S*::*RAP1*/Col-0 lines (Figure 6.5). One of the earliest events observed in HR is an oxidative burst due to the enhanced production of reactive oxygen intermediates (ROI) such as superoxide (O_2^-) and its dismutation product, hydrogen peroxide (H_2O_2). Nitric oxide (NO) is also generated and has been shown to serve as a signalling molecule in plant defence (Malik et al. 2011). It has been previously reported that loss of *GSNOR* led to an elevated HR which could be due to the accumulation of NO. However, as there was no clear difference between the mutant lines, this suggests that *RAP1* and *RAP2* might not be actively involved in AvrB-mediated HR. Although E3 ligase activity has been shown to be essential in

AvrPtoB-mediated-HR (Jones and Dangl 2006), *RAP1* and *RAP2* may not function in HR. Nonetheless, it would be worth testing other effectors to analyse the role of *RAP1/RAP2* in HR.

Virulent *Pst*DC3000 does not produce effectors (e.g. *avrB*) to trigger HR and therefore defence is dependent on basal resistance. The *atgsnor1-3* plants were found to be very susceptible to *Pst*DC3000 (Feechan et al. 2005) and therefore this plant line was used as the positive control for enhanced susceptibility to *Pst*DC3000. As expected, there was a striking increase in the number of colonies in *atgsnor1-3* leaves relative to wild-type (Figure 6.5). The *rap1* or *rap2* lines exhibited reduced resistance, suggesting that *RAP1* and *RAP2* were involved in disease resistance. The resistance to *Pst*DC3000 was further compromised in the *rap1/rap2* double mutants. There are examples in *Arabidopsis* of redundant gene function, for instance, the U-box family E3 ligases *PUB22/23/24* (Trujillo et al. 2008) and the SNARE family *SYP121/SYP122*(Zhang et al. 2007a). Robust disease-related phenotypes were observed only when all of the family members have been knocked out. Our finding suggested that *RAP1* and *RAP2* also function redundantly. However, there was still a significant difference in *Pst*DC3000 susceptibility between *atgsnor1-3* and *rap1/rap2* plants. It is speculated that the disease-related phenotype could be further enhanced if a triple/quadruple mutant of potential family members (i.e. *XBAT31, XBAT32* and *XBAT 33*) (Prasad and Stone 2010) is generated.

RAP1 proteins were found to be accumulated as a high molecular weight species upon *E. cichoracearum* infection (Figure 5.9). Therefore, it was speculated that *RAP1* may be involved in resistance against this pathogen. This has been verified in Chapter 6.2c (Figure 6.7) which shows that knockout of *RAP1*, *RAP2* or both had a significant impact on *E. cichoracearum* resistance. The strain of *E. cichoracearum* used here does not induce host defence responses in *Arabidopsis* (Vogel and Somerville 2000). It is still uncertain what mechanism *Arabidopsis* inhibits the germination of spores in young leaves. Interestingly, *RAP1* and *RAP2* expression is higher in young leaves (Figure 3.3) than in older leaves. Knockout of both *RAP1* and *RAP2* significantly increased susceptibility to *E. cichoracearum*, therefore these genes may be involved in the regulation of resistance against this pathogen. This assumption is supported by a report implicating a SNARE-protein in resistance to *E. cichoracearum*. The

corresponding gene *SYP121 (PEN1*) shares a similar expression profile with *RAP1* (Figure 3.4). Knockout of SNARE components *SYP121* and *SYP122* activated SA-independent powdery mildew resistance through the induction of a hypersensitive-like cell-death response which inhibited the penetration of the fungus (Zhang et al. 2007b). In addition, the *PR-1* expression level was also upregulated in *syp121-1/syp122-1* double mutant. Interestingly, SYP121 was shown to work as a negative regulator in the defence response, while RAP1 positively regulated the resistance against *E. cichoracearum*. Reduction of SYP121/SYP122 levels benefits the defence against *E. cichoracearum*, therefore it is speculated that RAP1 could be involved in the degradation of SYP121/SYP122 probably through proteasomic degradation. RAP1 could directly recognize SYP121/SYP122 for ubiquitin-mediated degradation or mediate the degradation of a positive regulator(s) of *SYP121/SYP122* (Fig 5.12). A report shows that *RAP1* expression was reduced when SHINE transcription factors (SHNs) were knocked down. SHNs control cuticle permeability by regulating the expression of cutin biosynthesis genes and wax formation in leaves (Shi et al. 2011). Germination and penetration are critical events for the successful invasion of a fungal pathogen (Mendgen et al. 1996), which these events are largely dependent on the interaction between hosts and pathogens. As the expression of *RAP1*, *PEN1* and *SHNs* are linked, it is speculated that *RAP1* mutants could have an altered physical barrier which favours the entry of powdery mildew.

6.3 Methyl Viologen (MV)

6.3.1 Enhances MV Resistance in *rap1* and *rap2* Plants

It has been reported that *ATGSNOR* mutants (*atgsnor1-3* and *par2-1*) were highly resistant to methy viologen (MV, other name: paraquat) (Chen et al. 2009). Methyl viologen accepts electrons from photosystem I and transfers them to oxygen and leads to the formation of the superoxide anion ($\cdot O_2^-$). MV has been shown to be an efficient inducer of cell death and has been used as a herbicide (Suntres 2002). *RAP1* and *RAP2* related mutant plants were also tested with MV. Figure 6.8showed that above 90% of cotyledons in all tested lines were developed when plants were grown in half MS medium. Addition of 1µM of MV completely inhibited the germination of Col-0 seeds, but about 60% of *atgsnor1-3* seeds could still form green cotyledons. Single mutants of *RAP1* or *RAP2* were also able to resist the effect of MV, where around 30% of seed germinated, however, developed cotyledons was typically slightly chlorotic. The resistance to MV was not apparent in *rap1/rap2* double mutants (A14/A91), only very few of them (<5%) were able to develop into seedlings and the seedlings were much smaller than the *atgsnor1-3*, *rap1* or *rap2* seedlings. Germination of *35S*::*RAP1*/Col-0 seeds was completely inhibited similar to that of wild-type.

The online microarray database NASCArrays (http://affymetrix.arabidopsis.info/) has provided expression profiles of individual gene. Noteworthy data (Figure 6.9) showed that *RAP1* expression was highly inducible by UV-B illumination. *RAP1* was induced rapidly within 30 minutes of treatment and after 1 hour *RAP1* transcript level were induced 13 fold higher than at time 0. *RAP1* expression was also sensitive to MV. Basal *RAP1* expression was rapidly suppressed after 30 minutes of MV treatment and further reduced to a very low level after 3 hours.

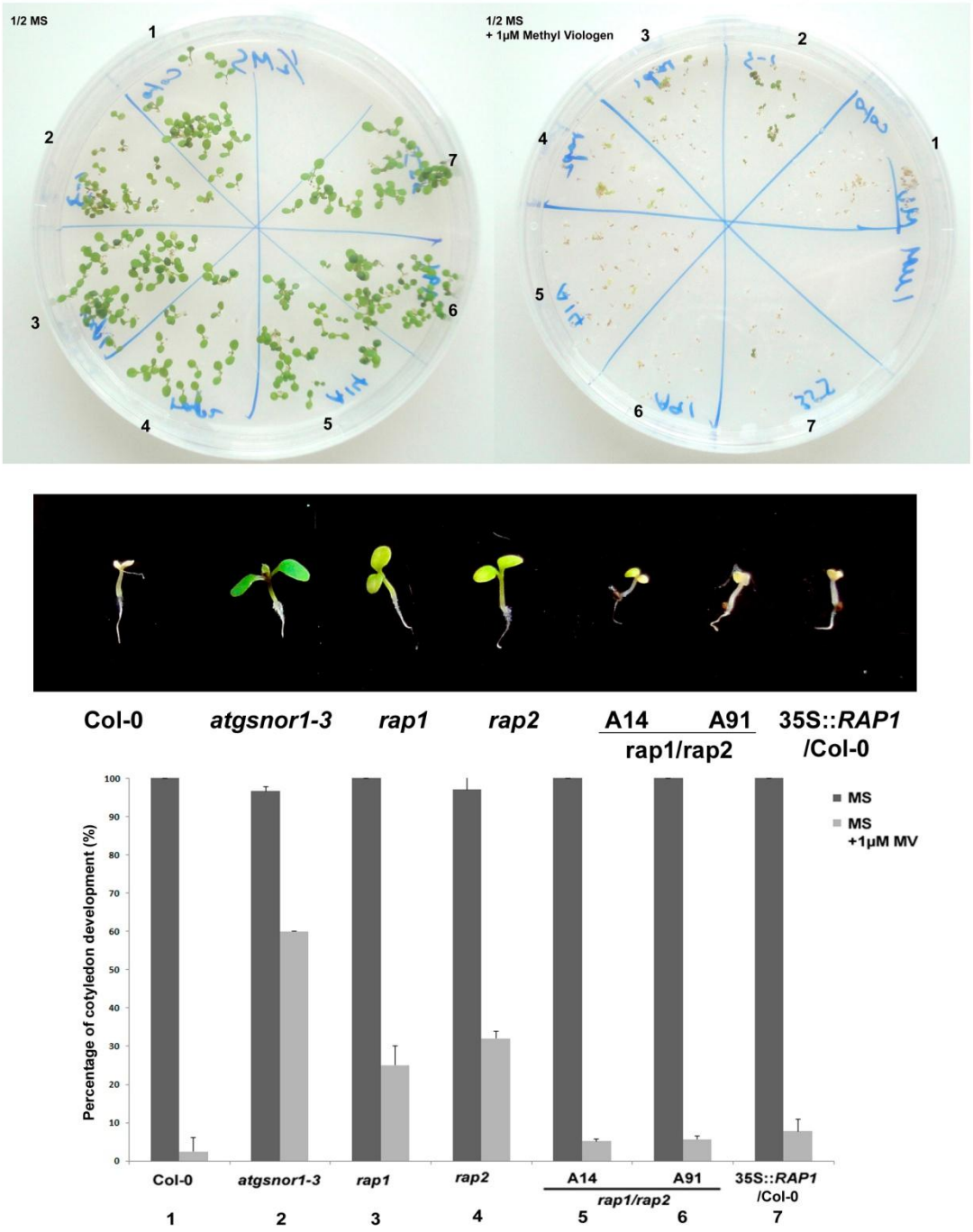

Figure 6.8 Enhanced resistance to MV for *atgsnor1-3*, *rap1* and *rap2* plants.
Seeds were sowed in either half MS with or without MV (1 µM final concentration) for 5 days. Percentage of cotyledon development was a result of two individual trials.

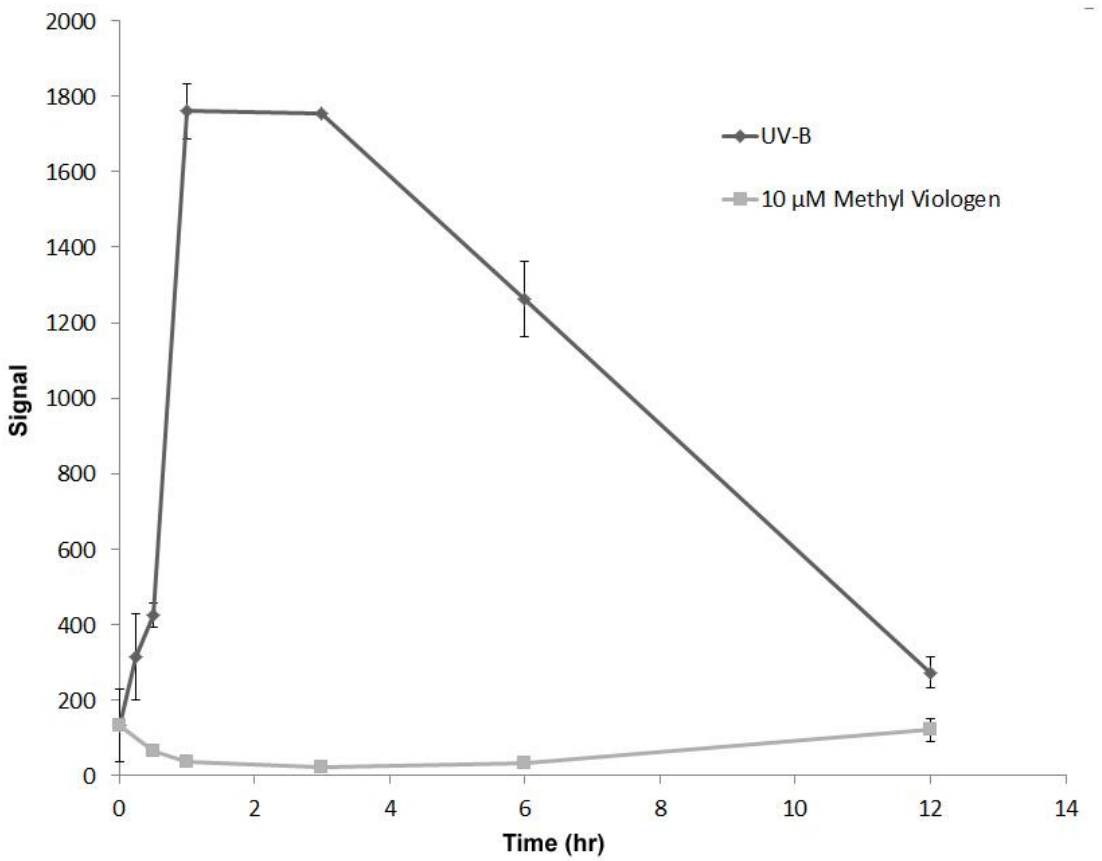

Figure 6.9 Expression of *RAP1* in response to UV-B and methyl viologen.
Arabidopsis shoots (from 16 days old plants) were treated with UV-B (15 min. 1.18 W/m2 Philips TL40W/12) or methyl viologen at final concentration of 10 µM. (data from NASCArrays)

6.3.2 Discussion: Methyl Viologen

The *GSNOR* loss-of-function mutants (*atgsnor1-3* and *par2-1*) in *Arabidopsis* had been reported to be resistant to methyl viologen (MV) or paraquat (Chen et al. 2009). MV has been used as a herbicide to kill green plant tissue by catalysing the formation of reactive oxygen species (ROS). In the germination test (Figure 6.8), enhanced resistance was observed in *atgsnor1-3* seedlings, and *rap1* and *rap2* seedlings also displayed resistance to MV with a level between wild-type and *atgsnro1-3*. Downregulation of *RAP1* also seems to have advantage to cope with the oxidative stress from MV in wild-type, as expression of *RAP1* was rapidly suppressed upon MV treatment (Figure 6.9). However, even though the *RAP1* expression was suppressed, the wild-type plants were killed by MV. It may suggest that anticipated reduction in *RAP1* expression would be required for the plants to acquire resistance to MV.

The mechanism behind the MV resistance in *GSNOR* knockout mutants is still uncertain. It has been suggested that S-nitrosylation of peroxiredoxin II E inhibited its activity in hydroperoxide reduction and peroxynitrite detoxification. Enhanced S-nitrosylation in *GSNOR* mutants may lead to accumulation of hydroperoxide and peroxynitrite that could be favourable condition against MV. Also, *Arabidopsis* METACASPASE9 activity is regulated by S-nitrosylation (Chen et al. 2009). The increase in S-nitrosylation may suppress the cell death induced by MV. On the other hand, the MV resistant phenotype in *GSNOR* knockout mutants could be simply due to a direct biochemical explanation that excess NO may accept the ROS generated from MV transforming into peroxynitrite (i.e. $\cdot O_2^- + \cdot NO \rightarrow ONO_2^-$). Peroxynitrite is thought to be relatively less toxic to plants (Peto et al. 2011).

It has been reported that an *Arabidopsis* mutant ozone-sensitive *radical-induced cell death1-1* (*rcd1-2*) was more resistant to MV and exhibits a higher tolerance to short-term ultraviolet-B (UV-B) treatments than the wild type. The report suggested that MV resistance of *rcd1-2* was due to the enhanced activities of the active oxygen species (AOS)-scavenging enzymes in chloroplasts and that the acquired tolerance to short-term UV-B exposure results from a higher accumulation of sunscreen pigments such as phenolic compounds (Fujibe et al. 2004). Interestingly, microarray data from NASCArrays has indicated that *RAP1* expression was highly induced by UV-B but suppressed by MV (Fig 6.9). This suggests that *RAP1* could be an important factor in

the homeostasis of cellular ROS. UV-B attacks DNA and photosystem II (PSII) and photoproducts are usually formed that can act as in situ sensors for UV penetration. UV-B is also known to induce stomatal closure via hydrogen peroxide (H_2O_2), and to affect ethylene biosynthesis. The mechanism was believed to be via ethylene-mediated H_2O_2 generation (He et al. 2011). The difference in chemistry between H_2O_2 (from UV-B) and $\cdot O_2^-$ (from MV) could lead to a significant variation in cellular redox balance and RAP1 might be involved in these redox signals (Figure 7.1). Additionally, it has been reported that UV-B triggered the generation of nitric oxide (NO) in plants (Zhang et al. 2011) and animals (Wu et al. 2010). An exposure of keratinocytes to UV-B led to the immediate generation of peroxynitrite ($ONOO^-$), with different kinetics from nitric oxide synthase (NOS) produced $NO/ONOO^-$. These findings also suggested that NO might be involved in redox balancing. Although there is a lack of evidence to establish the complex relationships of UV-B, ROS, NO and MV, understanding the properties of *RAP1* towards MV has at least provided some hints of how these potentially hazardous agents may be significantly involved in the regulation of many physiological pathways.

Chapter 7

7 General Discussion

Through the identification and analysis of mutant lines, certain physiological roles of *RAP1* have been implied in this study. *RAP1* might be involved in the defence against a variety of pathogens and regulation of various physiological responses (Figure 7.1). Our findings suggest that RAP1 is an E3 ligase integral to the ubiquitin-mediated degradation pathway. Further, the E3 ligase activity of RAP1 may be regulated by S-nitrosylation. *RAP1* together with *RAP2* were shown to belong to a gene family of E3 ligases. Evidence has also suggested that *RAP1* may be involved in the control of resistance/homeostasis towards various kinds of ROS. In summary, RAP1 could be a global regulator of many physiological pathways through the adjustment of cellular redox status.

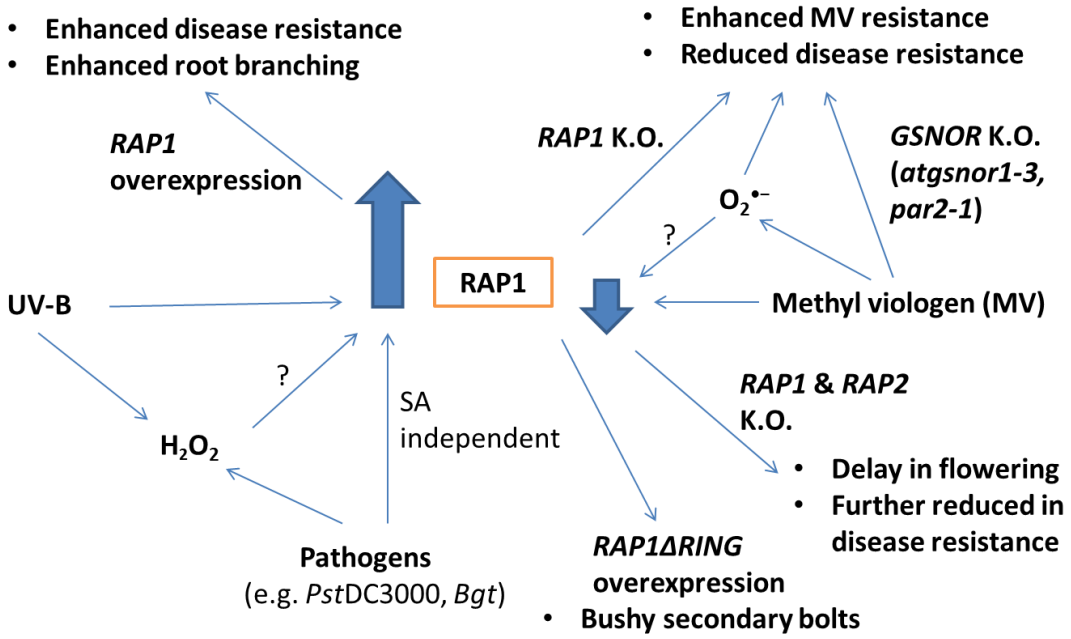

Figure 7.1 A schematic diagram to show the potential roles of *RAP1* in various physiological responses.

7.1 *RAP1* and *RAP2* Function Redundantly

As RAP1 and RAP2 are similar in protein sequence, it was speculated that these proteins may function redundantly. Neither *rap1* nor *rap2* demonstrated strong phenotypes in development or disease resistance. However, *rap1/rap2* double mutants showed delayed flowering and enhanced susceptibility to *Pst*DC3000 and *Arabidopsis* powdery mildew. In contrast, the expression profiles of *RAP1* and *RAP2* are significantly different. Also, *rap1* and *rap2* showed enhanced resistance to methyl viologen but not in the *rap1/rap2* double mutants. This suggests that RAP1 and RAP2 have overlapping functions but are components of different signalling pathways.

7.2 *RAP1* is Involved in Basal Defence

RAP1 was rapidly induced by wounding and a variety of pathogens. However, experimental data suggested that *RAP1* was more related to the defence required for basal resistance. Loss of *RAP1* led to enhanced susceptibility to *Pst*DC3000 and the effects were further amplified if both *RAP1* and the closely related *RAP2* were knocked out. RAP1 proteins were accumulated during *Arabidopsis* powdery mildew infection and the *rap1* mutants were more susceptible to *Arabidopsis* powdery mildew. On the other hand, *RAP1* may be less important for *R*-gene mediated resistance as there was no significant difference in the hypersensitive response between the *rap1*mutants and wild type plants. In addition, microarray data has shown that induction effect by *Pst*DC3000 (*avrRpm1*) was weaker than induction by *Pst*DC3000 (*hrcC*$^{-}$), *P. phaseolicola* and *Phytophthora infestans*.

RAP1 may regulate defence responses through redox-related regulation. Expression of *GSNOR* was highly sensitive to *RAP1* transcript levels, in particular overexpression of RAP1 significantly upregulated the expression of both *GSNOR* and *PR-1*. Also, *RAP1* expression was regulated by ROS-generating stresses such as UV-B and methyl viologen. Furthermore, *RAP1* showed SA-independent upregulation upon pathogen challenge and co-expressed with the SNARE encoding gene *SYP121*. This gene together with the closely related *SYP122* were shown to be involved in SA-independent resistance against *Arabidopsis* powdery mildew, suggesting *RAP1* may be involved in a hormone-independent defence pathway which could be redox-dependent.

It was also observed that, in general, knockout of *RAP1* did not lead to a dramatic reduction in disease resistance of pathogens. It is speculated that *RAP1* is involved in a broad range of pathogen resistance. Similarly, redox-related *GSNOR* gene was also involved in a broad-range of pathogen resistance but *gsnor* mutants exhibited greater susceptibility. There is only one *GSNOR* gene in *Arabidopsis* but at least 4 genes in the *RAP1*-family (Nodzon et al. 2004; Prasad and Stone 2010). Loss of *RAP1* and *RAP2* may still be insufficient to uncover the full extent of functional redundancy in the *RAP1* gene family. In this context, generation of a triple mutant of *PUB22/23/24* (U-box E3 ligases) was required to demonstrate the full role of these proteins in PAMP triggered immunity (Trujillo et al. 2008). In fact, *PUB24* was also one of the top 50 candidates that was co-expressed with *RAP1* (data not shown). It is suggested that a triple or even a quadruple mutant of *RAP* genes may be required to display the true importance of this gene family in plant defence responses.

7.3 S-Nitrosylation of RAP1 May Uncover the Relationship Between E3 Ligases and Cellular Redox Regulation

Published examples have mentioned that RING-type E3 ligases in neuronal cells can be S-nitrosylated and S-nitrosylation also inhibits the activity of the E3 ligases (Nakamura et al. 2010; Yao et al. 2004). In this study, a RING-type E3 ligase RAP1 was also shown to be S-nitrosylated and its activity was regulated by the concentration of applied NO-donors. The correlation between an E3 ligase and S-nitrosylation has provided an insight that physiological activities could be regulated by S-nitrosylation. There are 469 predicted RING-containing proteins in *Arabidopsis* (Stone et al. 2005) and the cysteine-rich domain of these proteins can be potentially modified by S-nitrosylation. The activities of these E3 ligases could be up-/down-regulated upon S-nitrosylation. As E3 ligase activity (ubiquitin-mediated degradation) is critical to determine the abundance of certain key regulators (e.g. transcription factors and kinases), S-nitrosylation of E3 ligases may therefore indirectly control a wide range of physiological responses.

Unlike other post-translational modifications such as phosphorylation and glycosylation, the regulatory mechanism of S-nitrosylation can be relatively transient because the S-NO bond is less stable and redox sensitive. E3 ligase activity could be readily adjusted by S-nitrosylation in response to the change in cellular redox status. It

is possible that E3 ligases could be a new type of redox sensor taking part in various physiological responses comparable to those identified in mammalian cells (Aracena-Parks et al. 2006; Nakamura and Lipton 2011; Wang et al. 2009b).

7.4 *RAP1* Could Be a Global Regulator of Redox-Mediated Responses

Apart from the defence-related phenotypes, *RAP1* was shown to be involved in a variety of developmental responses, such as root branching, time to flowering and development of secondary bolts. It is proposed that *RAP1* could be a global regulator controls these responses through redox-mediated mechanisms. It has been suggested that reactive oxygen species (ROS) could also be regulators of various physiological responses. However, only limited reports have commented on how plants detect and respond to the change in redox status (Spoel and Loake 2011). *RAP1* expression was shown to be independent of SA and other hormones but rapidly responsive to UV-B and methyl viologen (MV). As previously discussed (Chapter 6.3a), UV-B and MV could generate various kinds of ROS/RNS. Transcription factors that bind the *RAP1* promoter may be able to detect the change in redox status and control the levels of expression. It has been shown that RAP1 positively regulated the expression of *GSNOR*, therefore RAP1 may adjust the cellular redox environment through the regulation of *GSNOR*. Changes in GSNOR levels indirectly and directly control a variety of responses through S-nitrosylation/denitrosylation of proteins and the chemical reactions with other ROS/RNS. The substrate protein(s) of RAP1 could also be critical regulators that work cooperatively with RAP1 in the regulation of a variety of redox-mediated responses.

7.5 Conclusion

In this study, several questions about RAP1 have been answered: (1) RAP1 is an E3 ligase; (2) RAP1 can be S-nitrosylated *in vitro* and its E3 ligase activity can be regulated through the S-nitrosylation of cysteine residue C325 and; (3) RAP1 could be involved in growth and development and there is also evidence to suggest that RAP1 is a positive regulator in defence responses.

However, the complete roles of *RAP1* are yet to be uncovered. None of the upstream (*RAP1* activator/repressor) and downstream (substrate proteins) components of RAP1 have been isolated. For instance, identification of the substrate proteins of RAP1 will be one of the key experiments to be carried out in the future. Knowing the substrates of RAP1 will definitely help to figure out in which signalling pathways is RAP1 involving. Besides, there is no *in vivo* data to demonstrate the relationship between S-nitrosylation and RAP1, which can be achieved by studying of *RAP1* mutants in the presence of various NO donors or NO inhibitors. It is believed that many redox-related regulators exist in the *Arabidopsis* genome. Therefore, the continued identification of redox-related components will be a promising direction to help understand how cells regulate signals dynamically through changes in cellular redox status.

Bibliography

Abreu ME, Munne-Bosch S (2009) Salicylic acid deficiency in NahG transgenic lines and sid2 mutants increases seed yield in the annual plant Arabidopsis thaliana. J Exp Bot 60: 1261-1271

Achkor H, Diaz M, Fernandez MR, Biosca JA, Pares X, Martinez MC (2003) Enhanced formaldehyde detoxification by overexpression of glutathione-dependent formaldehyde dehydrogenase from Arabidopsis. Plant Physiol 132: 2248-2255

Alscher RG, Erturk N, Heath LS (2002) Role of superoxide dismutases (SODs) in controlling oxidative stress in plants. J Exp Bot 53: 1331-1341

Aracena-Parks P, Goonasekera SA, Gilman CP, Dirksen RT, Hidalgo C, Hamilton SL (2006) Identification of cysteines involved in S-nitrosylation, S-glutathionylation, and oxidation to disulfides in ryanodine receptor type 1. J Biol Chem 281: 40354-40368

Ausubel FM, Clay NK, Adio AM, Denoux C, Jander G (2009) Glucosinolate Metabolites Required for an Arabidopsis Innate Immune Response. Science 323: 95-101

Azevedo C, Sadanandom A, Kitagawa K, Freialdenhoven A, Shirasu K, Schulze-Lefert P (2002) The RAR1 interactor SGT1, an essential component of R gene-triggered disease resistance. Science 295: 2073-2076

Bachmair A, Novatchkova M, Potuschak T, Eisenhaber F (2001) Ubiquitylation in plants: a post-genomic look at a post-translational modification. Trends Plant Sci 6: 463-470

Bae W, Lee YJ, Kim DH, Lee J, Kim S, Sohn EJ, Hwang I (2008) AKR2A-mediated import of chloroplast outer membrane proteins is essential for chloroplast biogenesis. Nat Cell Biol 10: 220-227

Barroso JB, Corpas FJ, Carreras A, Rodriguez-Serrano M, Esteban FJ, Fernandez-Ocana A, Chaki M, Romero-Puertas MC, Valderrama R, Sandalio LM, del Rio LA (2006) Localization of S-nitrosoglutathione and expression of S-nitrosoglutathione reductase in pea plants under cadmium stress. J Exp Bot 57: 1785-1793

Bednarek P, Osbourn A (2009) Plant-Microbe Interactions: Chemical Diversity in Plant Defense. Science 324: 746-748

Benhar M, Forrester MT, Hess DT, Stamler JS (2008) Regulated protein denitrosylation by cytosolic and mitochondrial thioredoxins. Science 320: 1050-1054

Benhar M, Forrester MT, Stamler JS (2009) Protein denitrosylation: enzymatic mechanisms and cellular functions. Nat Rev Mol Cell Biol 10: 721-732

Benhar M, Thompson JW, Moseley MA, Stamler JS (2010) Identification of S-nitrosylated targets of thioredoxin using a quantitative proteomic approach. Biochemistry 49: 6963-6969

Bittel P, Robatzek S (2007) Microbe-associated molecular patterns (MAMPs) probe plant immunity. Curr Opin Plant Biol 10: 335-341

Borden KL, Freemont PS (1996) The RING finger domain: a recent example of a sequence-structure family. Curr Opin Struct Biol 6: 395-401

Bos JI, Armstrong MR, Gilroy EM, Boevink PC, Hein I, Taylor RM, Zhendong T, Engelhardt S, Vetukuri RR, Harrower B, Dixelius C, Bryan G, Sadanandom A, Whisson SC, Kamoun S, Birch PR (2010) Phytophthora infestans effector AVR3a is essential for virulence and manipulates plant immunity by stabilizing host E3 ligase CMPG1. Proc Natl Acad Sci U S A 107: 9909-9914

Bouchez O, Huard C, Lorrain S, Roby D, Balague C (2007) Ethylene is one of the key elements for cell death and defense response control in the Arabidopsis lesion mimic mutant vad1. Plant Physiol 145: 465-477

Bradford MM (1976) A rapid and sensitive method for the quantitation of microgram quantities of protein utilizing the principle of protein-dye binding. Anal Biochem 72: 248-254

Brodersen P, Malinovsky FG, Hematy K, Newman MA, Mundy J (2005) The role of salicylic acid in the induction of cell death in Arabidopsis acd11. Plant Physiol 138: 1037-1045

Broekaert WF, Delaure SL, De Bolle MF, Cammue BP (2006) The role of ethylene in host-pathogen interactions. Annu Rev Phytopathol 44: 393-416

Bronte V, Zanovello P (2005) Regulation of immune responses by L-arginine metabolism. Nat Rev Immunol 5: 641-654
Buhot N, Gomes E, Milat ML, Ponchet M, Marion D, Lequeu J, Delrot S, Coutos-Thevenot P, Blein JP (2004) Modulation of the biological activity of a tobacco LTP1 by lipid complexation. Mol Biol Cell 15: 5047-5052
Casademunt E, Carter BD, Benzel I, Frade JM, Dechant G, Barde YA (1999) The zinc finger protein NRIF interacts with the neurotrophin receptor p75(NTR) and participates in programmed cell death. EMBO J 18: 6050-6061
Chen R, Sun S, Wang C, Li Y, Liang Y, An F, Li C, Dong H, Yang X, Zhang J, Zuo J (2009) The Arabidopsis PARAQUAT RESISTANT2 gene encodes an S-nitrosoglutathione reductase that is a key regulator of cell death. Cell Res 19: 1377-1387
Chen YY, Huang YF, Khoo KH, Meng TC (2007) Mass spectrometry-based analyses for identifying and characterizing S-nitrosylation of protein tyrosine phosphatases. Methods 42: 243-249
Cheong JJ, Choi YD (2003) Methyl jasmonate as a vital substance in plants. Trends Genet 19: 409-413
Chico JM, Chini A, Fonseca S, Solano R (2008) JAZ repressors set the rhythm in jasmonate signaling. Curr Opin Plant Biol 11: 486-494
Clague MJ, Urbe S (2010) Ubiquitin: same molecule, different degradation pathways. Cell 143: 682-685
Craig A, Ewan R, Mesmar J, Gudipati V, Sadanandom A (2009) E3 ubiquitin ligases and plant innate immunity. J Exp Bot 60: 1123-1132
Dalle-Donne I, Rossi R, Colombo G, Giustarini D, Milzani A (2009) Protein S-glutathionylation: a regulatory device from bacteria to humans. Trends Biochem Sci 34: 85-96
Day B, Dahlbeck D, Staskawicz BJ (2006) NDR1 interaction with RIN4 mediates the differential activation of multiple disease resistance pathways in Arabidopsis. Plant Cell 18: 2782-2791
Delaure SL, Van Hemelrijck W, De Bolle MFC, Cammue BPA, De Coninck BMA (2008) Building up plant defenses by breaking down proteins. Plant Sci 174: 375-385
Delledonne M, Xia YJ, Dixon RA, Lamb C (1998) Nitric oxide functions as a signal in plant disease resistance. Nature 394: 585-588
Dombrowski JE, Bergey DR (2007) Calcium ions enhance systemin activity and play an integral

role in the wound response. Plant Sci 175: 335-344
Dou X, Wang Q, Qi Z, Song W, Wang W, Guo M, Zhang H, Zhang Z, Wang P, Zheng X (2011) MoVam7, a conserved SNARE involved in vacuole assembly, is required for growth, endocytosis, ROS accumulation, and pathogenesis of Magnaporthe oryzae. Plos One 6: e16439
Duan S, Chen C (2007) S-nitrosylation/denitrosylation and apoptosis of immune cells. Cell Mol Immunol 4: 353-358
Eckardt NA (2009) The Arabidopsis RPW8 resistance protein is recruited to the extrahaustorial membrane of biotrophic powdery mildew fungi. Plant Cell 21: 2543
Ecker JR, Davis RW (1987) Plant defense genes are regulated by ethylene. Proc Natl Acad Sci U S A 84: 5202-5206
Feechan A, Kwon E, Yun BW, Wang Y, Pallas JA, Loake GJ (2005) A central role for S-nitrosothiols in plant disease resistance. Proc Natl Acad Sci U S A 102: 8054-8059
Flores-Perez U, Sauret-Gueto S, Gas E, Jarvis P, Rodriguez-Concepcion M (2008a) A mutant impaired in the production of plastome-encoded proteins uncovers a mechanism for the homeostasis of isoprenoid biosynthetic enzymes in Arabidopsis plastids. Plant Cell 20: 1303-1315
Flores-Perez U, Sauret-Gueto S, Gas E, Jarvis P, Rodriguez-Concepcion M (2008b) A mutant impaired in the production of plastome-encoded proteins uncovers a mechanism for the

homeostasis of isoprenoid biosynthetic enzymes in Arabidopsis plastids. Plant Cell 20: 1303-1315
Forrester MT, Foster MW, Benhar M, Stamler JS (2009) Detection of protein S-nitrosylation with the biotin-switch technique. Free Radic Biol Med 46: 119-126
Foster MW, Hess DT, Stamler JS (2009) Protein S-nitrosylation in health and disease: a current perspective. Trends Mol Med 15: 391-404
Francis KE, Lam SY, Copenhaver GP (2006) Separation of Arabidopsis pollen tetrads is regulated by QUARTET1, a pectin methylesterase gene. Plant Physiol 142: 1004-1013
Fujibe T, Saji H, Arakawa K, Yabe N, Takeuchi Y, Yamamoto KT (2004) A methyl viologen-resistant mutant of Arabidopsis, which is allelic to ozone-sensitive rcd1, is tolerant to supplemental ultraviolet-B irradiation. Plant Physiol 134: 275-285
Gao M, Wang X, Wang D, Xu F, Ding X, Zhang Z, Bi D, Cheng YT, Chen S, Li X, Zhang Y (2009) Regulation of cell death and innate immunity by two receptor-like kinases in Arabidopsis. Cell Host Microbe 6: 34-44
Geng J, Carstens RP (2006) Two methods for improved purification of full-length mammalian proteins that have poor expression and/or solubility using standard Escherichia coli procedures. Protein Expr Purif 48: 142-150
Gfeller A, Farmer EE (2004) Keeping the leaves green above us. Science 306: 1515-1516
Goritschnig S, Zhang Y, Li X (2007) The ubiquitin pathway is required for innate immunity in Arabidopsis. Plant J 49: 540-551
Grant JJ, Loake GJ (2000) Role of reactive oxygen intermediates and cognate redox signaling in disease resistance. Plant Physiol 124: 21-29
Grant SR, Fisher EJ, Chang JH, Mole BM, Dangl JL (2006) Subterfuge and manipulation: type III effector proteins of phytopathogenic bacteria. Annu Rev Microbiol 60: 425-449
Gressel J (2010) Needs for and environmental risks from transgenic crops in the developing world. New Biotechnol 27: 522-527
Gu Z, Nakamura T, Lipton SA (2010) Redox reactions induced by nitrosative stress mediate protein misfolding and mitochondrial dysfunction in neurodegenerative diseases. Mol Neurobiol 41: 55-72
Hardtke CS, Okamoto H, Stoop-Myer C, Deng XW (2002) Biochemical evidence for ubiquitin ligase activity of the Arabidopsis COP1 interacting protein 8 (CIP8). Plant J 30: 385-394
He J, Yue X, Wang R, Zhang Y (2011) Ethylene mediates UV-B-induced stomatal closure via peroxidase-dependent hydrogen peroxide synthesis in Vicia faba L. J Exp Bot 62: 2657-2666
Heese A, Hann DR, Gimenez-Ibanez S, Jones AM, He K, Li J, Schroeder JI, Peck SC, Rathjen JP (2007) The receptor-like kinase SERK3/BAK1 is a central regulator of innate immunity in plants. Proc Natl Acad Sci U S A 104: 12217-12222
Hess DT, Matsumoto A, Kim SO, Marshall HE, Stamler JS (2005) Protein S-nitrosylation: purview and parameters. Nat Rev Mol Cell Biol 6: 150-166
Holmgren A (2008) Biochemistry. SNO removal. Science 320: 1019-1020
Holzmeister C, Frohlich A, Sarioglu H, Bauer N, Durner J, Lindermayr C (2011) Proteomic analysis of defense response of wildtype Arabidopsis thaliana and plants with impaired NO-homeostasis. Proteomics 11: 1664-1683
Hong JK, Yun BW, Kang JG, Raja MU, Kwon E, Sorhagen K, Chu C, Wang Y, Loake GJ (2008) Nitric oxide function and signalling in plant disease resistance. J Exp Bot 59: 147-154
Huang S, Kerschbaum HH, Engel E, Hermann A (1997) Biochemical characterization and histochemical localization of nitric oxide synthase in the nervous system of the snail, Helix pomatia. J Neurochem 69: 2516-2528
Huang X, Stettmaier K, Michel C, Hutzler P, Mueller MJ, Durner J (2004) Nitric oxide is induced by wounding and influences jasmonic acid signaling in Arabidopsis thaliana. Planta 218: 938-946
James C (2010) Global Status of Commercialized Biotech/GM Crops. ISAAA Brief No 42
Johnston JS, Pepper AE, Hall AE, Chen ZJ, Hodnett G, Drabek J, Lopez R, Price HJ (2005) Evolution of genome size in Brassicaceae. Ann Bot 95: 229-235

Jones JD, Dangl JL (2006) The plant immune system. Nature 444: 323-329
Jourd'heuil D, Jourd'heuil FL, Feelisch M (2003) Oxidation and nitrosation of thiols at low micromolar exposure to nitric oxide. Evidence for a free radical mechanism. J Biol Chem 278: 15720-15726
Kawasaki T, Nam J, Boyes DC, Holt BF, 3rd, Hubert DA, Wiig A, Dangl JL (2005) A duplicated pair of Arabidopsis RING-finger E3 ligases contribute to the RPM1- and RPS2-mediated hypersensitive response. Plant J 44: 258-270
Kemmerling B, Schwedt A, Rodriguez P, Mazzotta S, Frank M, Qamar SA, Mengiste T, Betsuyaku S, Parker JE, Mussig C, Thomma BP, Albrecht C, de Vries SC, Hirt H, Nurnberger T (2007) The BRI1-associated kinase 1, BAK1, has a brassinolide-independent role in plant cell-death control. Curr Biol 17: 1116-1122
Kendrick MD, Chang C (2008) Ethylene signaling: new levels of complexity and regulation. Curr Opin Plant Biol 11: 479-485
Kim HS, Delaney TP (2002) Arabidopsis SON1 is an F-box protein that regulates a novel induced defense response independent of both salicylic acid and systemic acquired resistance. Plant Cell 14: 1469-1482
Kim JH, Lee BW, Schroeder FC, Jander G (2008) Identification of indole glucosinolate breakdown products with antifeedant effects on Myzus persicae (green peach aphid). Plant J 54: 1015-1026
Koo YJ, Kim MA, Kim EH, Song JT, Jung C, Moon JK, Kim JH, Seo HS, Song SI, Kim JK, Lee JS, Cheong JJ, Choi YD (2007) Overexpression of salicylic acid carboxyl methyltransferase reduces salicylic acid-mediated pathogen resistance in Arabidopsis thaliana. Plant Mol Biol 64: 1-15
Koornneef A, Leon-Reyes A, Ritsema T, Verhage A, Den Otter FC, Van Loon LC, Pieterse CM (2008) Kinetics of salicylate-mediated suppression of jasmonate signaling reveal a role for redox modulation. Plant Physiol 147: 1358-1368
Kraft E, Stone SL, Ma L, Su N, Gao Y, Lau OS, Deng XW, Callis J (2005) Genome analysis and functional characterization of the E2 and RING-type E3 ligase ubiquitination enzymes of Arabidopsis. Plant Physiol 139: 1597-1611
Li J, Mahajan A, Tsai MD (2006) Ankyrin repeat: a unique motif mediating protein-protein interactions. Biochemistry 45: 15168-15178
Liu L, Hausladen A, Zeng M, Que L, Heitman J, Stamler JS (2001) A metabolic enzyme for S-nitrosothiol conserved from bacteria to humans. Nature 410: 490-494
Liu YC, Wu YR, Huang XH, Sun J, Xie Q (2011) AtPUB19, a U-Box E3 Ubiquitin Ligase, Negatively Regulates Abscisic Acid and Drought Responses in Arabidopsis thaliana. Mol Plant
Loake G, Grant M (2007) Salicylic acid in plant defence--the players and protagonists. Curr Opin Plant Biol 10: 466-472
Lorick KL, Jensen JP, Fang S, Ong AM, Hatakeyama S, Weissman AM (1999) RING fingers mediate ubiquitin-conjugating enzyme (E2)-dependent ubiquitination. Proc Natl Acad Sci U S A 96: 11364-11369
Malik SI, Hussain A, Yun BW, Spoel SH, Loake GJ (2011) GSNOR-mediated de-nitrosylation in the plant defence response. Plant Sci 181: 540-544
Meier S, Bastian R, Donaldson L, Murray S, Bajic V, Gehring C (2008) Co-expression and promoter content analyses assign a role in biotic and abiotic stress responses to plant natriuretic peptides. Bmc Plant Biol 8: 24
Mendgen K, Hahn M, Deising H (1996) Morphogenesis and mechanisms of penetration by plant pathogenic fungi. Annu Rev Phytopathol 34: 367-386
Meyer AJ (2008) The integration of glutathione homeostasis and redox signaling. J Plant Physiol 165: 1390-1403
Moreau M, Lee GI, Wang Y, Crane BR, Klessig DF (2008) AtNOS/AtNOA1 is a functional Arabidopsis thaliana cGTPase and not a nitric-oxide synthase. J Biol Chem 283: 32957-32967
Morrissey JP, Osbourn AE (1999) Fungal resistance to plant antibiotics as a mechanism of pathogenesis. Microbiol Mol Biol R 63: 708-+

Mou Z, Fan W, Dong X (2003) Inducers of plant systemic acquired resistance regulate NPR1 function through redox changes. Cell 113: 935-944
Nakamura T, Lipton SA (2007) S-Nitrosylation and uncompetitive/fast off-rate (UFO) drug therapy in neurodegenerative disorders of protein misfolding. Cell Death Differ 14: 1305-1314
Nakamura T, Lipton SA (2011) Redox modulation by S-nitrosylation contributes to protein misfolding, mitochondrial dynamics, and neuronal synaptic damage in neurodegenerative diseases. Cell Death Differ 18: 1478-1486
Nakamura T, Wang L, Wong CC, Scott FL, Eckelman BP, Han X, Tzitzilonis C, Meng F, Gu Z, Holland EA, Clemente AT, Okamoto S, Salvesen GS, Riek R, Yates JR, 3rd, Lipton SA (2010) Transnitrosylation of XIAP regulates caspase-dependent neuronal cell death. Mol Cell 39: 184-195
Noctor G (2006) Metabolic signalling in defence and stress: the central roles of soluble redox couples. Plant Cell Environ 29: 409-425
Nodzon LA, Xu WH, Wang Y, Pi LY, Chakrabarty PK, Song WY (2004) The ubiquitin ligase XBAT32 regulates lateral root development in Arabidopsis. Plant J 40: 996-1006
Noutoshi Y, Kuromori T, Wada T, Hirayama T, Kamiya A, Imura Y, Yasuda M, Nakashita H, Shirasu K, Shinozaki K (2006) Loss of Necrotic Spotted Lesions 1 associates with cell death and defense responses in Arabidopsis thaliana. Plant Mol Biol 62: 29-42
Ntoukakis V, Mucyn TS, Gimenez-Ibanez S, Chapman HC, Gutierrez JR, Balmuth AL, Jones AM, Rathjen JP (2009) Host inhibition of a bacterial virulence effector triggers immunity to infection. Science 324: 784-787
Ohme-Takagi M, Suzuki K, Shinshi H (2000) Regulation of ethylene-induced transcription of defense genes. Plant Cell Physiol 41: 1187-1192
Osbourn AE (1996) Preformed antimicrobial compounds and plant defense against fungal attack. Plant Cell 8: 1821-1831
Park SW, Kaimoyo E, Kumar D, Mosher S, Klessig DF (2007) Methyl salicylate is a critical mobile signal for plant systemic acquired resistance. Science 318: 113-116
Perez-Mato I, Castro C, Ruiz FA, Corrales FJ, Mato JM (1999) Methionine adenosyltransferase S-nitrosylation is regulated by the basic and acidic amino acids surrounding the target thiol. J Biol Chem 274: 17075-17079
Peto A, Lehotai N, Lozano-Juste J, Leon J, Tari I, Erdei L, Kolbert Z (2011) Involvement of nitric oxide and auxin in signal transduction of copper-induced morphological responses in Arabidopsis seedlings. Ann Bot 108: 449-457
Prasad ME, Schofield A, Lyzenga W, Liu H, Stone SL (2010) Arabidopsis RING E3 ligase XBAT32 regulates lateral root production through its role in ethylene biosynthesis. Plant Physiol 153: 1587-1596
Prasad ME, Stone SL (2010) Further analysis of XBAT32, an Arabidopsis RING E3 ligase, involved in ethylene biosynthesis. Plant Signal Behav 5: 1425-1429
Preuss D, Rhee SY, Davis RW (1994) Tetrad analysis possible in Arabidopsis with mutation of the QUARTET (QRT) genes. Science 264: 1458-1460
Reynolds JD, Ahearn GS, Angelo M, Zhang J, Cobb F, Stamler JS (2007) S-nitrosohemoglobin deficiency: a mechanism for loss of physiological activity in banked blood. Proc Natl Acad Sci U S A 104: 17058-17062
Ridnour LA, Thomas DD, Mancardi D, Espey MG, Miranda KM, Paolocci N, Feelisch M, Fukuto J, Wink DA (2004) The chemistry of nitrosative stress induced by nitric oxide and reactive nitrogen oxide species. Putting perspective on stressful biological situations. Biol Chem 385: 1-10
Roland P (2011) Plant Genetics, Sustainable Agriculture and Global Food Security. Genetics 188: 11-20
Romero-Isart N, Cols N, Termansen MK, Gelpi JL, Gonzalez-Duarte R, Atrian S, Capdevila M, Gonzalez-Duarte P (1999) Replacement of terminal cysteine with histidine in the metallothionein alpha and beta domains maintains its binding capacity. Eur J Biochem 259: 519-527

Rosebrock TR, Zeng L, Brady JJ, Abramovitch RB, Xiao F, Martin GB (2007) A bacterial E3 ubiquitin ligase targets a host protein kinase to disrupt plant immunity. Nature 448: 370-374
Sakamoto A, Ueda M, Morikawa H (2002) Arabidopsis glutathione-dependent formaldehyde dehydrogenase is an S-nitrosoglutathione reductase. FEBS Lett 515: 20-24
Santhanam L, Lim HK, Miriel V, Brown T, Patel M, Balanson S, Ryoo S, Anderson M, Irani K, Khanday F, Di Costanzo L, Nyhan D, Hare JM, Christianson DW, Rivers R, Shoukas A, Berkowitz DE (2007) Inducible NO synthase dependent S-nitrosylation and activation of arginase1 contribute to age-related endothelial dysfunction. Circ Res 101: 692-702
Schulze-Lefert P, Kwon C, Bednarek P (2008) Secretory pathways in plant immune responses. Plant Physiol 147: 1575-1583
Shi JX, Malitsky S, De Oliveira S, Branigan C, Franke RB, Schreiber L, Aharoni A (2011) SHINE transcription factors act redundantly to pattern the archetypal surface of Arabidopsis flower organs. PLoS Genet 7: e1001388
Shirasu K, Schulze-Lefert P (2003) Complex formation, promiscuity and multi-functionality: protein interactions in disease-resistance pathways. Trends Plant Sci 8: 252-258
Slaymaker DH, Navarre DA, Clark D, del Pozo O, Martin GB, Klessig DF (2002) The tobacco salicylic acid-binding protein 3 (SABP3) is the chloroplast carbonic anhydrase, which exhibits antioxidant activity and plays a role in the hypersensitive defense response. Proc Natl Acad Sci U S A 99: 11640-11645
Spoel SH, Loake GJ (2011) Redox-based protein modifications: the missing link in plant immune signalling. Curr Opin Plant Biol
Staswick PE (2008) JAZing up jasmonate signaling. Trends Plant Sci 13: 66-71
Stepanova AN, Alonso JM (2009) Ethylene signaling and response: where different regulatory modules meet. Curr Opin Plant Biol 12: 548-555
Stone SL, Hauksdottir H, Troy A, Herschleb J, Kraft E, Callis J (2005) Functional analysis of the RING-type ubiquitin ligase family of Arabidopsis. Plant Physiol 137: 13-30
Stone SL, Williams LA, Farmer LM, Vierstra RD, Callis J (2006) KEEP ON GOING, a RING E3 ligase essential for Arabidopsis growth and development, is involved in abscisic acid signaling. Plant Cell 18: 3415-3428
Suntres ZE (2002) Role of antioxidants in paraquat toxicity. Toxicology 180: 65-77
Tada Y, Spoel SH, Pajerowska-Mukhtar K, Mou Z, Song J, Wang C, Zuo J, Dong X (2008) Plant immunity requires conformational changes [corrected] of NPR1 via S-nitrosylation and thioredoxins. Science 321: 952-956
Teper-Bamnolker P, Samach A (2005) The flowering integrator FT regulates SEPALLATA3 and FRUITFULL accumulation in Arabidopsis leaves. Plant Cell 17: 2661-2675
Thaler JS, Humphrey PT, Whiteman NK (2012) Evolution of jasmonate and salicylate signal crosstalk. Trends Plant Sci 17: 260-270
Thines B, Katsir L, Melotto M, Niu Y, Mandaokar A, Liu G, Nomura K, He SY, Howe GA, Browse J (2007) JAZ repressor proteins are targets of the SCF(COI1) complex during jasmonate signalling. Nature 448: 661-665
Torres MA, Dangl JL (2005) Functions of the respiratory burst oxidase in biotic interactions, abiotic stress and development. Curr Opin Plant Biol 8: 397-403
Toufighi K, Brady SM, Austin R, Ly E, Provart NJ (2005) The Botany Array Resource: e-Northerns, Expression Angling, and promoter analyses. Plant J 43: 153-163
Trujillo M, Ichimura K, Casais C, Shirasu K (2008) Negative regulation of PAMP-triggered immunity by an E3 ubiquitin ligase triplet in Arabidopsis. Curr Biol 18: 1396-1401
Tsuda K, Katagiri F (2010) Comparing signaling mechanisms engaged in pattern-triggered and effector-triggered immunity. Curr Opin Plant Biol 13: 459-465
van Haver E, Alink G, Barlow S, Cockburn A, Flachowsky G, Knudsen I, Kuiper H, Massin DP, Pascal G, Peijnenburg A, Phipps R, Poting A, Poulsen M, Seinen W, Spielmann H, van Loveren H, Wal JM, Williams A (2008) Safety and nutritional assessment of GM plants and derived food and feed: The role of animal feeding trials. Food Chem Toxicol 46: S2-S70

Vernooij B, Friedrich L, Morse A, Reist R, Kolditz-Jawhar R, Ward E, Uknes S, Kessmann H, Ryals J (1994) Salicylic Acid Is Not the Translocated Signal Responsible for Inducing Systemic Acquired Resistance but Is Required in Signal Transduction. Plant Cell 6: 959-965

Vlot AC, Dempsey DA, Klessig DF (2009) Salicylic Acid, a multifaceted hormone to combat disease. Annu Rev Phytopathol 47: 177-206

Vlot AC, Klessig DF, Park SW (2008) Systemic acquired resistance: the elusive signal(s). Curr Opin Plant Biol 11: 436-442

Vogel J, Somerville S (2000) Isolation and characterization of powdery mildew-resistant Arabidopsis mutants. Proc Natl Acad Sci U S A 97: 1897-1902

Wang L, Tsuda K, Sato M, Cohen JD, Katagiri F, Glazebrook J (2009a) Arabidopsis CaM binding protein CBP60g contributes to MAMP-induced SA accumulation and is involved in disease resistance against Pseudomonas syringae. PLoS Pathog 5: e1000301

Wang L, Tsuda K, Truman W, Sato M, Nguyen le V, Katagiri F, Glazebrook J (2011) CBP60g and SARD1 play partially redundant critical roles in salicylic acid signaling. Plant J 67: 1029-1041

Wang P, Liu GH, Wu K, Qu J, Huang B, Zhang X, Zhou X, Gerace L, Chen C (2009b) Repression of classical nuclear export by S-nitrosylation of CRM1. J Cell Sci 122: 3772-3779

Wang YH (2008) How effective is T-DNA insertional mutagenesis in Arabidopsis? J Biochem Tech 1: 11-20

Wang YQ, Feechan A, Yun BW, Shafiei R, Hofmann A, Taylor P, Xue P, Yang FQ, Xie ZS, Pallas JA, Chu CC, Loake GJ (2009c) S-nitrosylation of AtSABP3 antagonizes the expression of plant immunity. J Biol Chem 284: 2131-2137

Wang YS, Pi LY, Chen X, Chakrabarty PK, Jiang J, De Leon AL, Liu GZ, Li L, Benny U, Oard J, Ronald PC, Song WY (2006) Rice XA21 binding protein 3 is a ubiquitin ligase required for full Xa21-mediated disease resistance. Plant Cell 18: 3635-3646

Weigel RR, Pfitzner UM, Gatz C (2005) Interaction of NIMIN1 with NPR1 modulates PR gene expression in Arabidopsis. Plant Cell 17: 1279-1291

Wi SJ, Ji NR, Park KY (2012) Synergistic Biosynthesis of Biphasic Ethylene and Reactive Oxygen Species in Response to Hemibiotrophic Phytophthora parasitica in Tobacco Plants. Plant Physiol 159: 251-265

Winter D, Vinegar B, Nahal H, Ammar R, Wilson GV, Provart NJ (2007) An "Electronic Fluorescent Pictograph" browser for exploring and analyzing large-scale biological data sets. Plos One 2: e718

Wu S, Wang L, Jacoby AM, Jasinski K, Kubant R, Malinski T (2010) Ultraviolet B light-induced nitric oxide/peroxynitrite imbalance in keratinocytes--implications for apoptosis and necrosis. Photochem Photobiol 86: 389-396

Wunsche H, Baldwin IT, Wu J (2011) S-Nitrosoglutathione reductase (GSNOR) mediates the biosynthesis of jasmonic acid and ethylene induced by feeding of the insect herbivore Manduca sexta and is important for jasmonate-elicited responses in Nicotiana attenuata. J Exp Bot

Xie DX, Feys BF, James S, Nieto-Rostro M, Turner JG (1998) COI1: an Arabidopsis gene required for jasmonate-regulated defense and fertility. Science 280: 1091-1094

Yamasaki H, Sakihama Y, Takahashi S (1999) An alternative pathway for nitric oxide production in plants: new features of an old enzyme. Trends Plant Sci 4: 128-129

Yao D, Gu Z, Nakamura T, Shi ZQ, Ma Y, Gaston B, Palmer LA, Rockenstein EM, Zhang Z, Masliah E, Uehara T, Lipton SA (2004) Nitrosative stress linked to sporadic Parkinson's disease: S-nitrosylation of parkin regulates its E3 ubiquitin ligase activity. Proc Natl Acad Sci U S A 101: 10810-10814

Yi X, Mroczko M, Manoj KM, Wang X, Hager LP (1999) Replacement of the proximal heme thiolate ligand in chloroperoxidase with a histidine residue. Proc Natl Acad Sci U S A 96: 12412-12417

Yu M, Yun BW, Spoel SH, Loake GJ (2012) A sleigh ride through the SNO: regulation of plant immune function by protein S-nitrosylation. Curr Opin Plant Biol

Yun BW, Feechan A, Yin M, Saidi NB, Le Bihan T, Yu M, Moore JW, Kang JG, Kwon E, Spoel SH, Pallas JA, Loake GJ (2011) S-nitrosylation of NADPH oxidase regulates cell death in plant immunity. Nature 478: 264-268

Zhang M, Dong JF, Jin HH, Sun LN, Xu MJ (2011) Ultraviolet-B-induced flavonoid accumulation in Betula pendula leaves is dependent upon nitrate reductase-mediated nitric oxide signaling. Tree Physiol 31: 798-807

Zhang Z, Feechan A, Pedersen C, Newman MA, Qiu JL, Olesen KL, Thordal-Christensen H (2007a) A SNARE-protein has opposing functions in penetration resistance and defence signalling pathways. Plant J 49: 302-312

Zhang ZG, Feechan A, Pedersen C, Newman MA, Qiu JL, Olesen KL, Thordal-Christensen H (2007b) A SNARE-protein has opposing functions in penetration resistance and defence signalling pathways. Plant J 49: 302-312

Zipfel C (2008) Pattern-recognition receptors in plant innate immunity. Curr Opin Immunol 20: 10-16

Zipfel C, Felix G (2005) Plants and animals: a different taste for microbes? Curr Opin Plant Biol 8: 353-360